William & Mary
CHARTERED 1693

W&M ScholarWorks

Reports

1964

# A Mathematical Analysis of the Dynamic Soaring Flight of the Albatross with Ecological Interpretations

Clarence D. Cone Jr.

Follow this and additional works at: https://scholarworks.wm.edu/reports

 Part of the Aerodynamics and Fluid Mechanics Commons, Marine Biology Commons, and the Ornithology Commons

## Recommended Citation

Cone, C. D. (1964) A Mathematical Analysis of the Dynamic Soaring Flight of the Albatross with Ecological Interpretations. Special scientific report (Virginia Institute of Marine Science); no. 50. Virginia Institute of Marine Science, College of William and Mary. https://doi.org/10.21220/V5P88C

This Report is brought to you for free and open access by W&M ScholarWorks. It has been accepted for inclusion in Reports by an authorized administrator of W&M ScholarWorks. For more information, please contact scholarworks@wm.edu.

# A MATHEMATICAL ANALYSIS OF THE DYNAMIC SOARING FLIGHT OF THE ALBATROSS WITH ECOLOGICAL INTERPRETATIONS

by

Clarence D. Cone, Jr.

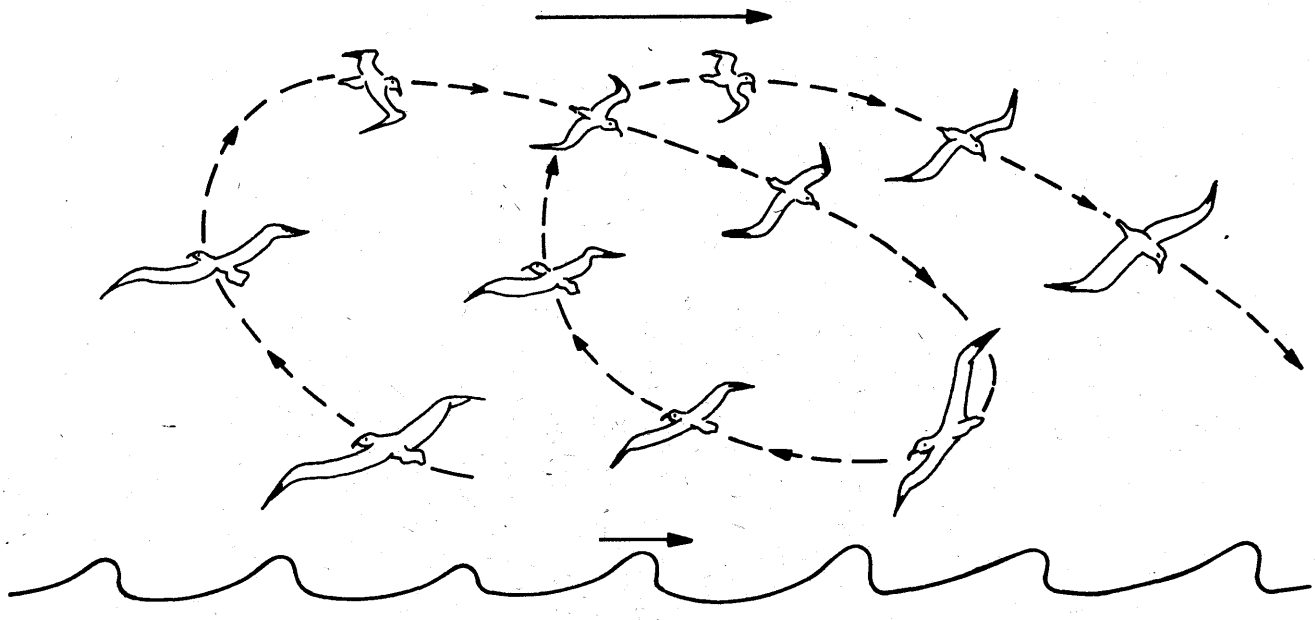

VIRGINIA INSTITUTE OF MARINE SCIENCE

SPECIAL SCIENTIFIC REPORT NO. 50

MAY 1964

VIRGINIA INSTITUTE OF MARINE SCIENCE

GLOUCESTER POINT, VIRGINIA

# A MATHEMATICAL ANALYSIS OF THE DYNAMIC SOARING FLIGHT OF THE ALBATROSS WITH ECOLOGICAL INTERPRETATIONS

by

Clarence D. Cone, Jr.

Special Scientific Report 50

W. J. Hargis, Jr.
Director

May 1964

ACKNOWLEDGMENTS

The author takes pleasure in acknowledging the cooperation and support given during the course of this study by Drs. William J. Hargis, Jr. and John L. Wood, Sr. of the Virginia Institute of Marine Science, and in expressing sincere appreciation to Dr. Philip S. Humphrey, Curator of Birds, U. S. National Museum, and Dr. Dean Amadon and Mr. Charles E. O'Brien, Department of Ornithology, American Museum of Natural History, for their interest and aid in making albatross study-skins and other specimens available for examination. Particular thanks are due to my wife, Charlotte M. Cone, who aided materially in various parts of the work. Finally, a special note of appreciation is extended to Dr. Michael P. Gaus and the National Science Foundation, whose interest and cooperation made possible this project in its present scope. The research work covered by this report was performed under a research grant of the National Science Foundation.

CONTENTS

# I. INTRODUCTION

The capability of flight plays a central role in the lives of most birds. Indeed, the existing morphological and ecological characteristics of many species are almost entirely dictated by the aerodynamic requirements of the highly developed flight modes they have acquired through evolutional specialization. In the case of such species, a clear understanding of the aerodynamic mechanisms underlying the particular flight modes can often provide a lucid insight into the basic physical relationships which govern a bird's characteristic activities and behavior.

This aerodynamic approach to the study of avian ecology is particularly useful in the case of soaring birds, where survival depends entirely upon the aerodynamic efficiency of the bird in exploiting the energy of special forms of air currents for sustained flight, and where the wing actions are sufficiently simple that the flight patterns can adequately be formulated for aerodynamic analysis. Such an approach was utilized by the author in a recent study[1*] of land birds which practice soaring flight in thermal air currents. By applying aerodynamic precepts to the analysis and interpretation of observed flight patterns, it was possible to explain, correlate, and even predict many facts of importance in the morphology and ecology of the land soarers. It is the purpose of the present study to apply a similar analysis to the dynamic soaring flight of sea birds, such as the albatross, and to utilize the results for establishing the significant factors in the ecology of the ocean soarers.

The magnificent soaring flight of the pelagic albatross and similar sea birds, although not readily observable because it takes place in remote regions of the ocean, is in its way every bit as fascinating and mysterious as that of the more easily observed land soarers. The source of the albatross' flight power, however, is quite different from that of the vulture or hawk. While the vulture secures its flight energy by steady circling in rising thermal shells[1,2,3], the albatross makes its way by a much more complex and difficult flight cycle. Operating in the thin shear layer of air generated near the water surface by the strong and relatively steady sea winds, the albatross has found a remarkable way to exploit the energy of horizontally-moving air flows. Unlike the steady and almost automatic soaring of the vulture, that of the albatross involves continuous voluntary maneuvering and control regulation. Yet, so perfectly adapted in structure and instinct is the albatross to its particular mode of flight that it performs its cycle with a geometrical precision of amazing exactness. We shall in this paper examine in detail the physical processes by which the albatross is able to accomplish such flight and to remain at sea for years at a time, covering untold thousands of miles, all without any significant expenditure of its own muscular energy for propulsion.

The paper commences with a description of typically observed soaring patterns and other pertinent flight characteristics of the albatross. Then using these observations as a basis, an idealized soaring cycle is

---

*Superscript numbers refer to references listed in Appendix A-1, page 99.

constructed, for purposes of analysis, which contains the four basic phases utilized in accomplishing dynamic soaring flight in shear layers. The mechanics of each of these four basic phases is subsequently investigated in detail, and the fundamental equations governing the motion and energy interchanges are formulated. The factors in the resulting equations, expressed in terms of the structural and aerodynamic parameters of the albatross, are analyzed as the development proceeds in order to delineate their relative importance and significance in the ecological regime of the bird. It is shown how the albatross can combine the basic phases of the ideal cycle with various secondary flight phases to obtain almost any desired flight path for travel purposes. Various related facts of importance in the general ecology of the bird are then discussed in light of the aerodynamic analyses, and ecological comparisons of land and ocean soarers are made on the basis of the aerodynamic requirements for the two different types of soaring flight. The mechanics of dynamic soaring in gusts, as used by some land birds, is also discussed and the exact correspondence to shear layer soaring is pointed out.

The basic equations and other relations developed in the aerodynamic analyses, as will be pointed out, require for their complete evaluation a considerable amount of quantitative field measurements and other data not presently available. The analyses yield, nevertheless, a clear picture of the physical factors involved in albatross ecology and bring into focus the specific field researches needed to establish the overall ecology of the albatrosses on a complete and comprehensive basis. It is shown that, when sufficient field data are obtained, the aerodynamic equations can be completely solved in a manner which will yield not only the quantitative aerodynamic properties of the albatross but also the effective properties of the wind shear layer in which the bird soars.

"Aeroecological" studies such as the present one necessarily involve the mechanical aspects of flight, and hence require full utilization of the principles and terminology of aerodynamics, together with the associated mathematics. The present paper involves a considerable amount of mathematical analysis which, although straight forward, may still prove somewhat abstruse for biologists unfamiliar with this discipline. In order to alleviate undue obscurity, therefore, the mathematical developments and derivations are presented in considerable detail, and the physical significances of the analyses are indicated as explicitly as possible. A large number of sketches and diagrams is included in order to increase the clarity of the presentation.

A number of appendices are presented at the end of the paper which give additional information and explanations intended to supplement the material in the main text. Particular attention is called to Appendices A-2, A-3, and A-4 which contain a definition list of the most frequently used symbols and discuss the classification basis and aerodynamic fundamentals of natural soaring flight. More detailed discussions of aerodynamic principles and terminology are available from standard aerodynamics textbooks. Appendix A-5 contains a classification and description of the various species of albatrosses comprising the order Procellariiformes.

The possibility of emulating natural dynamic soaring by use of sailplanes has long been an intriguing question to soaring enthusiasts. Consequently, Appendix A-6 has been included in order to indicate the application of the results of the present study on albatross soaring to establish the feasibility of dyanmic soaring flight by man. Unfortunately, the resulting conclusions make it appear doubtful that any generally useful degree of dynamic soaring by man will be developed, at least in the foreseeable future, despite a number of theoretical possibilities.

## II. OBSERVED CHARACTERISTICS OF ALBATROSS FLIGHT

This section presents a brief description of some of the more characteristic features of albatross flight. The descriptions given are based primarily on observations of the Wandering Albatross (Diomedea exulans), an albatross of the southern hemisphere and the largest flying sea bird. The essential features of this bird's flight appear common, however, to all the albatrosses and apply in principle to the other Procellariiformes which practice dynamic soaring.

Since the Wandering Albatross is a very large bird, its flight is easily followed at sea, even at considerable distances, and the flight patterns have been described by many observers. The remote areas of the south seas inhabited by exulans and most other albatross species (i.e. between 37° and 65° south latitude) were once rather heavily traversed by sailing vessels making use of the westerly winds prevailing there, and some useful information of a general nature has been compiled on the albatrosses of the region. In addition, a number of more systematic field studies and surveys of albatrosses have been carried out by various investigators, for example Murphy,[4] Mathews,[5] Richdale,[6] Dixon,[7] Hutton,[8] Idrac,[9] and Jameson.[10] Idrac, however, appears to be the only investigator to study albatross soaring flight from a truly technical standpoint.

Appendix A-5 (page 100) gives the classification scheme of the albatrosses and notes the principal ranges of the various species.

### SOARING FLIGHT

The basic requirement for albatross soaring is a brisk and steady wind, and albatrosses are found only where this condition is highly prevalent. In addition, the air space immediately above the surface must be free of all obstructions since the bird's flight is performed almost entirely within a thin boundary layer of air extending only 55 to 60 feet above the surface. These requirements are met only over the open sea where the relatively smooth water surface allows the prevailing winds to move with but a small amount of resistance, and where vast areas of unobstructed flight space exist. Using the practically boundless energy of the sea shear layers, the albatross, on its efficient wings, traverses vast expanses of sea from dawn to dusk in endless search of the squid and shrimp which form its diet. With the exception of the breeding season, when it returns to the small isolated islands where it nests, the albatross is truly pelagic, remaining far at

sea. There it ceaselessly orbits within the narrow wind shear layer above the water, alighting only briefly to claim its food from the sea.

## The Basic Flight Pattern

Let us first consider the basic flight pattern typical of albatross soaring at sea. The wind is brisk; the air well above the surface is moving with a speed of 40 miles per hour or more. Just above the surface of the water, however, the wind speed is considerably reduced, say only 10 miles per hour or less, having been slowed by the retarding action of the water surface. This region wherein the wind speed varies with altitude from a minimum at the surface to that of the full wind force at some distance above the water constitutes the important shear layer within which all soaring occurs.

We join the albatross at a point in the cycle when it is very near the surface, moving at high speed directly into the wind, and climbing rapidly as it progresses to windward. The bird continues to climb, rapidly losing speed as it rises, until it reaches an altitude of some 50 feet, where its ground speed to windward (i.e. relative to a stationary observer) has considerably decreased. It then executes a turn of 180° directly to leeward by smoothly banking its wings. During this turn the bird is observed to accelerate very rapidly so that, at the completion of the turn, it is moving to leeward at a very high rate of speed.

During all of the climb and turn, the bird has held its wings rigidly outstretched at their maximum span, but now the wings are suddenly folded into the shape of a shallow W and, simultaneously with this wing flexing, the bird commences a steep glide, almost a dive, toward the surface. The bird picks up still more speed during the dive and ends the leeward plunge with a sharp pullout just above the water surface. At this point, the albatross is moving with the maximum absolute velocity of its cycle.

Upon completion of the dive, the bird again turns into the wind, but this turning phase may take on one of two forms, depending upon the flight path the bird wishes to follow: it may immediately execute a full 180° turn into the wind, or it may perform only a partial turn, skim along a wave trough for some distance, and then turn into the wind. In either case, the turns are usually very steep, being made close to the surface with the wings banked to an almost vertical position. In fact, the turns are performed so close to the surface that the tip of the lower wing often cuts the water during the maneuver. At the completion of the low-level turn, the bird is once again moving directly into the wind at high speed, and, sometimes using the air flow off the crest of a wave for an initial boost, it commences another windward climb to begin a new cycle.

This circuitous pattern of climbing, turning downwind, diving, and turning upwind constitutes the basic flight cycle of the albatross. It permits the bird to remain continuously and effortlessly airborne, and to scan vast areas of sea in its search for food. By judiciously and instinctively varying the duration of each step in this cycle according to the

strength and direction of the prevailing wind, the albatross is able to regulate its resultant flight pattern so as to follow almost any desired path over the sea.

## Variations of the Basic Pattern

When the wind conditions are adequate, the albatross is capable of accomplishing a wide variety of useful soaring patterns in addition to the simple basic flight cycle described above. Many of these patterns may appear quite irregular and complex, depending upon the particular locomotion needs or desires of the bird at a given time. The four essential phases of the basic flight pattern, however, are implicitly contained in the total motion, each in its proper order, although the duration of each phase is subject to considerable variation. By injecting periods of simple gliding or coasting flight between the basic phases, by properly regulating the duration of each phase, and by performing the basic turns in the same or in opposite directions, consistently or alternately, the albatross constructs flight patterns which allow it to travel in practically any desired direction.

Following a leeward glide, or dive, the albatross may execute only a partial turn at low level and may skim along a wave trough for considerable distance before turning into the wind, as already mentioned. By always turning in the same direction along the waves, the bird makes rapid progress in a direction approximately transverse to the wind. In an analogous manner, the bird may perform a brief lateral coast or glide at high altitude following a windward climb. In some instances a bird may actually perform a lateral dive across the wind, instead of the usual leeward dive, in order to increase its lateral and windward rate of travel. Variation of the relative durations and speeds of the basic climb and dive phases results in the bird's making net progress to either leeward or windward, as the case may be. So skillful is the bird in performing the complex system of required motions that it can follow ships with ease and certainty, in all except very strong headwinds. The course of the ship relative to the prevailing wind is usually of little consequence to the bird provided the direct headwinds are not too strong. Albatrosses frequently follow vessels for several days at a time, disappearing at night, but reappearing off the stern again at daybreak.

The travel of an albatross in a given direction is usually accomplished by very indirect means, much like the tacking of a sailboat, and the bird performs a relatively complex pattern of motions in order to proceed along a particular mean course (such as in following a ship). For every mile of net displacement in a particular direction, the bird may have traversed many times that distance in actual flight path. This "excess" motion involved in albatross flight is not "wasted," however; it continuously carries the bird over fresh areas of water, the surface of which it closely scans for possible food.

It should be noted that observations of albatross soaring at sea must normally be made from ships, and the very presence of an observer's vessel

may influence the type of flight patterns observed. This situation exists because the birds are attracted by the vessel and their flight patterns are the result of their conscious endeavor to follow or remain in the vicinity of the ship. Thus, the flight patterns observed from a vessel are not necessarily those which the bird would pursue under completely natural conditions at sea; nevertheless, they clearly exhibit the basic phases involved in the dynamic soaring of the albatross, and illustrate the versatility of the bird's flight capabilities.

The presence of a vessel often allows the albatross to practice modes of flight which are quite foreign to its normal patterns. Such modes involve static soaring in the updrafts generated by the superstructure (or sails) of the vessel in its motion relative to the air. Albatrosses are able to statically balance themselves in such currents for long periods of time and to maintain a practically constant position relative to the ship. In coastal waters, gulls are routinely observed taking similar advantage of this free energy source. Such flight is exactly analagous to the soaring of land birds in the declivity currents existing on the windward slopes of hills.

## Limiting Flight Conditions

The amazing flight powers of the albatross are entirely dependent upon the presence of adequate wind, and the bird becomes incapable of sustained flight when the wind dies. Idrac[9] states that dynamic soaring ceases at wind speeds below 10 to 11 miles per hour at the surface and the bird must then resort to flapping flight to remain airborne. The relatively weak wing muscles are quite incapable of producing sustained flight of so large a bird, however, and during periods of calm the albatross alights and remains resting upon the surface, waiting the return of the wind. Some albatross species make almost habitual use of a few wing strokes at the termination of the windward climb. This is particularly characteristic of the species Diomedea nigripes, and may indicate a slight aerodynamic deficiency in ability to use shear layers of only moderate strength.

When the wind becomes excessively strong, such as in violent gales, dynamic soaring also ceases. The birds appear able to fly in very strong winds for a time, but as the gale intensifies, the birds disappear and are seen no more until the storm subsides. Idrac[9] says that the albatross is swept to leeward by winds exceeding 43 miles per hour.

Whatever the flight limitations placed on the albatross by the extremes of wind conditions, the continued survival of the bird is ample testimony that the frequency of occurrence of winds in the usable strength range is quite adequate for the bird's practical flight needs.

## Flight Along Wave Fronts

When moderate to strong winds blow over the sea, waves of appreciable amplitude are generated. The air moving over these wave forms can create updrafts of considerable strength on the windward sides, much like those

caused by hills on land. When these wave-generated upcurrents are strong enough, sea birds can use them for accomplishing static soaring. Even in cases where the upcurrents are insufficient to completely support the heavier birds like the albatross, flight energy can still be gained by the bird, and its flight path considerably lengthened by gliding or skimming through the upcurrent region, parallel to the waves. The low altitude skims characteristic of the albatross are an example of the use of this energy source. Other water birds, such as the pelicans and shearwaters, make frequent use of the waves by coasting along on the upcurrents as far as possible, and supplying additional energy as required by periodically flapping their wings.

## LANDING AND TAKE-OFF

While the albatross is capable of some degree of flapping flight, the use of the wings for this purpose is relatively rare compared to soaring. So perfectly adapted is the bird to the exploitation of the wind that the auxiliary power available from flapping is usually called upon only for the special demands of the take-off. Even in this case the bird appears to make a special effort to avoid the need for flapping its wings by utilizing the wind whenever possible. Some flapping-type wing motions may also be used in the landing process, but these motions are in the nature of a control or braking action. The albatross is very specifically designed for rapid sailing flight in the free wind over unobstructed seas. Flight at other than this "design" condition imposes some very difficult and often dangerous operational problems for the bird.

### Landing

Albatrosses alight frequently upon the surface to feed when the wind is strong. Not only is the landing much easier when the wind is brisk, but the more difficult process of the subsequent take-off is greatly simplified. In order to land under strong wind conditions the bird simply turns into the wind at the proper altitude level and, having lost a large part of its horizontal speed relative to earth, settles into the water. When the wind is weak, the landing is accomplished in much the same manner as that used by ducks. The large webbed feet are used as hydroplanes and the bird "planes" for some distance over the water before coming to rest. The ratio of wing span to body length for most albatrosses is about 5.5 so that the bird has very little room for strong wing flapping during landing (or take-off). Consequently, without the aid of the wind, the bird must make its landing approach at a relatively high ground speed, and depends upon its feet for the necessary braking action. The difficulty of landing results from the high value of the minimum or stalling airspeed of the bird, about 30-35 miles per hour.

When aided by use of the feet, landings on water under weak wind conditions are not particularly dangerous, although somewhat clumsy. High speed landings on the beaches of the nesting islands, however, pose a serious threat to the bird. Without the aid of the wind the bird must

"touch down" at 30 miles per hour or more and undergoes a rather violent impact with the ground. Since the feet are useless under such conditions, the bird takes the brunt of the impact on its well-feathered breast and often does a complete somersault before coming to rest and folding up the long wings. Such hard landings can be quite dangerous and may result in broken bones.

### Take-off

Take-off at sea is easily accomplished with the aid of the wind. In many cases when an albatross alights to feed, it remains on the surface only briefly and does not fold its wings. Paddling vigorously with its large webbed feet, it makes its way up the face of the nearest wave and launches itself into the wind from the crest. Without sufficient wind, the bird holds its huge wings fully extended and with violent leg action uses its feet to drive it across the water. Some 100 yards may be required before the bird is able to become airborne. The wings may be flapped vigorously through a small arc, but effective propulsive flapping does not become possible until the albatross has lifted clear of the water.

So difficult a process is the take-off for the albatross in low-speed winds that some species nest only on high prominences where they can take-off simply by jumping into the air. Those which nest on the beaches and lowland areas of islands usually take off only when the wind is sufficient. The birds select only those islands which offer long sloping beaches relatively free of surrounding shrubs and other obstructions. Even then, the difficulty in taking-off from land is usually insurmountable unless the wind is adequate; for the short, widely-spaced legs of the albatross are quite unsuited for rapid locomotion on land.

The foregoing discussion has been but a brief description of the most typical characteristics of albatross flight as observed in field studies. While a number of interesting descriptions of albatross flight patterns and habits appear in the literature, only a few are sufficiently detailed or accurate enough to be of any real value for technical flight studies. The available observations and field data are adequate for establishing the general mechanisms of albatross soaring but a great deal of additional quantitative field data must be obtained before we can specify the exact values of the various parameters which govern albatross soaring.

## III. THE AERODYNAMICS OF ALBATROSS FLIGHT

This section treats the aerodynamic mechanisms of albatross flight in considerable detail. Primary attention is devoted to the mathematical formulation and analysis of the dynamic soaring mode; but certain auxiliary modes of importance, such as landing and take-off, and wave soaring, are also discussed. The ecological significance of some of the more important aerodynamic results is pointed out as the development proceeds; additional ecological factors are discussed in the following Sections IV and V.

## THE BASIC SOARING CYCLE

The essential features of a typical dynamic soaring cycle were briefly described in the preceding Section II. It was noted that, although a broad range of variations exists in the individual phases comprising the total cycle, with some phases at times approaching vanishing duration, the sequence of the four basic phases is always the same. By consciously varying the duration and intensity of each phase of the cycle, the bird can regulate its displacement speed and direction so as to travel along almost any intended flight path.

Let us now consider the structure of the general soaring cycle in somewhat finer detail. For purposes of analysis, we divide the total cycle into four primary and two secondary phases. As indicated in Fig. 1, the primary phases, which constitute the basic soaring cycle, are: (1) the

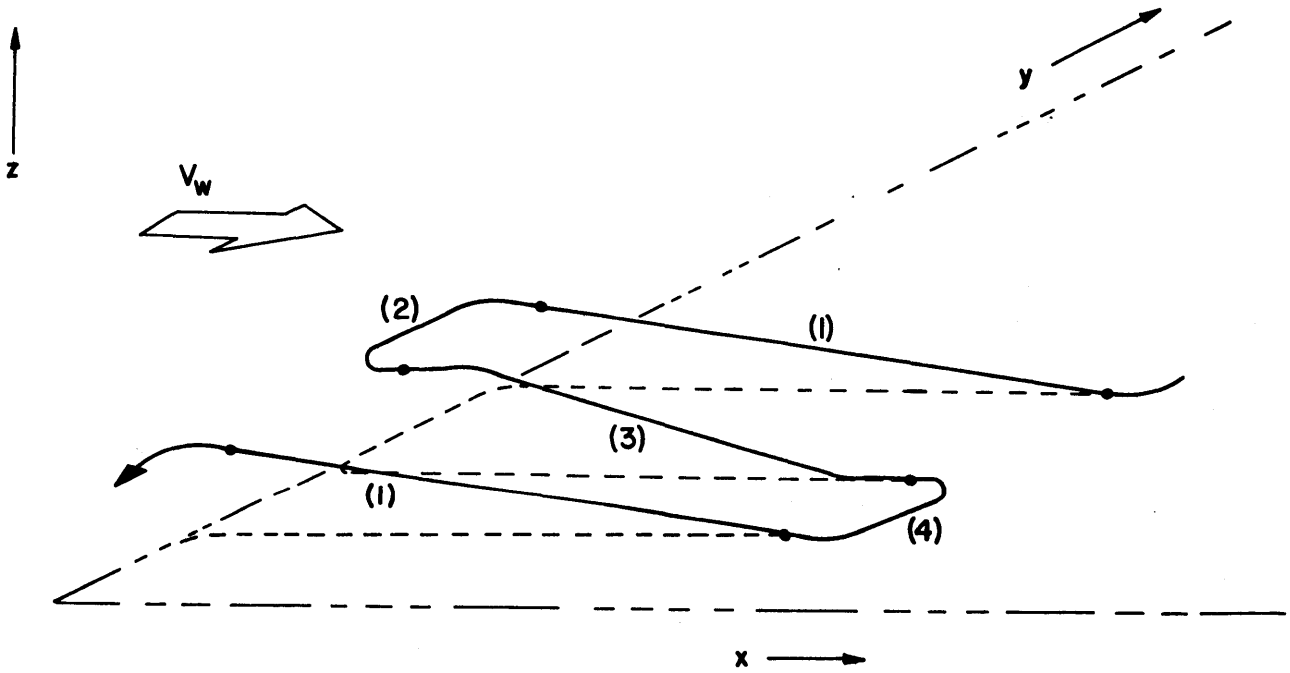


Fig. 1

windward climb, (2) the high altitude turn to leeward, (3) the leeward glide, and (4) the low altitude turn to windward. The secondary phases (Fig. 2) are (a) the high altitude coast or glide across the wind (following the windward climb), and (b) the low altitude coast across the wind (following the leeward glide). Each of the four primary phases involves a different type of aerodynamic action; the secondary phases are essentially constant-altitude glides spaced between the primary phases in order to

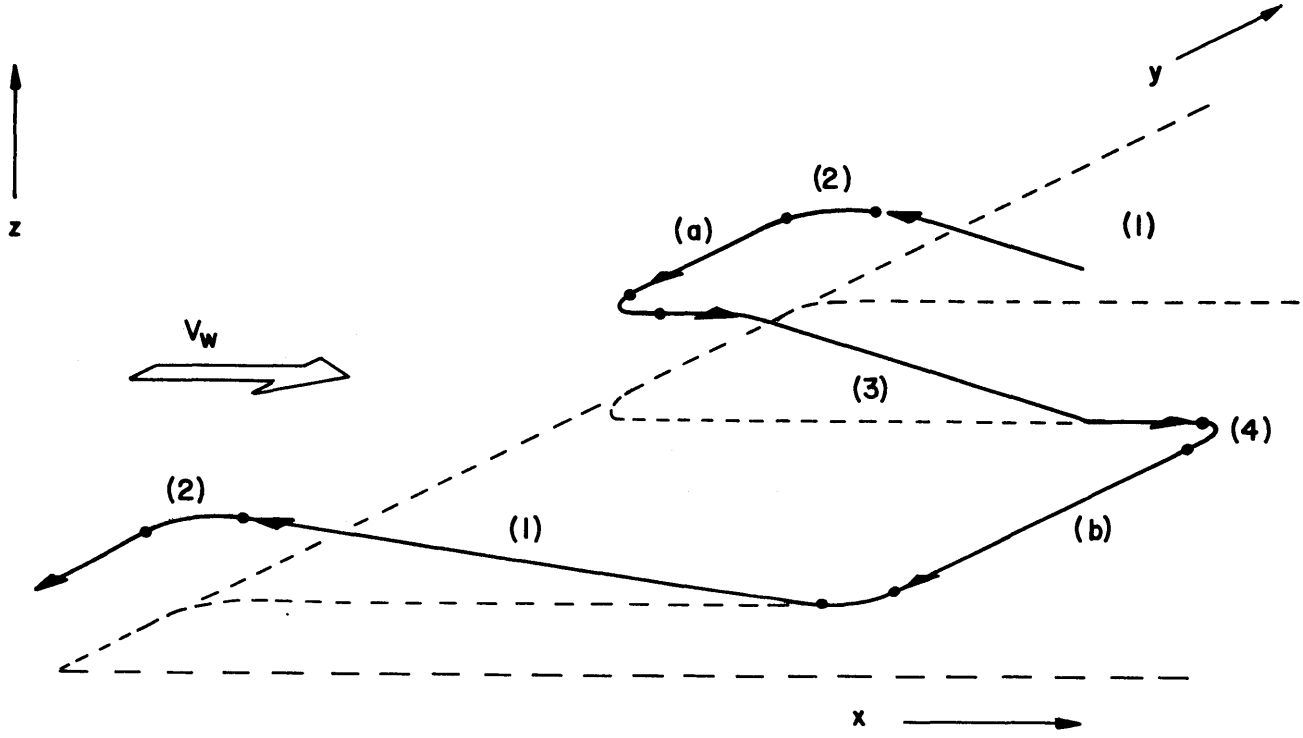


Fig. 2

control the mean course of the bird relative to earth. The durations of the secondary phases can be controlled to a considerable extent by the bird, but the maximum allowable durations at any particular time are governed by the energy available from the wind, as will be discussed later.

In order to more clearly illustrate the essential features of the aerodynamics involved, we shall for the present assume that the secondary coasting phases are absent, so that the total cycle consists only of a sequence of the four primary phases, as shown in Fig. 1. We shall refer to this simple idealized sequence as the basic cycle of dynamic soaring; it contains all the processes essential to flight in shear layers. The conditions at the end of one basic phase are coincident with those at the beginning of the following phase and a smooth, continuous cycle is thus produced. The bird's flight pattern consists of a periodic repetition of the simple basic cycle.

Starting at the beginning of the windward climb, the bird faces into the wind and, utilizing its existing supply of horizontal momentum to oppose the decelerating aerodynamic forces caused by its motion relative to the air, it rises to a typical height of 40 to 50 feet (Phase 1). Then the bird banks its wings and executes a turn to leeward, undergoing a rapid acceleration, relative to the earth, throughout the turn (Phase 2). Upon completion of this high altitude turn to the downwind direction, the bird commences a rather steep glide or dive and continues to accelerate along its glide path, for some distance (Phase 3). This high speed dive

continues until the bird is very near the water. Then, rolling into a nearly vertical bank, the bird simultaneously terminates the dive and turns sharply into the wind (Phase 4), to begin the subsequent windward climb.

The motion of the bird, relative to a stationary observer, is one which involves continuous acceleration. In the windward climb, the bird starts out with a high velocity (relative to earth), but this diminishes as the bird climbs. During the turn to leeward, the bird picks up a large amount of speed, and still more during the leeward glide. At the termination of the glide the bird has attained its maximum absolute velocity. Turning to windward at low altitude, the bird loses some velocity even before beginning the next climb (as a result of the finite wind velocity existing near the surface), and continues to decelerate throughout the climb of the subsequent cycle.

The fact that the albatross is in a continuous state of acceleration introduces considerable complexity into the aerodynamic analysis of the flight phases. However, as will be shown later, it is only by means of such velocity fluctuations and momentum changes that the bird can extract the wind energy necessary for its amazing endurance flights.

## ANALYSIS OF THE BASIC CYCLE

The analysis of the basic dynamic soaring cycle will be accomplished by considering the aerodynamics of each of the four primary phases separately at first, and the results will then be integrated to obtain the mechanics of the complete cycle.

### Properties of the Shear Layer

As a prelude to the discussion of the flight mechanics, it is desirable to consider briefly the general nature and more important properties of ocean shear layers. The properties of the shear layer play a critical role in dynamic soaring flight, for it is only by virtue of the difference in wind speed existing between the top and bottom of this layer that useful dynamic soaring is rendered possible. For brevity, we shall discuss only those properties of shear layers which are essential for the following flight analyses.

Aerodynamic Boundary Layers.- When air flows over a flat surface, the random motion of the molecules results in continuous collisions with the surface and most molecules rebound with less velocity (or momentum) in the flow direction than they had prior to the collision. These slower-moving molecules subsequently collide with other molecules farther above the surface, and consequently reduce the streamwise momentum of the more distant flow. As a result of the migration or diffusion of the low-speed (in free-stream direction) molecules away from the surface, a "boundary layer" of slowly moving air is created. Within this layer, the velocity increases from a value of zero at the surface to the value of the free flow above the layer. The effects of this molecular migration (viscous effects) are generally confined to the vicinity of the surface for fluids such as air

which have small viscosity values. The layers of air within the boundary flow slide smoothly over one another, and each exerts a retarding shear stress on the one above it. This viscous stress is the result of the low-momentum molecules of the lower layer migrating into the upper layer and slowing it by impact. Above the boundary layer, the velocity is constant with height and no shearing stresses exist. We shall not be concerned here with the nature of the viscous stresses, but only with the resulting variation of velocity in the flow direction with height.

The thickness of the aerodynamic boundary layer increases with distance in the direction of flow, as the mass of air which has been slowed down by the viscous stresses accumulates. For a laminar boundary layer, such as described above, the boundary layer thickness $\delta$ at any distance $x$ from the leading edge of the surface is given by

$$\delta \propto \left(\frac{\mu}{\rho V}\right)^{1/2} \times^{1/2} \qquad (1)$$

where

$\rho$ = density of the air
$\mu$ = viscosity of the air
$V$ = speed of flow outside the boundary layer

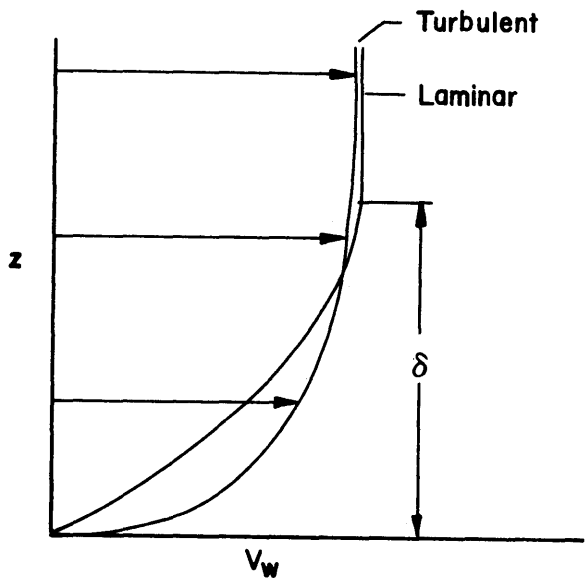


Fig. 3

Eq. (1) is valid until $x$ exceeds a certain critical distance; the smooth laminar flow within the boundary layer then becomes unstable and breaks up. The flow becomes very turbulent and $\delta$ increases considerably. In the turbulent layer, continuous mixing of the flow occurs and momentum transfer is accomplished by relatively large masses of air being transported up and down by turbulent eddies, instead of by the simple migration of independent molecules as in the laminar layer. The average velocity (in the flow direction) has a considerably different distribution in the turbulent boundary layer than in the laminar layer. Fig. 3 shows, schematically, the difference in the velocity profiles for the two cases. The turbulent layer has a much fuller profile near the surface due to the transport of high-velocity air from the free flow down into the lower portions of the layer, thus energizing it. In general, any mechanism which tends to induce turbulence or mixing in the boundary layer will result in fuller velocity

profiles near the surface. Due to the extremely large scale and surface roughness involved in the flow of wind over earth surfaces, earth boundary layers will generally be similar in form to turbulent aerodynamic boundary layers.

Large-Scale Boundary Layers Over Land. - The discussion of the small-scale aerodynamic boundary layer given above may be qualitatively applied to the large-scale boundary layers or shear layers generated by the natural wind in moving over land surfaces. In the case of earth boundary layers, however, the flow conditions are somewhat different in that very large obstructions protrude above the surface proper, and the relative degree of surface roughness is therefore very large. The air flow around trees, buildings, hills, and other surface obstructions generates heavy turbulence and the momentum of the air near the surface is greatly reduced; this momentum loss occurs in addition to that produced by the simple frictional retardation. The mixing of this low-velocity surface-air with the higher air strata is increased by thermal convections originating at the surface, and boundary layers of relatively great thicknesses are formed. The complexity of the variables governing the properties of land boundary layers generally precludes an accurate analytical treatment, and the quantitative properties of such flows are usually determined by experimental means.

A large number of experimental investigations have been carried out in past years on land boundary layers, primarily because of the need to know the wind velocity profiles for use in estimating wind loads in the design of buildings and other structures. As a result of these studies, it has been found that the wind profile $V_w(z)$ (wind speed $V_w$ as a function of altitude $z$) within the boundary layer can be fairly well represented by the relation

$$\frac{V_w}{V_w^*} = \left(\frac{z}{z^*}\right)^p \qquad (2)$$

where $V_w^*$ is the value of $V_w$ at the altitude $z^*$ (essentially the upper limit of the boundary layer). In general, $p$ and $z^*$ depend very much on the roughness of the terrain and on the turbulence of the air (which in turn depends upon the convective stability of the lower atmosphere). When the atmosphere is very unstable, the low-speed air near the surface is rapidly transported upward and mixed with the faster moving air of the free flow. Fast-moving air descends to replace the surface air and thus energizes the boundary layer. The value of $p$ in such cases tends toward zero and the boundary layer becomes very full near the surface. For smooth, stable airflows, $p$ tends toward 1.0, and the velocity profile $(z)$ becomes linear.

Fig. 4 shows a plot of the wind profiles given by eq. (2) for three types of terrain for which $p$ and $z^*$ were experimentally determined from a large number of actual wind profile measurements.[11] For purposes of comparison, the wind speed is expressed as a fraction of the wind speed existing at $z = z^*$. The profiles of Fig. 4 reveal some interesting facts. The boundary layer thickness $z^*$ decreases as the surface roughness

decreases. The decrease in $z^*$ is approximately proportional to the decrease in relative roughness. For the roughest terrain, $z^* = 1700$ feet, whereas for flat open land the layer is only about 900 feet thick.

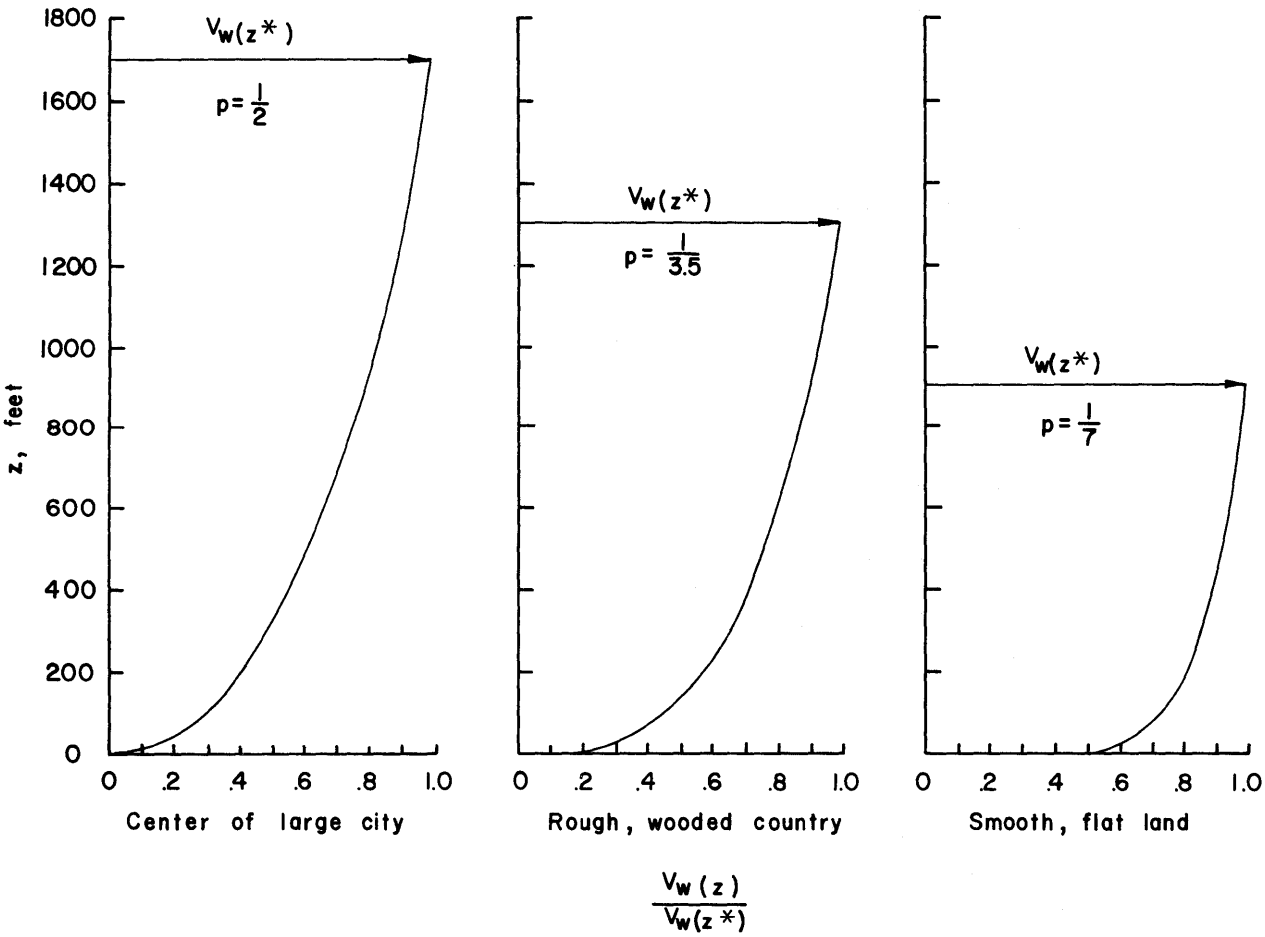


Fig. 4

The exponent p also decreases with decreasing roughness, so that the wind profiles for the smoother terrain are much fuller near the ground. In fact, the wind speed over open grassland attains 75 per cent of its maximum value at $z^*$ within the first 12.5 per cent of the boundary layer. This leads to very large wind gradients $dV_w/dz$ near the surface. The expression for the wind gradient, obtained by differentiating eq. (2), is

$$\frac{dV_w^*}{dz} = p \frac{dV_w^*}{z^{*p}} z^{p-1} \qquad (3)$$

The profiles of Fig. 4 are for neutrally stable atmospheric conditions (i.e. the lapse rate is adiabatic). For unstable conditions, p would decrease and each of the profiles would become fuller at the lower levels.

Large Scale Boundary Layers Over Water. - Experimental data for wind-generated boundary layers over water are relatively scarce, probably due to the fact that little practical need has existed for such data in the past. However, some idea of the nature of ocean boundary layers, or shear layers as we shall call them, can be obtained by extrapolating the trends given by data for land conditions. By comparing the profiles of Fig. 4, it can be expected that the wind profile for smooth water surfaces will be similar to that for smooth land, but with still smaller values for p and z*. The ocean shear layer will then possess a fuller velocity profile with very large gradients $dV_w/dz$ near the surface. It may also be expected that, under certain sea conditions,* the air near the water surface will be somewhat unstable due to its water vapor content, and this will lead to still smaller values of p, fuller profiles, and larger wind gradients. Thus, it would appear that for moderate wind speeds ($V_w^* \leq 35$ to 40 miles per hour), z* will be small, say on the order of a hundred feet or so, while the velocity reaches almost the maximum value of the free wind within a fraction of this distance, say 20 to 50 feet. These values are based on extrapolations of data for land surfaces, but they appear realistic in view of the data presently available for water shear layers ($p = 0.095$)[11] and from the observational data on actual flight characteristics of the albatross. These values of p and z* lead to relatively high shear rates $dV_w/dz$ near the surface [eq. (3)].

A fundamental difference exists, however, between land and water surfaces in regard to the action of the wind. On land, the surface shape and roughness (except for sand deserts) are independent of the wind speed $V_w$; but on water, the surface is unstable under shear and the wind generates wave patterns which react with the adjacent airflow to change its pattern. The surface distortion and altered airflow react with one another until, for a given wind speed, some equilibrium condition between surface shape and air-flow pattern is established. At low to moderate wind speeds, the water surface may be considered as essentially planar, and the shear layer profiles will be similar to those for smooth land. This condition will in all probability be the usual case existing for the normal range of wind speeds used by the albatross. It should be noted, however, that the waves themselves extract energy from the wind and thus reduce its momentum; this

---

*It is assumed here that the water temperature is equal to or greater than the air temperature. If the water is colder than the air, the boundary layer will of course be stabilized. The air-water temperature ratio may possibly exert a strong influence on just where the albatross can soar, as a result of its effect on the structure of the shear layer.

action is equivalent of course to increasing the surface roughness so far as the shear layer profile is concerned.

As the wind increases to higher speeds, larger waves are produced. These larger wave forms are approximately symmetrical, however, and have relatively gentle curvatures so that the air glides smoothly over them; the shear layer is still but slightly affected. (Fig. 5). When the wind becomes very strong, the airflow ultimately separates on the leeward side of the waves, the reverse airflow on this side causing them to develop a sharp crest, and the whole flow becomes extremely turbulent (Fig. 6). The air is filled with spindrift and spray torn from the wave crests. Under these conditions, the surface roughness would be relatively large and the high degree of turbulence would make dynamic soaring very difficult.

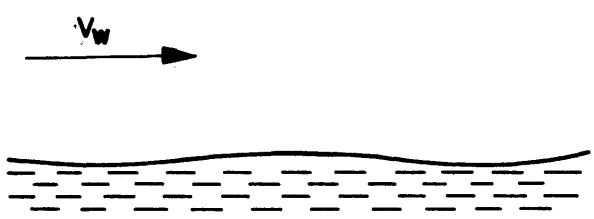


Fig. 5

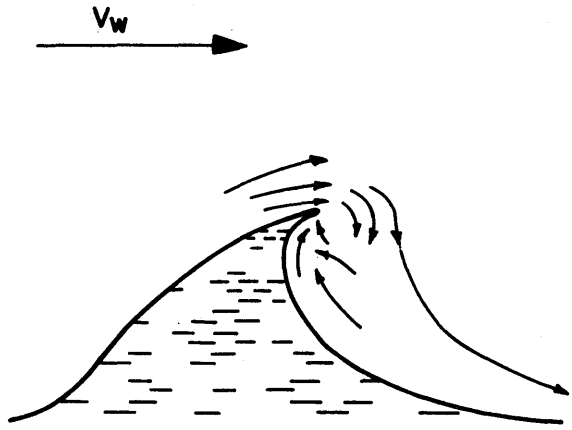


Fig. 6

The interactions between the water surface shape and the associated airflow would appear to have only minor effects on the soaring of albatrosses under normal conditions. In very high winds, however, the expected turbulence in the shear layer region would impose definite limits on the bird's soaring capability. Certain details of the surface wave – airflow interactions will be discussed later in this section. We shall assume in our present analyses that the wind profiles existing are those for relatively smooth water, or moderate wind speeds.

## The Windward Climb

From an aerodynamic standpoint, the windward climb is perhaps the most complex of the four basic flight phases. The primary function of the windward climb is to carry the bird from the region of low velocity near the surface to the region of high wind velocity at the top of the shear layer. Although some energy is taken from the wind during the climb, this phase does not provide the principal energy supply for dynamic soaring.

Formulation of the Equations of Motion. - Let us first consider the force and velocity systems associated with the windward climb. For this purpose we employ a set of orthogonal space coordinates x, z with origin

at the water surface and with axes oriented normal and parallel to the surface, as shown in Fig. 7. The flight path generated by the climb is assumed to lie in the x, z plane. The positive direction of the x-axis is taken to the right. The bird is represented in Fig. 7 as a point at altitude z above the surface, and moving to the left and upward with absolute velocity components (i.e. relative to earth) of $\hat{u}$ and $\hat{w}$. All vectors (force and velocity) are taken as positive in the positive direction of the coordinate axes. Thus, if the horizontal velocity relative to earth is denoted in Fig. 7 by the vector $\hat{u}$, then the magnitude u of this vector is a negative quantity. Since the vector $\hat{u}$ is directed to the left during the climb, $u = dx/dt$ is negative. The wind velocity relative to earth is denoted by the vector $\hat{V}_w$ and is positive as shown in Fig. 7. The wind velocity is an increasing function of altitude $\hat{V}_w(z)$ within the shear layer ($0 \leq z \leq z^*$), and maintains a constant value $V_w(z^*)$ above the shear layer ($z \geq z^*$). The velocity profile $V_w(z)$ is assumed to be independent of x, and is thus identical at all stations along the x-axis.

The bird is acted upon by two forces: the resultant aerodynamic force $\hat{R}$ due to the air pressure and frictional stress distributions over its wings and body, and the weight force $\hat{W}$ due to gravity. The weight force vector is constant in magnitude and direction, always acting in the negative direction of the z-axis. The aerodynamic force $\hat{R}$, however, depends upon the magnitude and direction of the resultant velocity $\hat{V}_R$ of the air relative to the bird. The aerodynamic velocity $\hat{V}_R$ is given vectorially by

$$\hat{V}_R = \hat{V}_w - (\hat{u} + \hat{w}) \qquad (4)$$

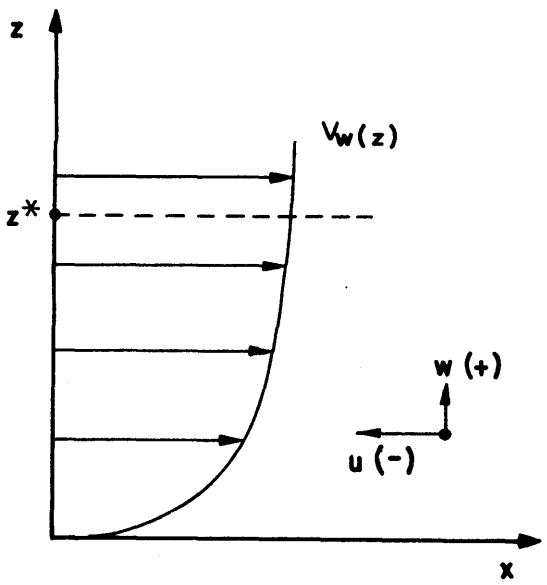


Fig. 7

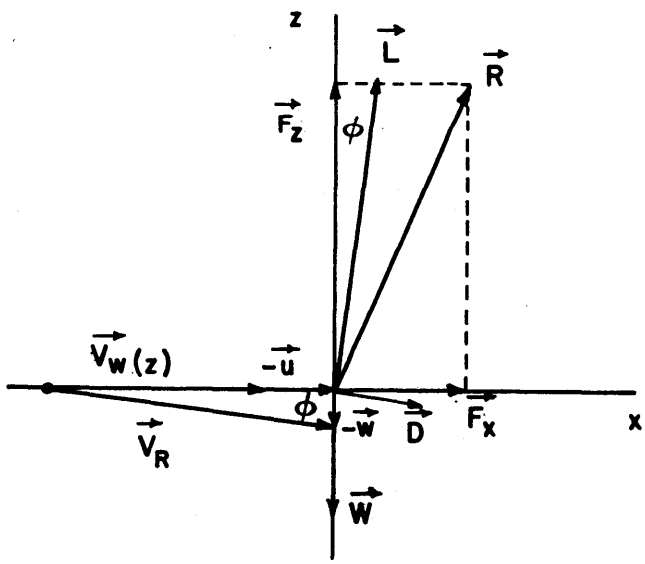


Fig. 8

Fig. 8 shows the various vector relationships. The aerodynamic force $\hat{R}$ is composed of the lift $\hat{L}$ and drag $\hat{D}$ of the bird.

$$\hat{R} = \hat{L} + \hat{D} \tag{5}$$

As is customary, $\hat{L}$ and $\hat{D}$ are taken as the force components normal and parallel, respectively, to $\hat{V}_R$. Referring to Fig. 8, it will be noted that $\hat{V}_R$ is inclined to the x-axis by an angle $\varphi$, due to the fact that the bird is climbing with the velocity $\hat{w}$. Thus, the lift vector will be inclined to the z-axis by the same angle, resulting in a component of the lift acting along the x-axis. This component of lift acts to decelerate the bird in the horizontal direction. The drag vector will have a component acting in the negative direction of the z-axis.

For purposes of analysis, it is convenient to resolve the resultant aerodynamic force $\hat{R}$ into the components $\hat{F}_x$ and $\hat{F}_z$ along the x- and z-axes, respectively. Thus, we have, using the unit vectors $\hat{i}$ and $\hat{k}$ for the x- and z-directions,

$$\hat{F}_x = (\hat{R} \cdot \hat{i})\, \hat{i} = [(\hat{L} + \hat{D}) \cdot \hat{i}]\, \hat{i} \tag{6}$$

$$\hat{F}_z = (\hat{R} \cdot \hat{k})\, \hat{k} = [(\hat{L} + \hat{D}) \cdot \hat{k}]\, \hat{k} \tag{7}$$

The magnitudes of these components are therefore given by

$$F_x = L \sin \varphi + D \cos \varphi \tag{8}$$

$$F_z = L \cos \varphi - D \sin \varphi \tag{9}$$

Equating the net force components to their respective time rates of change of momentum (Newton's second law) we obtain

$$F_x = \frac{W}{g} \frac{du}{dt} = (L \sin \varphi + D \cos \varphi) \tag{10}$$

$$F_z - W = \frac{W}{g} \frac{dw}{dt} = (L \cos \varphi - D \sin \varphi - W) \tag{11}$$

where $W$ is the bird's weight, $g$ is the gravitational acceleration, and $t$ denotes time. $W/g$ is of course the mass of the bird. The positive terms in eq. (10) denote that the force $\hat{F}_x$ is positive when $du/dt$ is positive, that is, when $u$ is increasing (positively) with time.

Equations (10) and (11) involve time as the independent variable, but since the wind speed is a function of altitude $z$, it is desirable to express these equations as functions of $z$ also. Using the definition of the climbing speed

$$w = \frac{dz}{dt} \tag{12}$$

we obtain

$$\frac{du}{dz} = \frac{g}{W} (L \sin \varphi + D \cos \varphi) \, w^{-1} \tag{13}$$

$$\frac{dw}{dz} = \frac{g}{W} (L \cos \varphi - D \sin \varphi - W) \, w^{-1} \tag{14}$$

These constitute the exact equations of motion for the bird during the climb phase. The trigonometric functions in these equations can of course be replaced by their equivalent forms

$$\sin \varphi = \frac{w}{V_R}$$

$$\cos \varphi = \frac{V_w - u}{V_R}$$

where

$$V_R = \sqrt{(V_w - u)^2 + w^2}$$

Equations (13) and (14) can be reduced to a simpler and more useful form by making use of the fact that $w$ is small relative to the airspeed during the climb, that is

$$w \ll (V_w - u) \tag{15}$$

Thus, since

$$\varphi = \tan^{-1} \frac{w}{V_w - u} \tag{16}$$

the inequality of relation (15) is equivalent to stating that $\varphi$ is a very small angle, and hence we can take

$$\varphi = \tan \varphi = \sin \varphi = \frac{w}{V_R} = \frac{w}{V} \tag{17}$$

$$\cos \varphi = 1 \tag{18}$$

Here $V = V_w - u$ is the magnitude of the aerodynamic velocity $\hat{V}_R$, to the above order of approximation. Using these relations and the fact that $D \ll L$ for the aerodynamically efficient albatross, the linearized forms of eqs. (13) and (14) become

$$\frac{du}{dz} = \frac{g}{W} \left(D + L \frac{w}{V}\right) w^{-1} \tag{19}$$

$$\frac{dw}{dz} = \frac{g}{W} (L - W) \, w^{-1} \tag{20}$$

Further reduction of these equations to coefficient form, using the conventional expressions for lift and drag

$$L = C_L \, 1/2 \, \rho \, V^2 \, S \tag{21}$$

$$D = C_D \, 1/2 \, \rho \, V^2 \, S \tag{22}$$

yields

$$\frac{du}{dz} = \frac{g}{w} \left( C_D + C_L \frac{w}{V} \right) 1/2 \, \rho \, \frac{V^2}{W/S} \tag{23}$$

$$\frac{dw}{dz} = \frac{g}{w} \left( C_L \, 1/2 \, \rho \, \frac{V^2}{W/S} - 1 \right) \tag{24}$$

Here $C_L$ and $C_D$ are the lift and drag coefficients, respectively, and $S$ is the wing area of the bird. Equations (23) and (24) constitute the linearized equations of motion for the windward climb.

These differential equations are still somewhat complex. They are nonlinear and mathematically coupled in both independent variables ($u$ and $w$ appear in both equations; $|u|$ is contained in $V$, since $V = V_w - u$). The complexity of these equations becomes evident when we note that the accelerations at any altitude $z$ depend upon both the velocities $u$ and $w$ which coexist at that altitude and hence upon the entire acceleration history of the bird up to the given altitude. The accelerations also depend upon the velocity distribution $V_w(z)$ of the wind in the shear layer. In addition, the drag coefficient $C_D$ is a function of the lift coefficient $C_L$, and the bird can vary $C_L$ at will merely by adjusting its aerodynamic control geometry (i.e., its wing and tail surfaces, and also the surfaces of its large webbed feet which are used for control) so as to trim at the desired angle of attack. Thus $C_L$ and $C_D$, in general, are also functions of altitude: $C_L = C_L(z)$, $C_D = C_D(C_L)$. Finally, we note that since the bird is capable of altering the shape and effective area of its wings, $W/S$ can also be varied with altitude as the bird desires.*

Before considering the general solutions of eqs. (23) and (24) or the exact eqs. (13) and (14), it is instructive to examine the physical significance of these expressions. By making use of certain basic observations on the nature of the bird's flight path during the climb, it is possible to simplify eqs. (23) and (24) considerably, and to arrive at a single equation whose interpretation yields some valuable information about the bird's aerodynamic characteristics and gives us a useful picture of the complex relationships which exist among the principal variables.

Analysis of the Equations of Motion. - It is a fact of observation that the vertical rise of the albatross during the greater part of the

*It will be shown later that the ability of the albatross to vary its wing loading $W/S$ plays an important role in the leeward glide phase.

windward climb is essentially uniform, that is, the velocity $w$ is practically constant except for a brief period at the beginning of the climb during which the bird accelerates vertically to the climbing speed $w$. Under the condition $w$ = constant, eq. (24) reduces to

$$\frac{dw}{dz} = 0 \tag{25}$$

for the major part of the climb. It then follows from eq. (24) [or more directly from eq. (20)] that

$$L = W \tag{26}$$

during the climb (in the linear equations). Eq. (26) expressed in coefficient form becomes

$$C_L \, 1/2 \, \rho \, V^2 \, S = W \tag{27}$$

which, upon rearrangement, yields

$$\frac{1}{C_L} = 1/2 \, \rho \, \frac{V^2}{W/S} \tag{28}$$

Substituting this relation in eq. (23) we obtain

$$\frac{du}{dz} = \frac{g}{w}\left(\frac{C_D}{C_L} + \frac{w}{V}\right) \tag{29}$$

Then solving eq. (27) for velocity $V$,

$$V = \sqrt{\frac{2 \, W/S}{\rho \, C_L}} \tag{30}$$

and substituting in Eq. (29), we arrive at the single relation

$$\frac{du}{dz} = g\left(\frac{1}{L/D}\,\frac{1}{w} + \sqrt{\rho/2 \, \frac{C_L}{W/S}}\right) \tag{31}$$

This form of the equation of motion is particularly suitable for analysis since the primary variables are expressed in terms of the conventional aerodynamic parameters $L/D$, $W/S$, $C_L$, and the climbing velocity $w$. The lift-drag ratio $L/D$ is an indication of the aerodynamic efficiency of the bird, and is a function of the lift coefficient $C_L$. The variation of $L/D$ with $C_L$ is obtained from the so-called drag polar diagram for the bird. Such a diagram is shown schematically in Fig. 9, assuming the wing to be rigid in shape.* The wing loading $W/S$ is the bird's weight divided

*In reality, the bird possesses a whole series of drag polars, one for each configuration, or shape, of its wing, since the wing shape can be varied by the bird at will. This subject will be discussed in more detail in the section on the leeward glide phase. (continued at bottom of next page)

by the wing area; this parameter determines the required magnitude of the lift coefficient for a given air speed [see eq. (27)]. The lift coefficient $C_L$ is a function of the angle of attack $\alpha$ (Fig. 10) and depends on the geometry, that is, the thickness and camber, of the wing sections. The point denoted by $C_{L_{max}}$ in Fig. 10 corresponds to the maximum attainable value of the lift coefficient. If $\alpha$ is increased beyond this point, the wing stalls; and a rapid loss of lift results.

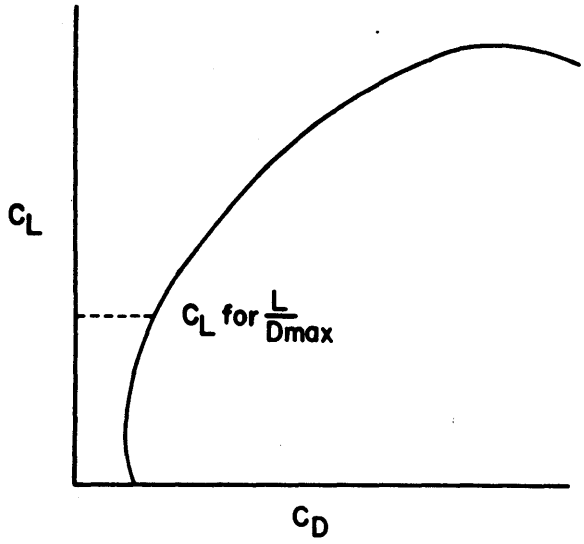


Fig. 9

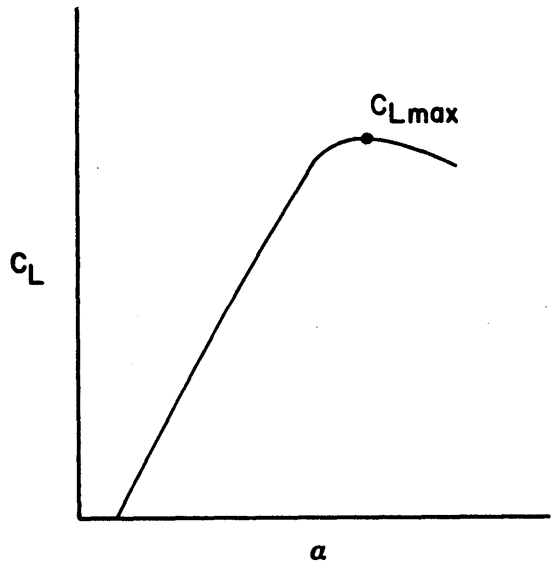


Fig. 10

The analysis of eq. (31) is based upon the fact that the bird must be able to attain a small minimum value of $du/dz$ in climbing flight. This in turn, requires that the magnitudes of the various parameters on the right hand side of eq. (31) must simultaneously have values that result in a small minimum value for the expression in parentheses. Analysis of the parameters in the light of this requirement allows us to explain the physical factors underlying the particular form and flight characteristics of the albatross. To see why the minimum value of $du/dz$ must be small, however, we must first examine the physical significance of this derivative.

Consider the bird at a point just above the surface and beginning the windward climb. At this instant the bird's horizontal speed $u$ has some definite value, say $u = u_o$; the absolute value of $u$ will continuously decrease as the bird rises due to the decelerating action of $F_x$. If the wind speed $V_w(z)$ does not increase as rapidly as $u$ decreases, the aerodynamic velocity $V = (V_w - u)$*

For the climbing phase, the wings are held rigidly outstretched so that a single drag polar applies. This polar will undoubtedly be very similar to those of modern high-aspect -ratio sailplanes. However, during the climb the flow field behind the albatross' wing may not be steady since the bird is decelerating (that is, $C_L$ may be changing), so that the induced drag may not be the same as would be measured in steady flow, as in the wind-tunnel. The induced drag relationships for a decelerating wing are developed in ref. 13.

*Note here that $u$ has a negative value so that $V = V_w - u \equiv V_w + |u|$.

will decrease and the bird must increase $C_L$ in order to maintain $L = W$. Ultimately, at some altitude $z_f$, $u$ will decrease to a limiting value $u_f$ such that the velocity becomes so small that the bird's wing stalls, that is, $C_L$ has reached its maximum value $C_{L_{max}}$ according to the relation

$$W = C_{L_{max}} \, 1/2 \, \rho \, (V_w - u_f)^2 \, S \tag{32}$$

The altitude $z_f$ at which this condition occurs will depend of course on the wind-speed profile $V_w(z)$. If $V_w$ were large enough, $\hat{u}_f$ could even have the same direction as the wind, without wing stall; the bird would then be moving "backward" relative to the earth. In general, however, the bird will not climb to the point of wing stall, since it must reserve a margin of $C_L$ to allow execution of the subsequent turn to leeward, as will be discussed in more detail later on. Hence, if we set some maximum allowable limit on $C_L$, say $C_{L_f}$, where $C_{L_f} < C_{L_{max}}$, then $u_f$ will correspond to the condition where the airspeed $V$ satisfied this value of $C_L$, that is,

$$W = C_{L_f} \, 1/2 \, \rho \, (V_w - u_f)^2 \, S \tag{33}$$

The altitude $z_f$ at which $u_f$ occurs obviously depends upon the rate at which $V_w$ increases with $z$ as well as the rate at which $u$ decreases.

Now if $du/dz$ is large at all points of the climb, the change in $u$, $\Delta u$ $(= u_2 - u_1)$, will be large for any small altitude rise $\Delta_z = z_2 - z_1$, since the absolute velocity decrease $\Delta u$ is given by

$$\Delta u = \int_{z_1}^{z_2} \frac{du}{dz} \, dz \tag{34}$$

Thus, since $V_w$ increases with altitude, for a given velocity decreases $\Delta u$, the aerodynamic velocity $V$ $(= V_w - u)$ will be less if $du/dz$ is large, because the altitude gain $\Delta z$ needed to produce $\Delta u$ will be correspondingly small. The value of $C_L$ must therefore be larger at each point in the climb. Hence, for a specified maximum limiting value of $C_L$, $C_{L_f}$, the minimum allowable absolute value of $u$, $u_f$, will be reached at a lower value of altitude $z_f$ if $du/dz$ is large. It is clear, therefore, that the magnitude of $du/dz$ determines, upon integration, how high the albatross can rise in the windward climb for any given wind profile $V_w(z)$ and initial horizontal component of absolute velocity $u_o$. These relations are illustrated in Fig. 11.

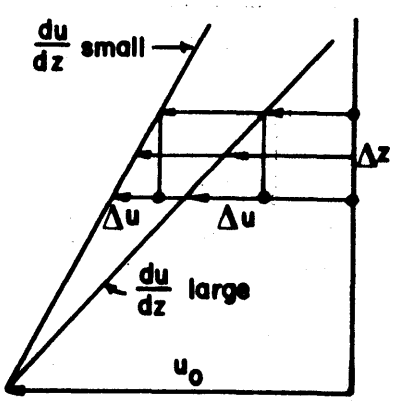


Fig. 11

If the derivative $du/dz$ were too large, the albatross could not rise to

any appreciable altitude in the shear layer. Hence, even though the wind might be quite strong at the upper limit of the shear layer ($z = z^*$), the bird could not gain sufficient altitude in the climb to make the ensuing turns necessary to complete the cycle. But even if the altitude reached were sufficient to allow the turn to leeward to be completed, the bird still may not possess enough x-momentum after the turn to windward to continue the cycling process. This condition arises because of the implicit effect of the altitude gained in a given climb on the initial horizontal velocity $u_o$ available at the beginning of the succeeding climb. As will be discussed in detail in the subsequent section on the leeward turn, the primary energy input to the bird in dynamic soaring comes from the high altitude turn to leeward, and the amount of energy gained depends upon the wind speed $V_W$ at the altitude where the turn to leeward is accomplished. If the turn to leeward cannot be made at a sufficiently high altitude (where $V_W$ is large enough), the gain in energy may be insufficient to allow the next cycle to be completed.

On the other hand, if $du/dz$ is sufficiently small that the bird can reach the upper limit of the shear layer $z^*$ with an airspeed $V_W(z^*) - u(z^*)$ which is equal to or greater than the limiting value imposed by $C_{L_f}$, that is if

$$[V_W(z^*) - u(z^*)] \geqq \sqrt{2 \frac{W}{S} (\rho C_{L_f})^{-1}} \tag{35}$$

then the bird can attain maximum energy from the turn to leeward and hence a maximum value of $u_o$ for the succeeding climb.

It is interesting to note that it would not be advantageous for the bird to climb to altitudes greater than $z^*$, even if $du/dz$ were sufficiently small to permit this. Above $z^*$ $V_W$ no longer increases, while $|u|$ can only decrease. Hence upon turning to leeward at altitudes greater than $z^*$, the absolute velocity of the bird would be less than if the turn had been made at $z^*$. This appears to be one of the principal reasons why the flight of the albatross is confined to the narrow altitude range of the shear layer; flight is most efficient in this region.

It is obvious that the practical significance of the magnitude of $du/dz$ ultimately depends upon the magnitude and shape of the wind profile $V_W(z)$. If the wind is strong and $dV_W/dz$ is large through an appreciable depth of the shear layer, then $du/dz$ can also be relatively large without adversely affecting the bird's dynamic soaring ability. Even though $|u|$ may decrease rapidly with altitude in such a case, the increase in $V_W$ could be sufficient to prevent a net decrease in the aerodynamic velocity until an adequate altitude has been reached. If the wind is weak, however, it is obvious that $du/dz$ must be correspondingly small if the necessary altitude is to be gained. It thus appears that the aerodynamic parameters of the albatross must be such as to produce values of $du/dz$ sufficiently small to allow soaring in weak or moderate winds. The lower limit of usable wind speed (which actually determines the minimum value of $du/dz$ required)

must be small enough that the frequency of occurrence of this and all higher wind speeds is sufficiently great to guarantee the bird an adequate flight capability for its travel needs.

A very small minimum value of $du/dz$ is quite desirable in that it would guarantee the bird's soaring ability over a wide range of wind conditions, but the minimum value actually required depends upon the average oceanic wind conditions. As will be shown later the aerodynamic properties required for the attainment of very low values of $du/dz$ are incompatible with those for other important aerodynamic operations such as the take-off and landing, and hence some compromise must be made. In any event, we may be quite certain that the compromise of aerodynamic characteristics which the albatross has arrived at through the process of evolution quite adequately balances all the demands of its present oceanic environment.

Having now established the physical significance of $du/dz$ and the requirement that it have a small minimum value, the various factors in the right hand side of eq. (31) can be considered. The desired condition is that the value of the expression

$$\frac{1}{L/D}\frac{1}{w} + \sqrt{\frac{\rho}{2}}\sqrt{\frac{C_L}{W/S}} \tag{36}$$

be small. For this to be true it is necessary that, from a relative standpoint,

(1) $L/D$ be large (3) $C_L$ be small

(2) $w$ be large (4) $W/S$ be large

as can be seen by inspection. The factor $\sqrt{\rho/2}$ is of course taken as constant over the small altitude range used by the albatross.

The requirement of a large value for $L/D$ [condition (1)] is well satisfied by the bird's aerodynamic design. The albatross has a form which, by all conventional aerodynamic standards, should be most efficient. The bird is superbly streamlined and the wings are faired smoothly into the body. The body feathers produce an exceptionally smooth surface as do the wing coverts. The wing has a relatively high aspect ratio $A$ ($= b^2/S$), approximately 13, and as is well known in aeronautical design a wing of large aspect ratio is one of the prime requirements for obtaining large values of $L/D$. The wing sections of the bird are very thin and moderately cambered, thus meeting another basic requirement for high aerodynamic efficiency.

As mentioned previously, $L/D$ is a function of the lift coefficient $C_L$. To satisfy conditions (1) and (3) simultaneously it is thus necessary that the maximum value of $L/D$ occur at relatively small values of $C_L$. Aerodynamic data indeed indicate that a high aspect ratio wing composed of thin, cambered wing sections has precisely this property. It is thus clear

why the long, narrow wing of the albatross, so characteristic of the oceanic soarers, takes the particular form it does.

Condition (2) states that the rate of climb $w$ should be large. However, $w$ cannot take on arbitrarily large values, since it implicitly affects $C_L$, $L/D$, and $W/S$. To examine this complex relationship, let us consider the bird at the end of its low altitude turn to windward, where $w = o$ and $u = u_i$. In order to accelerate to the (constant) climbing speed $w$, the bird must increase its angle of attack such that the lift becomes greater than the weight; vertical acceleration then follows according to eq. (24). During this period of vertical acceleration, $L$ will be large and consequently so will $D$. The action of the aerodynamic forces during this period will cause $u$ to decrease (in absolute value), as will be discussed in detail in the subsequent section on the energy interchange mechanisms of the climb (page 34). Thus, if $w$ is large, $u$ at the start of the climb (that is, when $w$ has attained its constant value) will be correspondingly reduced in absolute value and the aerodynamic velocity will be less at each altitude. If $V$ is small, then $C_L$ must be large, according to the relation

$$C_L V^2 = \frac{2}{\rho} \frac{W}{S} \tag{37}$$

This effect is contrary to condition (3). If $C_L$ becomes excessively large, $L/D$ will decrease. This is contrary to the requirements of condition (1). Finally, if $W/S$ is large, in accord with condition (4), it is evident from eq. (37) that $C_L$ must be very large if $w$ is large, leading to even greater adverse effects. It is clear that the climbing velocity $w$ cannot be unduly large, but must approach some optimum value where the integrated effects involving $C_L$, $L/D$, and $W/S$ will make expression (36) take on a sufficiently small value. The magnitude of this optimum value of $w$ is of course dependent on the nature and strength of the wind velocity profile $V_w(z)$. The relative magnitudes of $L/D$, $C_L$, and $w$ must be such as to allow the bird use of an adequate range of wind speeds for satisfying its soaring needs.

Condition (3), as already discussed, is intimately connected with the other three conditions. The requirement of a large value of $L/D$ at a small value of $C_L$ is quite compatible with the type of wing possessed by the albatross. From eq. (37), however, $C_L$ must vary proportional to $1/V^2$ as the bird rises. In the general case, the aerodynamic velocity $V$ probably varies somewhat with altitude $z$, $[V(z) = V_w(z) - u(z)]$, and hence $C_L$ must vary (assuming $W/S$ to remain constant during the climb).* This variation of $C_L$ will cause $L/D$ to change according to the function of $L/D\ (C_L)$. Hence, it would appear highly desirable for the $L/D\ (C_L)$ curve of the bird to be very flat near $L/D_{max}$. The velocity $V$ would usually be expected to decrease with altitude, since $|u|$ is decreasing. However, if $dV_w/dz$ is greater than $du/dz$, it is entirely possible that $V$ could even increase, temporarily, with altitude, or remain constant. This would require that $C_L$ decrease or remain constant. The variation of $C_L$ with $z$

*This assumption is supported by observations of the climb, where the wings are held fully extended and rigid.

is of course entirely under the control of the bird, through regulation of its angle of attack. Undoubtedly, the bird instinctively uses the optimum variation of $C_L$ for the particular wind conditions encountered at any given time.

Condition (4) indicates that the albatross should possess a high wing loading W/S. But, as is evident from eq. (37), W/S cannot become too large, or else $C_L$ will be increased to detrimental proportions. In reality, the albatross does possess a relatively high wing loading (2.5 $lb/ft^2$ for Diomedea exulans) as compared to that of the land soarers (0.78 $lb/ft^2$ for Cathartes aura and 1.23 $lb/ft^2$ for Coragyps atratus). This value is apparently an optimum one for the dynamic soaring requirements of the albatross; it obviously allows a small enough value of du/dz to permit dynamic soaring in such weak winds as the bird may have to use.

To summarize the results of this section, it has been shown that eq. (31) clearly explains why the albatross possesses the exceptional streamlining, high aspect ratio wing, and high wing loading which characterize the dynamic soaring birds of the ocean. It has been shown also that the primary variables L/D, w, $C_L$, and W/S are rather complexly related, aerodynamically, and that their interactions are intimately connected with the properties of the wind profile, $V_w(z)$ and $dV_w/dz$. The general relationship of these variables can be summarized schematically as follows

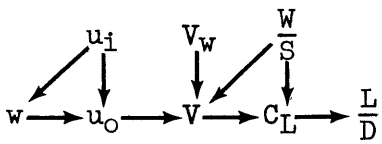


(38)

The bird, by control of its angle of attack, accelerates to the vertical velocity w at the start of the climb. Simultaneously, however, the initial x-component of velocity $u_i$ is decreased to $u_o$, by an amount that depends on the final magnitude of w. The value of $u_o$ in turn, combines with the value of the wind speed $V_w$ near the surface to determine the initial aerodynamic velocity V. Then V, in combination with the wing loading W/S, determines the lift coefficient and associated L/D. The particular value of w used under given wind conditions of $V_w(z)$ and $dV_w/dz$, in conjunction with W/S, thus sets the subsequent functions $C_L(z)$ and du/dz which ultimately determine the altitude which the bird will gain in the climb.

Solution of the Equations of Motion. - The preceding analysis yielded a useful picture of the interactions existing between the aerodynamic parameters involved in the windward climb. In order to describe the climb in exact detail, however, it is necessary to obtain the solution of the equations for actual flight conditions.

From a mathematical standpoint, the solution of eqs. (19) and (20) [or of eqs. (13) and (14)] for u(z) and w(z) is a straightforward process and can be carried out by numerical integration when the functions $V_w(z)$, $C_L(z)$, and L/D ($C_L$), along with W/S, are specified. In the case of the actual albatross flight, however, direct solutions cannot be obtained since

the pertinent functions appearing in the equations are not known. That is, the wind profile $V_w(z)$ and the aerodynamic efficiency $L/D$ $(C_L)$ are unknown, in general, and the function $C_L(z)$ is undetermined, being subject to arbitrary control by the bird. While $V_w(z)$ could probably be measured without great difficulty, direct experimental measurement of $L/D$ $(C_L)$ for the albatross would be almost impossible. Thus, solutions of eqs. (19) and (20) can be obtained only when $V_w(z)$, $C_L(z)$, and $L/D$ $(C_L)$ are assumed or otherwise specified.

By using special functions in the general solution, however, it becomes possible to investigate in detail the individual effects of any of the basic parameters on the efficiency of the windward climb, especially those of different wind profiles, and the general solution procedure thus becomes a useful tool for analytical studies of the climb aerodynamics. The general method of solution of the basic differential equations is consequently developed in section "a" below.

On the other hand, if $du/dz$, $dw/dz$, $u$, and $w$ were known at a sufficient number of points in the shear layer, the equations could alternately be solved for two of the three unknown functions $V_w(z)$, $C_L(z)$, and $L/D$ $(C_L)$. If $V_w(z)$ were determined independently by experimental means, the $C_L(z)$ and $L/D$ $(C_L)$ for the albatross could be determined. It is shown in section "b" below that it is possible by means of a simple photographic analysis of the climb to determine not only $C_L(z)$ and $L/D$ $(C_L)$, but also $V_w(z)$ (when an additional equation is used) for actual flight paths of the albatross.

a. The general solution

The most general form of the linearized equations of motion is given by eqs. (19) and (20)

$$\frac{du}{dz} = g\left(\frac{1}{L/D}\cdot\frac{1}{w}+\frac{1}{V}\right)\frac{L}{W} \tag{39}$$

$$\frac{dw}{dz} = g\left(\frac{L}{W}-1\right)w^{-1} \tag{40}$$

Using the relation $V = V_w - u$ and the coefficient forms for the aerodynamic forces, eqs. (39) and (40) become

$$\frac{du}{dz} = g\left(\frac{1}{L/D}\cdot\frac{1}{w}+\frac{1}{V_w-u}\right)\ C_L\,\frac{1}{2}\,\rho\,(V_w-u)^2\,\frac{1}{W/S} \tag{41}$$

$$\frac{dw}{dz} = g\left(C_L\,\frac{1}{2}\,\rho\,(V_w-u)^2\,\frac{1}{W/S}-1\right)w^{-1} \tag{42}$$

These equations contain no restrictions except those imposed by the linearization process,* that is, $w \ll V_w - u$. In particular, no restrictions have been imposed on $w$, and this velocity is free to vary with altitude, $w = w(z)$

The solution of these simultaneous equations consists in determination of the velocity patterns $u(z)$ and $w(z)$ for the entire windward climb. The nonlinearity of the equations precludes a direct solution in terms of simple functions and we must resort therefore to numerical methods of solution. This consists of a step by step integration of eqs. (41) and (42) and proceeds as follows.

We assume that during the entire climb, $W/S$ is constant. The justification of this assumption has been given previously. We also assume that the wind velocity profile $V_w(z)$ within the shear layer ($0 \leq z \leq z^*$) is known from experimental data. Above $z^*$, the upper limit of the shear layer, $V_w$ assumes the constant value $V_w(z^*)$. The variation of $C_L$ with $z$ is entirely at the bird's disposal. The only limit is that $C_L$ cannot exceed $C_{L_{max}}$, where the wing stalls. The lift-drag ratio $L/D \equiv C_L/C_D$ is a function only of $C_L$, as previously noted. The values of the gravitational acceleration constant $g$ and the air mass density $\rho$ are of course taken as constants.

To begin the integration we must specify the initial values of $z_o$, $u_o$, $w_o$, $V_{w_o}$, and $C_{L_o}$, respectively. The value of $(L/D)_o$ is determined by the value of $C_{L_o}$. In general, the integration may be commenced at any altitude, that is, for $z_o > 0$ and $w_o > 0$, provided the other initial conditions are also known at this altitude. It is of more general interest, however, to begin the integration at $z_o = 0$ (i.e. at the surface) and with $w_o = 0$ so as to obtain the entire flight path of the bird, including the period of initial vertical acceleration. Unfortunately, this procedure leads to difficulty in that the factor $1/w$ in the equations takes the meaningless form $1/0$ for $w_o - 0$ at $z_o$. This difficulty requires special treatment, and will be considered in detail subsequently. For the present we shall assume that $z_o$ is a small, but finite value, and that $w_o$ is also finite. Under these conditions the integration can proceed smoothly.

The first step is to insert all the initial values and constants into eqs. (41) and (42) and thus determine the initial values of $du/dz$ and $dw/dz$ denoted by $(du/dz)_o$ and $(dw/dz)_o$, respectively. Then, choosing an arbitrary, but small, increment of altitude $(\Delta z)_1$, we determine the velocity values at altitude $z_1$, where

$$z_1 = z_o + (\Delta z)_1 \tag{43}$$

by means of the relations

$$u(z_1) = u_o + (\Delta u)_1 = u_o + \left(\frac{du}{dz}\right)_o (\Delta z)_1 \tag{44}$$

---

*The exact equations (13) and (14) can be treated by the same procedure as is outlined here for the linearized equations.

$$w(z_1) = w_o + (\Delta w)_1 = w_o + \left(\frac{dw}{dz}\right)_o (\Delta z)_1 \tag{45}$$

We now have $u$ and $w$ at the new altitude $z_1$. $V_w$ at $z_1$ is also known from the wind profile equation $V_w(z)$. The value of $C_L$ at $z_1$ is generally arbitrary, however, since the bird can vary $C_L$ at will, independently of all other variables, merely by trimming at the appropriate angle of attack. Hence, unless we know the $C_L(z)$ function actually used by the bird from experimental data,* we must assume the functional relation between $C_L$ and $z$ for the integration to proceed. The resulting velocity histories $u(z)$ and $w(z)$ will of course be heavily influenced by the nature of the function $C_L(z)$. For general studies of the climb mechanics the arbitrariness of $C_L(z)$ allows us to examine the effects of this parameter in detail, by comparing the results obtained for $u(z)$ and $w(z)$ as the form of $C_L(z)$ is varied. With a specified function $C_L(z)$ (experimental or assumed), the corresponding function $L/D$ $(C_L)$ is determined by means of the drag polar $C_D$ $(C_L)$, so that all values on the right sides of eqs. (41) and (42) are known at $z_1$.

We merely repeat the same procedure used above [eqs. (44) and (45)], substituting the values of the variables at $z_1$ for the new "initial" conditions. Thus we obtain from eqs. (41) and (42)

$$\left(\frac{du}{dz}\right)_1 = g\left(\frac{1}{(L/D)_1} \cdot \frac{1}{w_1} + \frac{1}{V_{w_1} - u_1}\right) C_{L_1} \frac{1}{2} \rho (V_{w_1} - u_1)^2 \frac{1}{W/S} \tag{46}$$

$$\left(\frac{dw}{dz}\right)_1 = g\left(C_{L_1} \frac{1}{2} \rho (V_{w_1} - u_1)^2 \frac{1}{W/S} - 1\right) \frac{1}{w_1} \tag{47}$$

where $u$, $w_1$, $C_{L_1}$, and $V_{w_1}$ indicate the values of the functions at $z_1$,

$$\begin{aligned} u_1 &= u(z_1) \\ w_1 &= w(z_1) \\ C_{L_1} &= C_L(z_1) \\ V_{w_1} &= V_w(z_1) \end{aligned} \tag{48}$$

Then the velocity values at the new altitude $z_2$,

$$z_2 = z_1 + (\Delta z)_2 \tag{49}$$

---

*Such data can be determined by photographic recordings, as will be discussed in section "b".

are obtained from the relations

$$u_2 = u(z_2) = u_1 + (\Delta u)_2 = u_1 + \left(\frac{du}{dz}\right)_1 (\Delta z)_2 \tag{50}$$

$$w_2 = w(z_2) = w_1 + (\Delta w)_2 = w_1 + \left(\frac{dw}{dz}\right)_1 (\Delta z)_2 \tag{51}$$

Repeating the process, using a very small value for $\Delta z$ increments, the functions $u(z)$ and $w(z)$ can be tabulated and plotted for any desired lift coefficient variation $C_L(z)$.

It should be noted that the accuracy of the integration depends upon the magnitude of the $\Delta z$ interval (or intervals) used. A check on the accuracy is obtained by comparing the plots (or tabulated values) of $u(z)$ and $w(z)$ for a given value of $\Delta z$, against the same functions obtained by using a smaller value of $\Delta z$. When the plots no longer change appreciably as the magnitude of $\Delta z$ is decreased, the curves have approached the exact solution as closely as is necessary for computational purposes.

The simple integration procedure outlined here is equivalent to using Taylor series integration, retaining only first order terms. Any of the more sophisticated methods of numerical integration, such as the Adams or Kutta-Runge methods, could of course be used. If sufficiently small values of $\Delta z$ are employed, however, the Taylor series method is suitably accurate.

In general investigations of the effects of the function $C_L(z)$, the integration would be carried only to some limiting value of $C_L$ which is imposed by physical restrictions. For example, one such restriction might be the wing stall. That is, when $C_{L_{max}}$ is exceeded, the wing stalls and lift is lost. The value of $z$ at which the angle of attack exceeds that for $C_{L_{max}}$ will therefore set the approximate maximum value of $z$ attained, for then $w$ rapidly becomes negative and the bird falls. If $\alpha$ is not allowed to exceed that for $C_{L_{max}}$, the bird will continue to climb, assuming that $V_w - u$ is sufficient throughout the climb to maintain a positive value of $w$ up to and beyond the altitude where $C_{L_{max}}$ occurs. It may indeed happen, however, that $V_w - u$, for the specified $C_L(z)$, is not sufficient to maintain $F_z \geqq W$ up to the altitude specified for $C_{L_{max}}$; hence the bird will decelerate vertically ($dw/dz$ will become negative) once $F_z$ becomes less than $W$, and will lose altitude after $w$ becomes negative. In this case, only a part of the specified $C_L(z)$ curve will be possible, since a maximum value of $z$ has occurred; the maximum altitude gain will always correspond to the point where $w$ becomes zero.

By using various $C_L(z)$ functions [and corresponding $L/D$ $(C_L)$ relations] in the solution of the equations of motion, and comparing the results, it is possible to learn a great deal about the relative effectiveness of these functions in allowing altitude gain during the climb phase, for given wind conditions $V_w(z)$. The effects of varying the wind profile function $V_w(z)$ can also be investigated. By programming the integrations of eqs. (41) and (42)

on an electronic computer, solutions can be rapidly and simply obtained for any desired inputs of $C_L(z)$, L/D ($C_L$), and $V_w(z)$.

Let us now consider the case where the solution is desired starting from the initial conditions $z_o \doteq 0$ and $w_o = 0$. It is immediately apparent that eqs. (41) and (42) will involve the undefined factor $1/w_o = 1/0$ for the calculation of $(du/dz)_o$ and $(dw/dz)_o$. This condition arises because of the use of relation (12)

$$\frac{dz}{dt} = w$$

to eliminate dt in the basic eqs. (10) and (11).

To proceed with the integration in this case, we replace eqs. (41) and (42) with the forms

$$\frac{du}{dt} = g\left(\frac{1}{L/D} + \frac{w}{V_w - u}\right) C_L \frac{1}{2} \rho (V_w - u)^2 \frac{1}{W/S} \tag{52}$$

$$\frac{dw}{dt} = g\left(C_L \frac{1}{2} \rho (V_w - u)^2 \frac{1}{W/S} - 1\right) \tag{53}$$

Inserting the initial values $u_o$, $w_o = 0$, $C_{L_o}$, $V_{w_o}$, and $(L/D)_o$ in these equations, we can obtain $(du/dt)_o$ and $(dw/dt)_o$ as before. Then choosing an arbitrary, small time increment $\Delta t$, we can determine $u_1$ and $w_1$ from

$$u_1 = u(t_1) = u_o + \left(\frac{du}{dt}\right)_o (\Delta t)_1 \tag{54}$$

$$w_1 = w(t_1) = w_o + \left(\frac{dw}{dt}\right)_o (\Delta t)_1 \tag{55}$$

where $w_o = 0$. Now, to find what value of $\Delta z$ corresponds to the time increment $(\Delta t)_1$, we use the relation

$$\Delta z = \int_o^{(\Delta t)_1} \frac{w_1}{(\Delta T)_1} t \, dt = \frac{w_1}{2} (\Delta t)_1 \tag{56}$$

$$z_1 = z_o + \Delta z \tag{57}$$

Thus we have $u_1$, $w_1$, and $z_1$. These values may now be substituted directly in eqs. (46) and (47) and the integration carried out in terms of $\Delta z$ as before.

The numerical integration of eqs. (41) and (42) may be used to investigate the effect of the climbing velocity $w$ on the horizontal velocity $u$. The nature of this effect was mentioned previously on page 26, in connection with condition (2). If the bird is considered to have the initial conditions $z_o = 0$, $w_o = 0$, $(dw/dz)_o = 0$, and $u = u_1$, the condition $L_o = W = C_{L_o} 1/2\ \rho (V_{w_o} - u_1)^2 S$ must exist. If then $C_L$ is increased, $dw/dz$ will become positive and $w$ will increase. Simultaneously, $u$ will decrease by an amount which depends on the manner in which $C_L$ was varied during the period of vertical acceleration and, of course, on the wind profile $V_w(z)$. If the vertical acceleration is subsequently reduced to zero (by regulation of $C_L$) after some desired value of $w$ is attained, the bird will climb at a constant rate. The value of $u$, say $u_o$, at this altitude where $w$ becomes constant will then ultimately determine how high the bird can rise in the shear layer. Under the condition $dw/dz = 0$, $L = W$ (i.e. $F_z = W$), and eqs. (41) and (42) reduce to

$$\frac{du}{dz} = g\left(\frac{1}{L/D} \cdot \frac{1}{w} + \frac{1}{V_w - u}\right) \tag{58}$$

for the part of the climb during which $w$ is constant. Then $C_L$ at each value of $z$ is no longer arbitrary, but is uniquely determined by the condition $C_L = W/S \cdot 2/\rho \cdot (V_w - u)^{-2}$ up to the maximum value of $z$ at $C_{L_{max}}$. Thus it is possible to determine quantitatively how $w$ affects $u_o$ and the maximum altitude attainable when various $C_L(z)$ functions are used during the initial vertical acceleration period.

b. Solution for the aerodynamic characteristics

If an accurate record is obtained of the bird's flight path (relative to earth) during the climb by photographic or other means such as theodolite triangulation, it is possible to solve the equations of motion for the values of the unknown parameters $C_L(z)$ and $L/D(z)$. To obtain an accurate photographic record, the camera must be mounted perpendicular to and at a considerable distance from the plane of the flight path so as to avoid errors due to parallax. The camera must be fixed relative to earth during the recording and a fixed reference point must appear in the photograph. By making multiple exposures at known time intervals (or equivalently, by using a motion picture camera with known film speed), the entire flight path of the bird during the climb can be recorded.

The resulting flight path thus obtained can be converted to actual full-scale dimensions by using a known characteristic length (say the body length) of the bird. If the body length of the bird were known to be 2.2 feet, for example, and the corresponding length in the photograph (or its projection) is 1.3 centimeters, then the actual dimensions of the flight path in feet are obtained by multiplying all distances on the photograph (measured in centimeters) by the scale factor 2.2 ft/1.3 cm or 1.69. Using this procedure, a plot of the full scale flight path can be constructed, using time as a parameter. Such a plot is shown schematically in Fig. 12, where the points on the curve denote the known time intervals. Alternately, more involved triangulation

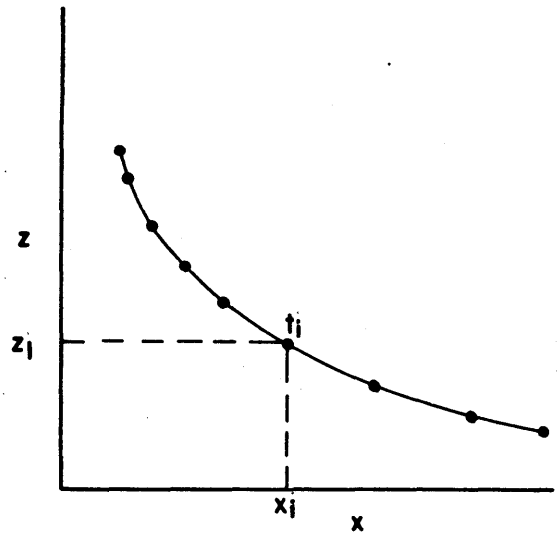


Fig. 12

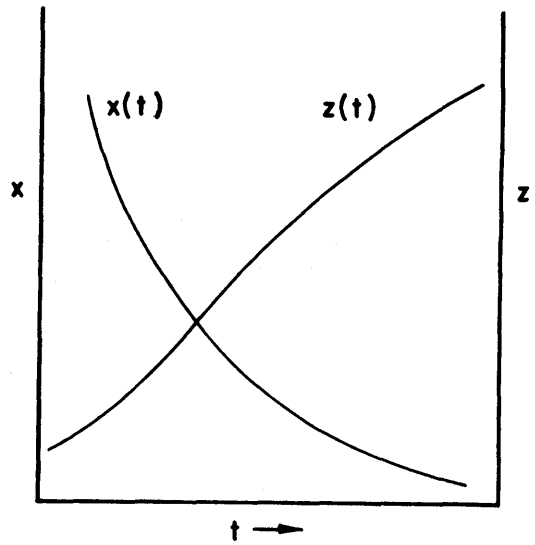


Fig. 13

methods, such as used in aircraft and balloon tracking systems, could also be used under proper conditions to establish the flight path.

From this plot of the actual flight path, the functions $z(t)$ and $x(t)$ can be determined and plotted as shown in Fig. 13. These plots will in turn allow the determination of $w(z) = dz/dt$ and $u(t) = dx/dt$, and subsequently $dw/dz$ and $du/dz$. In order to determine the functions $C_L(z)$ and $L/D(z)$ used by the bird, we make use of eq. (24) for the vertical acceleration

$$\frac{dw}{dz} = \frac{g}{w}\left(C_L \frac{1}{2}\rho\,(V_w - u)^2 \frac{1}{W/S} - 1\right) \tag{59}$$

We assume that $V_w(z)$ is known. Since $dw/dz$, $w$, and $u$ are now also known functions of $\dot{z}$ and $W/S$ is a known constant, eq. (59) can be solved for $C_L(z)$ directly. Then, using eq. (23) for the horizontal acceleration

$$\frac{du}{dz} = g\left(\frac{1}{L/D}\frac{1}{w} + \frac{1}{V_w - u}\right) C_L \frac{\rho}{2}\frac{(V_w - u)^2}{W/S} \tag{60}$$

the function $L/D(z)$, or $L/D\,(C_L)$, can be determined. Thus, by means of the known actual solutions $w(z)$ and $u(z)$ (as determined by experimental measurement), the equations of motion allow us to determine two very important aerodynamic characteristics of the albatross, $C_L(z)$ and $L/D\,(C_L)$.

In order to obtain the above solutions it was necessary that the wind profile $V_w(z)$ existing at the time of the photographic recording be known. In lieu of actual wind profile measurements (which would not be too difficult to obtain over a 70-foot altitude layer), a theoretical or approximation function would have to be used for $V_w(z)$. On the other hand, it is possible to determine $V_w(z)$ from the photographic recordings, provided we assume the

function $L/D\ (C_L)$ to be known with sufficient accuracy. In all probability, the relation between $L/D$ and $C_L$ for the albatross will be quite similar to that for modern high performance sailplanes having laminar-flow airfoils and an aspect ratio equivalent to that of the bird. In this case, eq. (59) can be solved for $(V_w - u)$ in terms of $C_L$. Substitution for $(V_w - u)$ in eq. (60) then yields a relation from which the function $C_L(z)$ can be determined using the known $L/D\ (C_L)$ relation. With $C_L(z)$ determined, eq. (59) can be solved for $(V_w - u)$ as a function of $z$, from which $V_w(z)$ follows, since $u(z)$ is known. In the foregoing procedures, the fact that the functions $w(z)$ and $u(z)$ are in graphical form requires, of course, that the calculations be carried out for a series of individual values of the altitude $z$.

If another simultaneous equation involving $V_w$, $C_L$, and $L/D$ were available in addition to eqs. (59) and (60), it would be possible to determine all three functions $V_w(z)$, $C_L(z)$, and $L/D\ (C_L)$ directly from single photographic or other record of the flight path. Such an equation is given by the energy-balance relations which are developed in the following section. It is indicated at the close of that section how the simultaneous solutions for $V_w(z)$, $C_L(z)$, and $L/D(z)$ can all be obtained from a single flight path record.

Energy Analysis of the Windward Climb.- At the beginning of the climb, the bird is moving directly into the wind, just above the surface $z = z_o$, with $u = u_o$ and $w = w_o = 0$. Thus the bird possesses an initial supply of kinetic energy in the amount of $1/2\ w/g\ u_o^2$. As the bird begins its climb and rises through the shear layer, energy is extracted from the wind. Simultaneously, energy is being dissipated by the action of the aerodynamic drag force and is being supplied to increase the bird's kinetic energy and potential energy by $1/2\ w/g\ w^2$ and $W\ (z - z_o)$. It is of interest to investigate the details of this energy interchange process.

Let us first consider the energy required to accomodate the aerodynamic drag force $\hat{D}$. This energy is transferred directly to the air in such a manner that it is ultimately dissipated into heat by viscous action. This energy will be called the dissipation energy and denoted by the symbol $\Delta E_d$. It is equal to the working of the drag force $\hat{D}$ relative to the total aerodynamic velocity $\hat{V}_R$,

$$\Delta E_d = \int_{t_o}^{t_1} \hat{D} \cdot \hat{V}_R \, dt \tag{61}$$

Here $t_1 - t_o$ denotes an arbitrary interval of time and $\Delta E_d$ the dissipation energy expended during this interval. Since, from eq. (4),

$$\hat{V}_R = \hat{V}_w - \hat{u} - \hat{w}$$

eq. (61) can be written as

$$\Delta E_d = \int_{t_o}^{t_1} \hat{D} \cdot (\hat{V}_w - \hat{u} - \hat{w}) \, dt \tag{62}$$

Expanding eq. (62) we obtain

$$\Delta E_d = \int_{t_o}^{t_1} \hat{D} \cdot V_w \, dt + \int_{t_o}^{t_1} \hat{D} \cdot - \hat{u} \, dt + \int_{t_o}^{t_1} \hat{D} \cdot - \hat{w} \, dt \qquad (63)$$

The last two integrals have positive values as can be seen from the vector sketch of Fig. 14. All vector operations are carried out in the positive sense herein so that confusion with signs is avoided in the resulting scalar equations. Hence

$$\Delta E_d = \int_{t_o}^{t_1} D \, V_w \cos \varphi \, dt - \int_{t_o}^{t_1} D \, u \cos \varphi \, dt + \int_{t_o}^{t_1} D \, V_w \sin \varphi \, dt \qquad (63a)$$

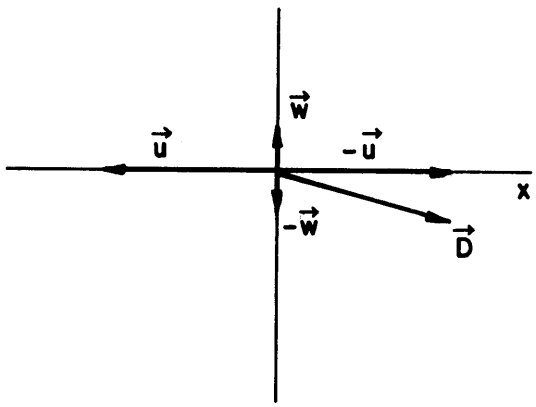


Fig. 14

Eq. (63) shows that the dissipation energy is supplied both by the wind and the absolute velocity of the bird. The energy is extracted from these sources in exact proportion to the relative magnitudes of the velocities. In particular, it is noted that the vertical velocity w of the bird causes an increase in the dissipation energy.

Let us now consider what happens to the original kinetic energy supply $1/2 \, W/g \, u_o^2$ of the bird during the climb. The work done by the bird in moving with the velocity $\hat{u}$ against the force $\hat{F}_x$ in the time interval $t_1 - t_o$ is

$$\int_{t_o}^{t_1} \hat{F}_x \cdot \hat{u} \, dt = \int_{t_o}^{t_1} \frac{W}{g} \frac{d\hat{u}}{dt} \cdot \hat{u} \, dt = - \frac{1}{2} \frac{W}{g} (u_o^2 - u_1^2) \qquad (64)$$

The left integral of this equation can also be written in terms of the components of $\hat{F}_x$,

$$\int_{t_o}^{t_1} \hat{F}_x \cdot \hat{u} \, dt = \int_{t_o}^{t_1} D \cos \varphi \, \hat{i} \cdot \hat{u} \, dt + \int_{t_o}^{t_1} L \sin \varphi \, \hat{i} \cdot \hat{u} \, dt \qquad (65)$$

or

$$\int_{t_o}^{t_1} \hat{F}_x \cdot \hat{u} \, dt = \int_{t_o}^{t_1} D \cos \varphi \, u \, dt + \int_{t_o}^{t_1} L \sin \varphi \, u \, dt \qquad (65a)$$

Combining eqs. (64) and (65a) we obtain

$$-\int_{t_o}^{t_1} D \cos\varphi \, u \, dt - \int_{t_o}^{t_1} L \sin\varphi \, u \, dt = \frac{1}{2}\frac{W}{g}(u_o^2 - u_1^2) \qquad (66)$$

This equation shows that the initial kinetic energy possessed by the bird is used in two ways: (1) to provide a part of the dissipation energy, as indicated by the first integral on the left and (2) to provide the energy for work done by the force $L \sin\varphi$. Eq. (63a) shows that the force $L \sin\varphi$ is not involved in the dissipation energy and hence must be concerned with the potential energy increase $W(z_1 - z_o)$, and kinetic energy increase $1/2\ W/g\ w^2$.

The work done by the vertical force $\hat{F}_z$ is given by

$$\int_{t_o}^{t_1} \hat{F}_z \cdot \hat{w} \, dt = \int_{t_o}^{t_1} L \cos\varphi \, \hat{j} \cdot \hat{w} \, dt - \int_{t_o}^{t_1} D \sin\varphi \, \hat{j} \cdot \hat{w} \, dt \qquad (67)$$

or

$$\int_{t_o}^{t_1} \hat{F}_z \cdot \hat{w} \, dt = \int_{t_o}^{t_1} L \, w \cos\varphi \, dt - \int_{t_o}^{t_1} D \, w \sin\varphi \, dt \qquad (67a)$$

Also,

$$\int_{t_o}^{t_1} \hat{F}_z \cdot \hat{w} \, dt = \int_{t_o}^{t_1} \left(\frac{W}{g}\frac{d\hat{w}}{dt} - \hat{W}\right) \cdot \hat{w} \, dt \qquad (68)$$

or

$$\int_{t_o}^{t_1} \hat{F}_z \cdot \hat{w} \, dt = \int_{w_o}^{w_1} \frac{W}{g} w \, dw + \int_{z_o}^{z_1} W \, dz = \frac{1}{2}\frac{W}{g}(w_1^2 - w_o^2) + W(z_1 - z_o) \qquad (69)$$

Thus, equating eqs. (67a) and (69) we obtain

$$\frac{1}{2}\frac{W}{g}(w_1^2 - w_o^2) + W(z_1 - z_o) = \int_{t_o}^{t_1} L \, w \cos\varphi \, dt - \int_{t_o}^{t_1} D \, w \sin\varphi \, dt \qquad (70)$$

The terms on the left represent the kinetic energy of the vertical motion and tha gain in potential energy of the bird, respectively.

By combining eqs. (66) and (70) we obtain the general expression for the overall energy balance

$$\frac{1}{2}\frac{W}{g}(w_1^2 - w_o^2) + W(z_1 - z_o) - \int_{t_o}^{t_1} D\, u \cos\varphi\, dt + \int_{t_o}^{t_1} D\, w \sin\varphi\, dt$$

$$= \frac{1}{2}\frac{W}{g}(u_o^2 - u_1^2) + \int_{t_o}^{t_1} L\, u \sin\varphi\, dt + \int_{t_o}^{t_1} L\, w \cos\varphi\, dt \qquad (71)$$

Then adding $\int_{t_o}^{t_1} D\, V_w \cos\varphi\, dt$ to each side of eq. (71) and using eq. (63a), we obtain

$$\frac{1}{2}\frac{W}{g}(w_1^2 - w_o^2) + W(z_1 - z_o) + \Delta E_d = \frac{1}{2}\frac{W}{g}(u_o^2 - u_1^2) + \int_{t_o}^{t_1} L\, w \cos\varphi\, dt$$

$$+ \int_{t_o}^{t_1} L\, u \sin\varphi\, dt + \int_{t_o}^{t_1} D\, V_w \cos\varphi\, dt \qquad (72)$$

Now applying the exact relations

$$\cos\varphi = \frac{V_w - u}{V_R}$$

$$\sin\varphi = \frac{w}{V_R} \qquad (72a)$$

we obtain the final (exact) expression for the energy equation

$$\underbrace{\frac{1}{2}\frac{W}{g}(w_1^2 - w_o^2)}_{\text{K.E. increase}} + \underbrace{W(z_1 - z_o)}_{\text{P.E. increase}} + \underbrace{\Delta E_d}_{\substack{\text{Dissi-}\\\text{pation}\\\text{Energy}}} = \underbrace{\frac{1}{2}\frac{W}{g}(u_o^2 - u_1^2)}_{\text{K.E. decrease}} +$$

$$\underbrace{\int_{t_o}^{t_1} L\frac{w}{V_R} V_w\, dt + \int_{t_o}^{t_1} D\, V_w \cos\varphi\, dt}_{\text{Energy from wind}} \qquad (73)$$

Here $V_R$ has the value $[(V_w - u)^2 + w^2]^{1/2}$ .

To summarize the results obtained above, we note that the change in kinetic energy $1/2\ W/g\ (u_o^2 - u_1^2)$ associated with the horizontal motion of the bird provides all that portion of the dissipation drag expressed by $\int_{t_o}^{t_1} \hat{D} \cdot \hat{u}\ dt$ and a part of the kinetic and potential energies $1/2\ W/g\ (w_1^2 - w_o^2)$ and $W(z_1 - z_o)$. It also supplies a part of the dissipation energy for the term $\int_{t_o}^{t_1} \hat{D} \cdot \hat{w}\ dt$. The remainder of the energy requirements are furnished by the wind, according to the last two integrals on the right side of eq. (73). It is seen that the energy for increasing the kinetic energy of vertical motion and potential energy, plus the dissipation energy associated with w, is supplied by both the wind and the initial kinetic energy of horizontal motion of the bird, in direct proportion to the velocities $V_w$ and u, respectively.

The dissipation energy $\int_{t_o}^{t_1} \hat{D} \cdot \hat{V}_w\ dt$ is never really taken from the air; the ordered motion of the wind $V_w$ is merely converted to the "random" motion associated with the dissipation processes (vortex and viscous wakes).

Eq. (73) can be derived more directly, of course, by treating both force components $F_x$ and $F_z$ simultaneously in one equation. Thus, denoting by $\Sigma\hat{F}$ the sum of all forces acting on the bird at any instant, we have by Newton's second law

$$\Sigma\hat{F} = \frac{W}{g} \frac{d\hat{V}_a}{dt}$$

where $\hat{V}_a$ is the absolute velocity of the bird. Then taking the scalar product of each side of the above equation with $\hat{V}_a$, the working of all forces is obtained:

$$\int_{t_o}^{t_1} \Sigma\hat{F} \cdot \hat{V}_a\ dt = \frac{W}{g} \int_{t_o}^{t_1} \frac{d\hat{V}_a}{dt} \cdot \hat{V}_a\ dt$$

Expanding this relation we obtain

$$\int_{t_o}^{t_1} (\hat{L} + \hat{D} + \hat{W}) \cdot (\hat{u} + \hat{w})\ dt = \frac{W}{g} \int_{t_o}^{t_1} \frac{d}{dt} (\hat{u} + \hat{w}) \cdot (\hat{u} + \hat{w})\ dt$$

$$\int_{t_o}^{t_1} (\hat{L} \cdot \hat{u} + \hat{L} \cdot \hat{w} + \underbrace{\hat{D} \cdot \hat{u} + \hat{D} \cdot \hat{w}}_{\text{Dissipation}} + \underbrace{\hat{W} \cdot \hat{u}}_{=0} + \underbrace{\hat{W} \cdot \hat{w}}_{\text{P.E.}})\ dt = \underbrace{\frac{1}{2} \frac{W}{g} (u_1^2 - u_o^2) + \frac{1}{2} \frac{W}{g} (w_1^2 - w_o^2)}_{\text{K.E.}}$$

The terms $\hat{L} \cdot \hat{u}$ $(= L\ u \sin \varphi = L\ w/V_R\ u)$ and $\hat{L} \cdot \hat{w}$ $(= L\ w \cos \varphi = L \frac{V_w - u}{V_R} w)$ reduce to $L\ w/V_R\ V_w$, so that adding $\int_{t_o}^{t_1} \hat{D} \cdot \hat{V}_w\ dt$ to each side and expanding the products yields eqs. (73) identically.

In a preceding section (page 26), it was stated that the horizontal velocity component $u$ and the vertical velocity component $w$ are not independent, and that if $w$ is made large, as a result of the vertical acceleration, the value of $u$ will correspondingly decrease, assuming the conditions prior to the acceleration to be $u = u_i$, $w = 0$, $z = z_i$. This relationship between $u$ and $w$ during the vertical acceleration, for a given initial value of $u_i$, can be developed in an approximate form by using the preceding energy relations. Using eq. (66) and the expression $dt = dz/w$ we have

$$-\int_{z_i}^{z_1} D \frac{u}{w} \cos \varphi \, dz - \int_{z_i}^{z_1} L \frac{u}{V_R} dz = \frac{1}{2} \frac{W}{g} (u_i^2 - u_o^2) \qquad (74)$$

During the vertical acceleration period at the beginning of the climb, that is, at very low altitude, $V_w \ll u$ and hence we can take $-u = V_R$ approximately. The integral $-\int_{z_i}^{z_o} D \frac{u}{w} \cos \varphi \, dz$ can be expressed in the form $n \int_{z_i}^{z_o} L \, dz$ as follows.

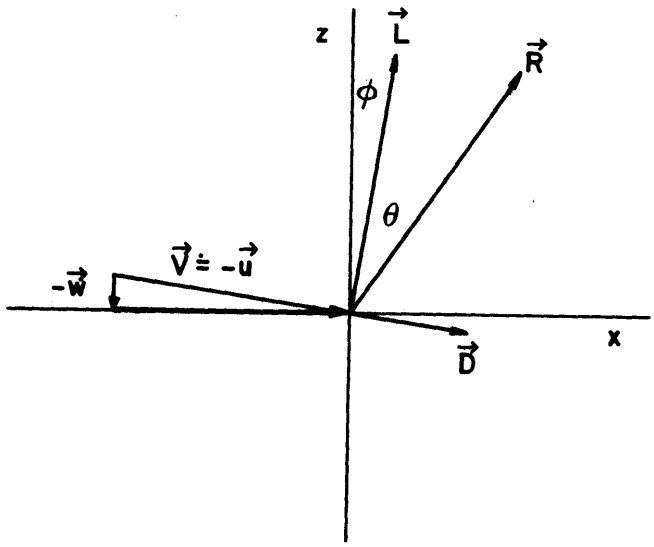


Fig. 15

From Fig. 15 we have

$$R \cos (90^\circ - (\varphi + \theta)) = -L \frac{w}{u} D \cos \varphi \qquad (75)$$

Assuming $L \doteq R$, eq. (75) becomes

$$L \sin (\varphi + \theta) + L \frac{w}{u} = D \cos \varphi \qquad (76)$$

Now let $\theta = n\varphi$ where $n$ gives an average or effective value of $\theta$ (or $L/D$) during the vertical acceleration period.

Then

$$L\left[\sin \left\{\varphi(1+n)\right\} + \frac{w}{u}\right] = D \cos \varphi \qquad (77)$$

But since $\varphi$ and $\theta$ are both small angles ($\theta$ must be small for large values of $L/D$ since $\theta = \tan^{-1} D/L$), we have

$$\sin [\varphi (1 + n)] = -\frac{w}{u} (1 + n) \qquad (78)$$

and

$$D \cos \varphi = -L \frac{w}{u} (1 + n - 1) = -n L \frac{w}{u} \qquad (79)$$

$$-\int_{z_i}^{z_o} D \cos \varphi \frac{u}{w} dz = n \int_{z_i}^{z_o} L \, dz \qquad (80)$$

The constant n gives the effective value of L/D for the entire vertical acceleration period in terms of the angle $\varphi$. Using eq. (80) in eq. (74) we obtain

$$n \int_{z_i}^{z_o} L \, dz + \int_{z_i}^{z_o} L \, dz = \frac{1}{2} \frac{W}{g} (u_i^2 - u_o^2) \tag{81}$$

The lift L can be written as

$$L = W + \frac{W}{g} w \frac{dw}{dz} \tag{82}$$

so that

$$\int_{z_i}^{z_o} L \, dz = \int_{z_i}^{z_o} W \, dz + \int_{o}^{w} \frac{W}{g} w' \, dw' \tag{83}$$

Thus eq. (81) becomes

$$\frac{1}{2} \frac{W}{g} (u_i^2 - u_o^2) = (1 + n) \left[ W(z_o - z_i) + \frac{1}{2} \frac{W}{g} w^2 \right] \tag{84}$$

The factor n in this equation accounts for the dissipation energy lost during the acceleration up to the vertical velocity w. Eq. (84) can be written as

$$\frac{1}{2} \frac{W}{g} u_i^2 = (1 + n) \left[ W(z_o - z_i) + \frac{1}{2} \frac{W}{g} w^2 \right] + \frac{1}{2} \frac{W}{g} u_o^2 \tag{85}$$

This equation gives the explicit relation between $u_o$ and w and clearly shows that $u_o$ will decrease as w increases for given values of $u_i$ and n. Since n is inherently positive, a part of the available kinetic energy $1/2 \, W/g \, (u_i^2 - u_o^2)$ is dissipated by the drag experienced during the acceleration while the remainder goes to increase the kinetic energy of the vertical motion and the potential energy. It is clearly desirable to have n as small as possible and hence a large value of L/D is necessary.

It is possible, of course, to determine the relationship between u and w exactly when $V_w(z)$, $C_L(z)$, and L/D ($C_L$) are given, by direct integration of the equations of motion as discussed previously in "Solution of the Equations of Motion" on page 27.

It was stated in the preceding part "b" (page 33) that the energy equation would allow the simultaneous determination of $V_w(z)$, $C_L(z)$, and L/D ($C_L$) from photographic data. To indicate how this solution is obtained, we must develop the energy equation in a form which lends itself to this purpose. We first rewrite eq. (73) in the form

$$\frac{1}{2}\frac{W}{g}(w^2 - w_o^2) + W(z - z_o) - \int_{t_o}^{t} D\, u \cos\varphi\, dt + \int_{t_o}^{t} D\, w \sin\varphi\, dt = \frac{1}{2}\frac{W}{g}(u_o^2 - u^2) + \int_{t_o}^{t} L \frac{w}{V_R} V_w\, dt \quad (86)$$

Differentiating both sides of this equation with respect to $t$ we obtain

$$\frac{W}{g} w \frac{dw}{dt} + W \frac{dz}{dt} - D\, u \cos\varphi + D\, w \sin\varphi = -\frac{W}{g} u \frac{du}{dt} + L \frac{w}{V_R} V_w \quad (87)$$

In terms of $dz$, eq. (87) becomes

$$\frac{W}{g} w^2 \frac{dw}{dz} + Ww - D\, u \cos\varphi + D\, w \sin\varphi = -\frac{W}{g} u\, w \frac{du}{dz} + L \frac{w}{V_R} V_w \quad (87a)$$

Since $\cos\varphi = \frac{V_w - u}{V_R}$ and $\sin\varphi = \frac{w}{V_R}$, eq. (87a) can be rewritten as

$$\frac{W}{g} w^2 \frac{dw}{dz} + Ww - D\, u \frac{V_w - u}{V_R} + D \frac{w^2}{V_R} = -\frac{W}{g} u\, w \frac{du}{dz} + L \frac{w}{V_R} V_w \quad (88)$$

This equation is exact, that is, it has not been linearized in any way. For use with the flight path data, the quantities $w$, $u$, $dw/dz$, and $W$ are known. The unknown variables are $D$, $L$, and $V_w$. The velocity $V_R = [(V_w - u)^2 + w^2]^{1/2}$ contains $V_w$ implicitly.

Eq. (88) can be linearized by applying the assumptions $\cos\varphi = 1$, $V_R = V_w - u$, and $\sin\varphi = w/(V_w - u)$. Thus we obtain

$$\frac{W}{g} w^2 \frac{dw}{dz} + Ww - D\, u + D \frac{w^2}{V_w - u} = -\frac{W}{g} u\, w \frac{du}{dz} + L \frac{wV_w}{V_w - u} \quad (89)$$

for the linearized form of the energy equation.

In order to solve for the unknown variables we use eqs. (19) and (20)

$$\frac{du}{dz} = \frac{g}{W}\left(D + L \frac{w}{V_w - u}\right) w^{-1} \quad (19)$$

$$\frac{dw}{dz} = \frac{g}{W}(L - W)\, w^{-1} \quad (20)$$

along with eq. (89). (All of these equations are of the linearized form for simplicity; however, eqs. (13) and (14) along with eq. (88) could be used to obtain the exact solutions if desired.) To determine $V_w(z)$, $L(z)$, and $D(z)$, we solve the three simultaneous eqs. (19), (20), and (89) over a range of values of $z$ for which the flight path data are available. To cite one procedure, we solve eq. (20) for $L$. Substituting this value of $L$ in eqs. (19) and (89), we obtain two equations in $D$ and $V_w$. Solving eq. (19) for $D$ in terms of $V_w$ and substituting for $D$ in eq. (89), we can finally obtain the value of $V_w$. Then from eq. (19) we can obtain the value of $D$.

Obtaining the solutions for several values of $z$, the unknown functions $D$, $L$, and $V_w$ can be constructed. The coefficients $C_D$, $C_L$, and $C_L/C_D$ can be determined from the relations $C_D = D/[\rho/2(V_w - u)^2 S]$ and $C_L = L/[\rho/2(V_w - u)^2 S]$ if desired. Thus from experimental measurement of the flight path, all the major functions which govern the albatross' motion during the windward climb can be quantitatively determined.

The High Altitude Turn to Leeward

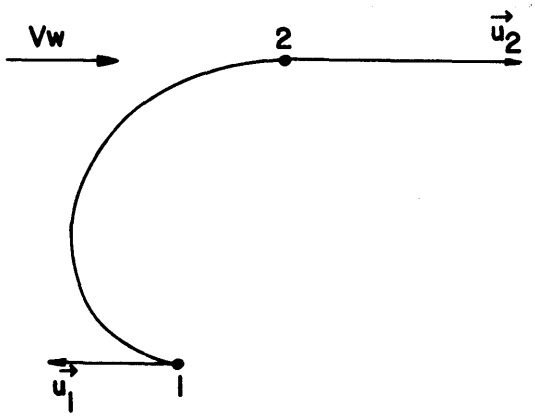


The high altitude turn to leeward is perhaps the most important phase of the basic soaring cycle, since it furnishes the primary energy supply for dynamic soaring by the albatross. Yet, aerodynamically, it is probably the simplest phase of all. By executing a simple 180° gliding turn from windward to leeward near the top of the shear layer, the albatross extracts from the horizontal wind the energy necessary to power its amazing endurance flights.

**Fig. 16**

The Kinetic Energy Gain of the Leeward Turn.- Consider the bird at the end of the windward climb, when it has reached its maximum altitude $z = z_f$ near the top of the shear layer and is moving upwind with an absolute velocity $\hat{u}$ (it is assumed that the vertical velocity component has decreased to zero at $z_f$, $w = 0$). The bird banks its wings and commences a turn toward the leeward direction. We shall assume that this turn is accomplished at essentially constant altitude $z = z_f$; in reality it is actually a gliding turn in which the bird loses some slight amount of altitude, but we can neglect this fact in our present analysis. We employ a set of $x$, $y$ coordinate axes to describe the turn, and all vector quantities are taken as positive in the positive direction of the coordinate axes. Under the assumption of constant altitude, the wind speed $V_{wf} = V_w(z_f)$ is constant at all points in the plane of the turn.

At the beginning of the turn (point 1 in Fig. 16), the bird possesses an aerodynamic velocity $\hat{V}_c = \hat{u}_1 - \hat{V}_{wf}$.* The absolute speed $u_1$ of the bird is therefore,

$$u_1 = V_c + V_{wf} \tag{90}$$

Here $V_c$ has a negative value; eq. (90) can be written alternately as $u_1 = V_c - V_{wf}$. The bird maintains a constant airspeed $V_c$ throughout the turn; hence the absolute velocity $\hat{u}_2$ at the end of the turn (point 2 in Fig. 16) has the magnitude

$$u_2 = V_c + V_{wf} \tag{91}$$

where both $V_c$ and $V_{wf}$ are positive; $|u_2| = |V_c| + V_{wf}$. Corresponding to these two absolute velocities, the bird possesses kinetic energy of

$$\begin{aligned} KE_1 &= \frac{1}{2}\frac{W}{g}(V_c - V_{wf})^2 \\ KE_2 &= \frac{1}{2}\frac{W}{g}(V_c + V_{wf})^2 \end{aligned} \tag{92}$$

Here $V_c$ denotes the (constant) absolute value of the airspeed. From eq. (92) it is seen that the bird has gained kinetic energy in turning from point 1 to point 2 in the amount

$$\Delta KE_{1,2} = \frac{1}{2}\frac{W}{g}[(V_c + V_{wf})^2 - (V_c - V_{wf})^2] \tag{93}$$

or

$$\Delta KE_{1,2} = 2\frac{W}{g} V_c V_{wf} \tag{94}$$

This kinetic energy supply may be used as the bird desires for various flight purposes, such as distance travel in a particular direction. Two basic restrictions are placed upon the use of this energy, however. First, enough of it must be saved to allow the subsequent windward climb to proceed, and second, all turns and partial turns made subsequent to the completion of the leeward turn must be made at very low altitudes, near the water surface. The reason for the first restriction we have already discussed in the preceding section on the windward climb; the reason for the second one will be discussed in the following section on the low altitude turn to windward.

The gain in kinetic energy as given by eq. (94) is seen to be proportional to the product of the airspeed in the turn and the wind speed at the altitude of the turn. It is clear that, for maximum energy gain, the turn must be made at

---

*In reality $V_c$ is the horizontal component of the aerodynamic velocity; under the present assumption $w = 0$, it becomes the total aerodynamic velocity.

the altitude where $V_c\, V_{wf}$ is a maximum. Since $V_c = |u_1| + V_{wf}$, maximum energy gain may well occur at altitudes below the top of the shear layer, if $|u|$ decreases too rapidly with altitude (i.e., $du/dz$ large). The maximum attainable energy gain in such cases may be relatively small. In order to obtain the largest gain, with regard to the maximum allowed by the wind speed available, it is necessary that the decrease in $|u|$ with altitude be sufficiently small that $V_c$ ( $= |u_1| + V_{wf}$) reaches its maximum value at or above the top of the shear layer (where $V_w$ is also maximum).

Eq. (94), written in terms of $|u_1|$ becomes

$$\Delta KE_{1,2} = 2 \frac{W}{g} ( |u_1|\, V_{wf} + V_{wf}^2) \qquad (95)$$

This relation shows the importance of the bird having a small value for $|du/dz|$ for use of weak winds, as discussed previously in "Analysis of the Equations of Motion", page 20. For large energy gains, it is desirable that $|u_1|$ be large when $V_{wf}$ is essentially equal to $V_w$*; when the wind is weak, $|du/dz|$ must be very small if any useful amount of kinetic energy is to be obtained, since then even $V_w$* becomes small.

It should be noted that $|u_1|$ depends not only on $du/dz$ but also on $u_o$, the horizontal velocity at the beginning of the windward climb, since

$$u_1 = u_o + \int_o^{z_1} \frac{du}{dz}\, dz \qquad (96)$$

The magnitude of $u_o$ is, in turn, implicitly dependent upon the velocity (or energy) gained in the preceding leeward turn. Thus, if the gain in $|u|$ during the turn ( $|u_2| - |u_1|$ ) is small, $u_o$ will be small, and may not be sufficient for the requirements of the succeeding windward climb. From eq. (95) it is clear that even if $|du/dz|$ is relatively small, as the wind speed decreases the gain in kinetic energy will decrease, and ultimately will become less than that required for sustained soaring.

Mechanisms of the Energy Gain. - The preceding discussion was based upon the simple kinematic relationship between the initial and final absolute velocities of the bird in the turn. It is of interest, however, to consider the dynamics of the turn as well, in order to examine more explicitly the process by which the bird extracts its flight energy from the horizontal wind.

Before considering the actual leeward turn conditions, it will be helpful to examine the aerodynamic relations existing during a turn in still air, that is, a turn in which the wind speed is zero, since the aerodynamic forces and velocities in the leeward turn (with wind) are exactly the same as in a still-air turn. The more complex absolute motion of the actual leeward turn (with wind) can then be simply obtained by vectorially adding the wind velocity $\hat{V}_{wf}$ to the aerodynamic velocity $\hat{V}_c$ of the still-air case.

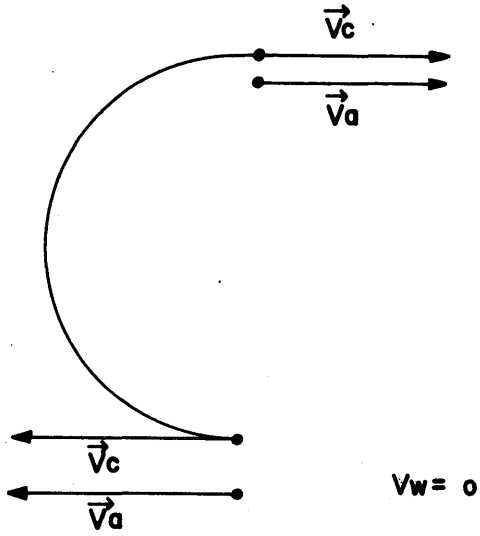


Fig. 17

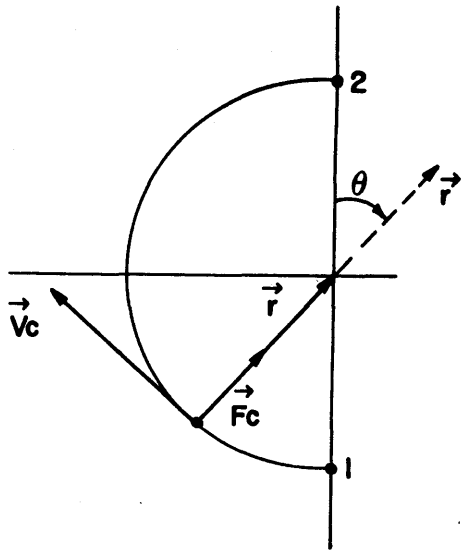


Fig. 18

Consider a bird at the start of a gliding turn in still air ($\hat{V}_w = 0$) with an airspeed $\hat{V}_c$ (where the sinking velocity $\hat{w}$ is assumed negligible). The initial absolute velocity $\hat{u}$ of the bird at the beginning of the turn is then equal to $\hat{V}_c$ (Fig. 17). The bird executes a 180° turn by banking its wings so that a component $\hat{F}_c$ of the lift acts horizontally to pull the bird around the turn, and since there is no wind, the absolute velocity $\hat{V}_a$ of the bird* at any point is equal to the aerodynamic velocity $\hat{V}_c$. The centripetal force $\hat{F}_c$ produces a constant radial acceleration according to the relation

$$\hat{F}_c = \frac{W}{g} \frac{V_c^2}{r^2} \hat{r} \tag{97}$$

where $r$ is the radius of the resulting turn (Fig. 18). The position vector $\hat{r}$ connects the bird and the center of the turn, and is positive in the direction of the center. The angle $\theta$ in Fig. 18 denotes the angular displacement of the vector $\hat{r}$ from its initial "vertical" position ($\theta = 0°$). Thus, as the bird turns from point 1 to point 2 it generates a smooth semicircle of radius $r$; $\hat{V}_c$ and $\hat{F}_c$ remain perpendicular to one another and rotate through 180°. The bird completes the turn ($\theta = 180°$) with the same absolute speed it started with; no energy gain has occurred.

---

*The vector $\hat{V}_a$ denotes the absolute velocity of the bird. It has the components $\hat{u}$ and $\hat{v}$ parallel to the $x$ and $y$ coordinate axes, respectively. At the beginning and end of the turn, $\hat{V}_a = \hat{u}$ since $\hat{v} = 0$ at these points (see Fig. 19).

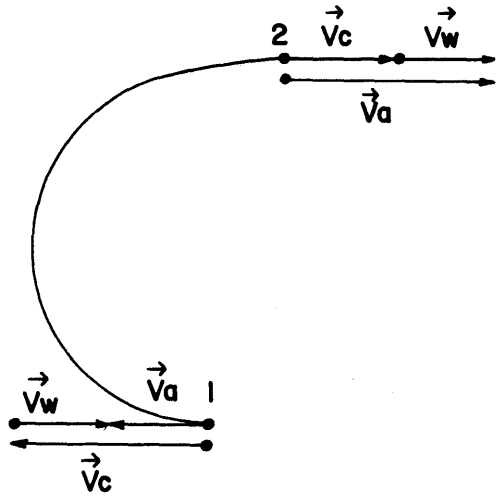


Fig. 19

Now consider the actual case of the leeward turn as previously discussed where a wind of magnitude $\hat{V}_{wf}$ exists at the altitude of the turn. This actual case can be obtained directly from the still-air case described in the preceding paragraph by superposing on both the air and the bird an absolute velocity $\hat{V}_{wf}$. This results in the creation of a wind $\hat{V}_{wf}$, and the conditions then become as shown in Fig. 19; the absolute velocity $\hat{u}$ of the bird has been decreased by the amount $\hat{V}_{wf}$, but the aerodynamic velocity $\hat{V}_c$ remains unchanged since both air and bird received the same absolute velocity change $\hat{V}_{wf}$. Since the aerodynamic velocity is the same in both cases, it follows that the motion of the bird relative to the air, and the aerodynamic force $\hat{F}_c$ will also be unaltered. The vectors $\hat{V}_c$ and $\hat{F}_c$ will again rotate at a uniform angular rate through 180° as the bird turns from windward to leeward. The flight path relative to earth will be different from the still-air case, however since now $\hat{V}_a = \hat{V}_c + \hat{V}_{wf}$ instead of simply $\hat{V}_a = \hat{V}_c$. It is clear that in the actual leeward turn a gain in kinetic energy will occur.

The gain in kinetic energy experienced during the leeward turn is equal to the work $w_k$ done by the centripetal force $\hat{F}_c$ on the bird during the turn. Using the relations of Fig. 20, the rate at which this work is done is given by

$$\frac{dw_k}{dt} = \hat{F}_c \cdot \hat{V}_a \tag{98}$$

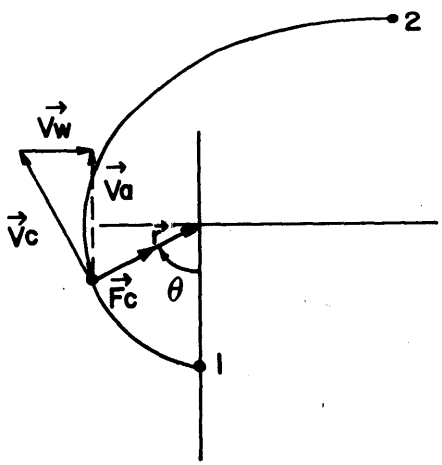


Fig. 20

or

$$\frac{dw_k}{dt} = \hat{F}_c \cdot (\hat{V}_c + \hat{V}_{wf}) \tag{99}$$

The centripetal force is given by eq. (97). Thus,

$$\frac{dw_k}{dt} = \hat{F}_c \cdot \hat{V}_{wf} = \frac{W}{g}\frac{V_c^2}{r} V_{wf} \sin\theta \tag{100}$$

since $\hat{F}_c \cdot \hat{V}_c = 0$. The vector $\hat{r}$ is positive between points 1 and 2 so that eq. (100) gives the rate at which the bird is receiving energy. Physically, this means that the bird, in order to turn in the leeward direction, must

impart momentum to the air in a direction opposite to that of the wind. Since the air is moving with an initial absolute speed $V_{wf}$, this reduction in the x-momentum of the air corresponds to a loss in its kinetic energy. The energy lost by the air is transferred to the bird.

The total work done by the centripetal force during the turn from point 1 to point 2 is obtained by integrating the instantaneous power being supplied [eq. (100)] over the time required to make the turn. Thus

$$w_{k_{1,2}} = \int_{t_1}^{t_2} \frac{W}{g} \frac{V_c^2}{r} \; V_{wf} \sin\theta \; dt \tag{101}$$

Let $\theta = \omega t$ where $\omega$ is the constant angular velocity of rotation of the bird in the turn,

$$\omega = \frac{V_c}{r} \tag{102}$$

Then

$$dt = \frac{d\theta}{\omega} = \frac{r}{V_c} d\theta \tag{103}$$

and

$$w_{k_{1,2}} = \int_0^{\pi} \frac{W}{g} V_c \; V_{wf} \sin\theta \; d\theta = 2 \frac{W}{g} V_c \; V_{wf} \tag{104}$$

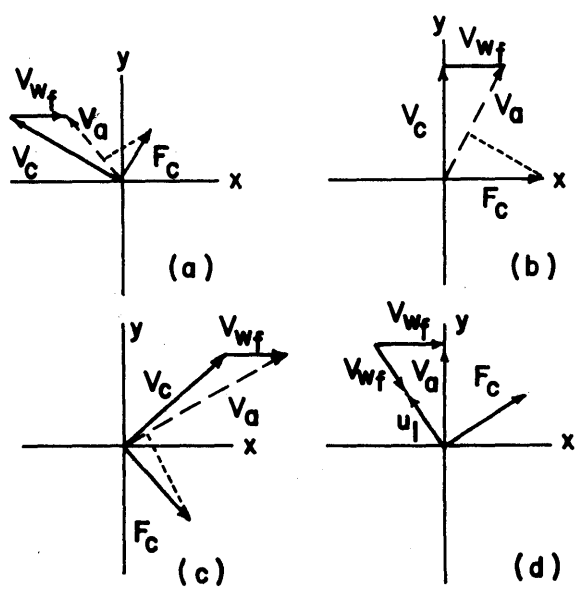


Fig. 21

The total work done by $\hat{F}_c$ is thus equal to the kinetic energy gained by the bird during the turn [eq. (94)].

The nature of the kinetic energy gain can be seen by examining the force-velocity relationship at various points (various $\theta$ values) along the turn path. Fig. 21(a) shows the conditions at the point where $\theta = 30^\circ$ or just after the turn has commenced. The absolute velocity $\hat{V}_a$ has increased relative to its initial value $\hat{u}_1$ at the beginning of the turn ($\theta = 0^\circ$). Hence the bird has already gained kinetic energy, although it is still moving with a component of its absolute velocity in the upwind direction (i.e., $\hat{u}$ is still negative). The fact that a component of the force $\hat{F}_c$ is acting in the direction of $\hat{V}_a$ means, of course, that the bird is accelerating (and thus gaining kinetic energy) in

the direction of motion. It will be shown in the next paragraph that the bird retains all its initial kinetic energy due to $\hat{u}_1$ and that the total energy at any other point is equal to this initial energy plus that due to the work of $\hat{F}_c$. At $\theta = 90^\circ$ [Fig. 21(b)] the bird has gained even more absolute speed and kinetic energy and is now moving with a component of $\hat{V}_a$ in the downwind direction ($\hat{u}$ positive). The value of $\theta$ for which $\hat{u} = 0$ is clearly less than $90^\circ$; this value is obtained for the condition where $\hat{V}_a$ lies along the y-axis. The bird is still accelerating in the direction of $\hat{V}_a$. Near the end of the turn [Fig. 21(c)], $V_a$ is rapidly approaching its maximum value $\hat{V}_a = \hat{V}_c + V_{wf}$. The force component acting along $\hat{V}_a$ has now decreased to a small value, however, and the acceleration is rapidly approaching zero. By comparing the diagrams of Fig. 21 it can be easily seen that the absolute velocity of the bird, and hence the kinetic energy, increases continuously throughout the turn. The accelerating force, on the other hand, increases from zero at $\theta = 0^\circ$ up to a maximum, and then decreases again to zero at $\theta = 180^\circ$.

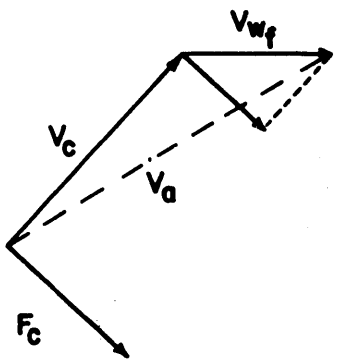


Fig. 22

At the start of the turn, the bird possesses an amount of kinetic energy $1/2\ W/g\ u_1^2$ due to its absolute speed $u_1$ in the upwind direction. As the bird turns it retains all of this energy even though the value of $|\hat{u}|$ is continuously decreasing during the first half of the turn. The additional increase in kinetic energy above the initial value, at any point of the turn, is equal to the work done by the wind on the bird. This is easily shown by consideration of Fig. 21(d), which gives the vector diagram for the point $\theta = \theta_a$, where $\hat{u} = 0$ and $\hat{V}_a$ lies along the y-axis. The condition we wish to verify is that

$$\frac{1}{2}\frac{W}{g}V_a^2 - \frac{1}{2}\frac{W}{g}u_1^2 = \int_0^{\theta_a}\frac{W}{g}V_c\,V_{wf}\sin\theta\,d\theta \qquad (105)$$

Expanding the left side of this equation, we obtain

$$\frac{1}{2}\frac{W}{g}(V_a^2 - u_1^2) = \frac{1}{2}\frac{W}{g}(V_{wf}^2 + 2u_1V_{wf} + u_1^2 - V_{wf}^2 - u_1^2) = u_1V_{wf}\frac{W}{g} \qquad (106)$$

since from Fig. 21(d), $V_a^2 = (u_1 + V_{wf})^2 - V_{wf}^2$. Evaluating the right side of eq. (105) we obtain

$$\int_0^{\theta_a}\frac{W}{g}V_c\,V_{wf}\sin\theta\,d\theta = \frac{W}{g}V_c\,V_{wf}(1 - \cos\theta_a) \qquad (107)$$

From Fig. 21(d)

$$\cos \theta_a = \frac{V_{wf}}{u_1 + V_{wf}} \tag{108}$$

and the right side of eq. (105) becomes

$$\frac{W}{g} (u_1 + V_{wf}) V_{wf} \left[ \frac{u_1 + V_{wf} - V_{wf}}{u_1 + V_{wf}} \right] = u_1 V_{wf} \frac{W}{g} \tag{109}$$

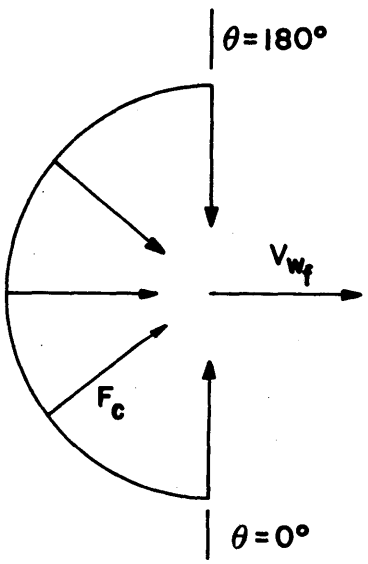


Fig. 23

Thus eq. (105) is proved for the point $\theta_a$; it is equally true for all values of $\theta$.

From the diagram of Fig. 22, it is evident that only $\hat{V}_{wf}$ has a component in the direction of $F_c$ and consequently all work done on the bird comes from the energy of the horizontal wind. As can be seen in Fig. 23, $\hat{V}_{wf}$ has a component in the direction of $F_c$ for the entire region $\theta^o \leqq \theta \leqq 180^o$.

Geometry of the Flight Path. - The flight path generated by the leeward turn is, mathematically, a segment of a trochoid. A trochoid is the curve generated by the tip of

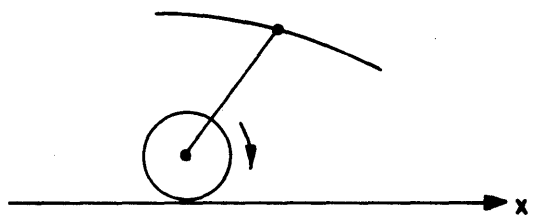


Fig. 24

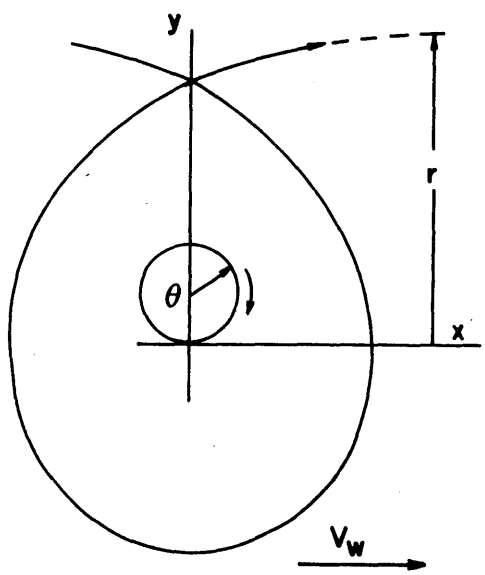


Fig. 25

a radial line segment extending from the center of a circle, as the circle rolls along the x-axis, (Fig. 24). In the present case, the bird is making a semi-circle of radius $r$ relative to the air, while the air is moving with speed $V_{wf}$ relative to the earth. From the trochoid geometry shown in Fig. 25, the radius of the corresponding trochoid circle is thus seen to be

$$\frac{V_{wf}}{V_c} r \tag{110}$$

A simple analysis of the trochoid geometry yields the equations of the leeward turn in terms of the parameter $\theta$

$$\frac{x}{r} = \frac{V_{wf}}{V_c} \theta - \sin \theta \tag{111}$$

$$\frac{y}{r} = \frac{V_{wf}}{V_c} - \cos \theta \tag{112}$$

Here $\theta$ denotes angular displacement of the radius $r$ as the bird turns.

Since $\theta$ is related to the time $t$ by

$$\theta = \omega t = \frac{V_c}{r} t \tag{113}$$

eqs. (111) and (112) can be written as follows

$$x = V_{wf} t - r \sin \frac{V_c}{r} t \tag{114}$$

$$y = \frac{V_{wf}}{V_c} r - r \cos \frac{V_c}{r} t \tag{115}$$

The velocity components $u$ and $v$ of the absolute motion are then obtained directly by time differentiation of eq. (114) and (115)

$$u = \frac{dx}{dt} = V_{wf} - V_c \cos \frac{V_c}{r} t \tag{116}$$

$$v = \frac{dy}{dt} = V_c \sin \frac{V_c}{r} t \,. \tag{117}$$

The total speed $V_a$ is then obtained from the relation

$$V_a = (u^2 + v^2)^{1/2} \tag{118}$$

whence

$$V_a = \left( V_{wf}^3 - 2 V_{wf} V_c \cos \frac{V_c}{r} t + V_c^2 \right)^{1/2} \tag{119}$$

The acceleration components $a_x$ and $a_y$ are obtained by a second differentiation of eqs. (114) and (115)

$$a_x = \frac{d^2x}{dt^2} = \frac{V_c^2}{r} \sin \frac{V_c}{r} t \tag{120}$$

$$a_y = \frac{d^2y}{dt^2} = \frac{V_c^2}{r} \cos \frac{V_c}{r} t \tag{121}$$

The total acceleration is thus given by

$$a = \frac{V_c^2}{r} \tag{122}$$

This is, of course, the centripetal acceleration produced by the aerodynamic force component $\hat{F}_c$. It is possible to determine the acceleration components directly from the centripetal force equation. Using Newton's second law, we have

$$\hat{F}_c \cdot \hat{i} = \frac{W}{g} \frac{V_c^2}{r} \sin \theta = \frac{W}{g} \frac{d^2x}{dt^2} \tag{123}$$

$$\hat{F}_c \cdot \hat{j} = \frac{W}{g} \frac{V_c^2}{r} \cos \theta = \frac{W}{g} \frac{d^2y}{dt^2} \tag{124}$$

where $\hat{i}$ and $\hat{j}$ are unit vectors along the x and y axes, respectively. Since $(V_c/r)t \equiv \theta$, the acceleration components given by eqs. (123) and (124) are identical with those of eqs. (120) and (121).

During the leeward turn the bird will actually be sinking with a constant vertical velocity $\hat{w}$. The flight path during the turn will thus be a segment of a spiral trochoid. The sinking speed of the bird results in a loss of potential energy; this energy furnishes the power needed to accommodate the aerodynamic drag. This is the reason, of course, why it was possible in the preceding analysis to assume that the aerodynamic velocity $\hat{V}_c$ was of constant magnitude.

The altitude lost during the turn is given by

$$\Delta z = \int_0^{t'} w \, dt \tag{125}$$

where $t'$ is the time required to make the turn,

$$t' = \frac{\pi}{V_c} r \tag{126}$$

At the end of the leeward turn, the bird is at an altitude $z_f - \Delta z$, where $z_f$ is the initial altitude at the commencement of the turn. For efficient energy extraction it is obviously desirable that $\Delta z$ (or $w$) be small so that the wind speed $V_{wf}$ at the terminal altitude will be large. This requires that the bird's $L/D$ in the turn be large. Thus, the high aspect ratio of the albatross is seen to satisfy another basic requirement for efficient dynamic soaring. In general, optimum values of wing bank angle and flight speed (or $C_L$) exist for each radius of turn, which will make $w$ a minimum. The rather complex relation between $w$, $C_L$, $C_D$, $V_c$, and $r$ in a spiral turn has been treated in considerable detail in previous papers by the author[3,12] and therefore will not be discussed here.

The high altitude turn to leeward leaves the bird with an energy supply in the form of a large velocity relative to earth. From this supply the bird draws the energy needed to perform all flight maneuvers, up through the windward climb of the succeeding cycle. Further consideration of how much energy the bird obtains from the leeward turn and how this energy is subsequently used will be given in a following section on the complete flight cycle (page 64). The mechanics of the leeward turn of the albatross are exactly the same as for the circling flight of land soaring birds.[3] Only the albatross, however, can extract energy from the horizontal wind; this is made possible by the existence of the shear layer with its velocity difference.

## The Leeward Glide

At the completion of the high altitude turn to leeward, the albatross has acquired considerable energy, but so long as the bird remains near the top of the shear layer this energy is unavailable for practical use. To see why this is so, let us consider what happens when the bird attempts to turn from the leeward direction. As shown in Fig. 26, the centripetal force $\hat{F}_c$ will then have a component acting in a direction opposite to that of $\hat{V}_{wf}$, and the bird will be doing work on the air. Hence, the bird will lose speed and kinetic energy. In fact, upon turning a full 180° back to the windward direction, it will have lost exactly the same amount of energy that it initially gained in the leeward turn. The net energy gain in making a complete 360° turn is therefore zero. Thus, it is clearly impossible for the bird to extract energy from the uniform horizontal wind by any type of circling maneuver. This results from the fact that all turns must be made <u>relative to the air</u>.

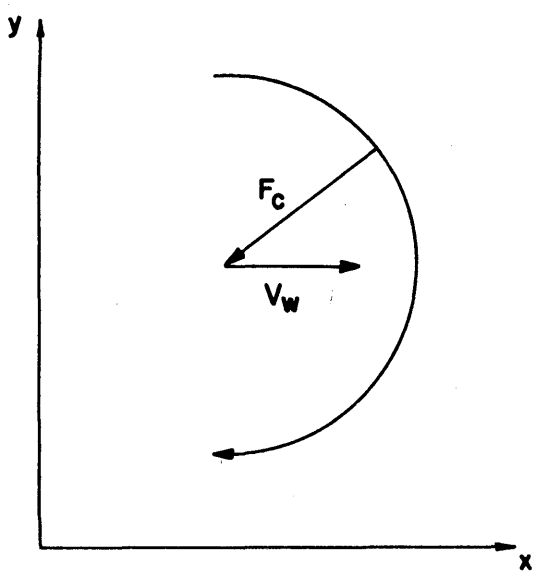


Fig. 26

If, however, the bird were able to reach the lower region of the shear layer with a high absolute speed, a turn from the leeward direction could be made

with only a small loss of kinetic energy, since then $\hat{V}_w$ would be small. Consequently, following a 90° or 180° turn from leeward at low altitude, the bird would still possess a large part of the kinetic energy gained in the high altitude turn, and could use this energy for coasting flight across or even directly into the wind, reserving enough momentum for the next climb, of course. The purpose of the leeward glide, therefore, is to get the bird down through the shear layer to the region of low wind velocity where turns can be made without great loss of useful kinetic energy. It is clear that only by virtue of the difference in wind speed between the top and bottom of the shear layer is it possible for the albatross to extract useful energy from the horizontal wind.

In performing the leeward glide, it is obviously desirable that the albatross reach the lower level of the shear layer with as large an absolute velocity as possible, so that the useful quotas of kinetic energy and momentum will be large. Were it not for the variation of wind speed within the shear layer, the leeward glide could be easily and efficiently accomplished by a simple equilibrium glide down to the surface. The wind speed variation $V_w(z)$ which does exist, however, greatly complicates the aerodynamics of the glide and poses some difficult requirements which the bird must meet if maximum kinetic energy and momentum are to be obtained. The details of these requirements and the bird's solution are discussed in this section. It is shown that the analysis predicts and explains an important and commonly observed feature of the leeward glide, namely, the "reefing-in" or flexing of the wings.

Velocity and Energy Relations of the Leeward Glide. - At the end of the leeward turn, the albatross is at some altitude $z_2$ near the top of the shear layer and is moving downwind with aerodynamic velocity $\hat{V}_c$ and absolute velocity $\hat{V}_a$, where $\hat{V}_a = V_c + V_w(z_2)$. In performing the leeward glide, it seems logical that the bird would have one of two general purposes to accomplish. First, it may endeavor to reach the lower level of the shear layer with as much kinetic energy as possible so that it will have a maximum energy supply for performing such secondary flight maneuvers as coasting crosswind or upwind; or secondly, it may desire to make as much progress to leeward as possible during the glide. The basic flight requirements for either of these two endeavors are essentially the same. In either case it is obviously desirable for the bird to make the most efficient use of its potential energy of altitude in accomplishing its intended purpose.

In order to analyze the mechanics of the leeward glide, it is convenient and instructive to make use of the gliding diagram shown in Fig. 27. This diagram is simply a plot of the horizontal and vertical components $\hat{u}$ and $\hat{w}$ of the equilibrium aerodynamic gliding velocity $\hat{V}$ for a range of values of the angle of attack $\alpha$ (or lift coefficient $C_L$). The diagram is constructed by using the drag polar $C_D$ ($C_L$) and wing loading $W/S$ of the bird.*

---

*It can be assumed, purely for purposes of illustration, that the polar $C_D$ ($C_L$) is obtained experimentally by holding the wing shape rigid while rotating the wing through the angle of attack range in an airstream and measuring the forces; $W/S$ is then constant for this given wing shape for a given bird. From a realistic standpoint, of course, such a procedure would be extremely difficult to accomplish with a live bird.

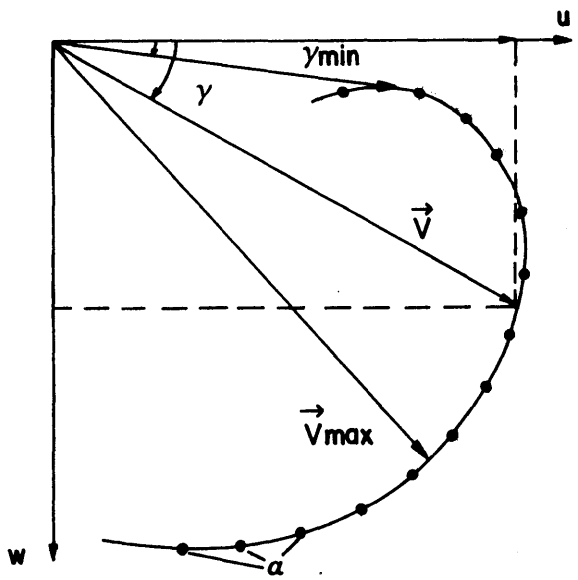


Fig. 27

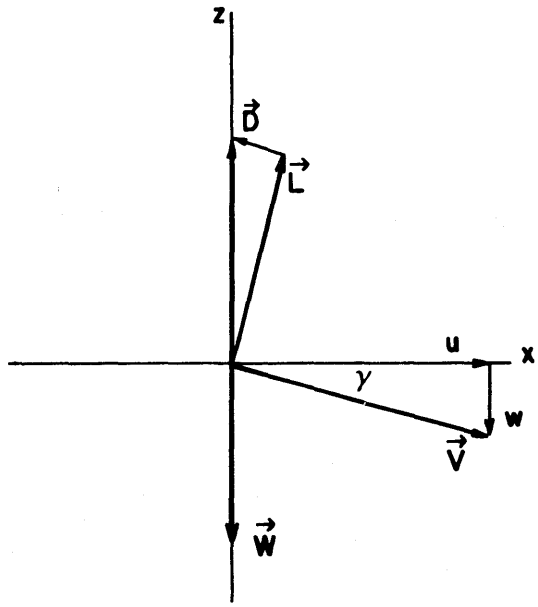


Fig. 28

From Fig. 28, which shows the conditions existing in an equilibrium glide, it follows that

$$u = \left(\frac{2}{\rho\, C_L}\right)^{1/2} \left(\frac{W}{S}\right)^{1/2} \cos^{3/2}\gamma \tag{127}$$

$$w = \left(\frac{2}{\rho\, C_L}\right)^{1/2} \left(\frac{W}{S}\right)^{1/2} \cos^{1/2}\gamma \sin\gamma \tag{128}$$

where the aerodynamic gliding angle $\gamma$ is a function only of $C_L$,

$$\gamma = \text{ctn}^{-1}\frac{C_L}{C_D} = \text{ctn}^{-1}\frac{L}{D} \tag{129}$$

For a given wing loading, u and w will vary as the angle of attack (or $C_L$) is varied, and a curve of the type illustrated in Fig. 27 will be generated. The length of the vector $\hat{V}$ drawn from the origin to any point on the curve thus gives the gliding speed directly, and the angle $\gamma$ of the vector gives the aerodynamic glide inclination (relative to the air) for the particular angle of attack $\alpha$ (or $C_L$) corresponding to that point. The longest vector which can be drawn gives the maximum possible equilibrium gliding velocity attainable with the given wing loading. The minimum gliding angle $\gamma_{min}$ corresponds to the tangent line to the curve and gives the maximum value of L/D.

The gliding diagram thus gives the velocity $\hat{V}$ of the bird relative to the air for each trimmed value of $\alpha$, or $C_L$, so that in the case of a glide in

still air it gives also the absolute velocity $\hat{V}_a$. When a wind $\hat{V}_w$ exists, the gliding diagram allows the absolute velocity $\hat{V}_a$ to be obtained quite simply by vector addition directly on the diagram. To obtain $\hat{V}_a$ in both magnitude and direction, the wind vector $\hat{V}_w$ is added to the aerodynamic velocity $\hat{V}$, as shown in Fig. 29. The angle $\gamma_e$ then gives the inclination of the resultant

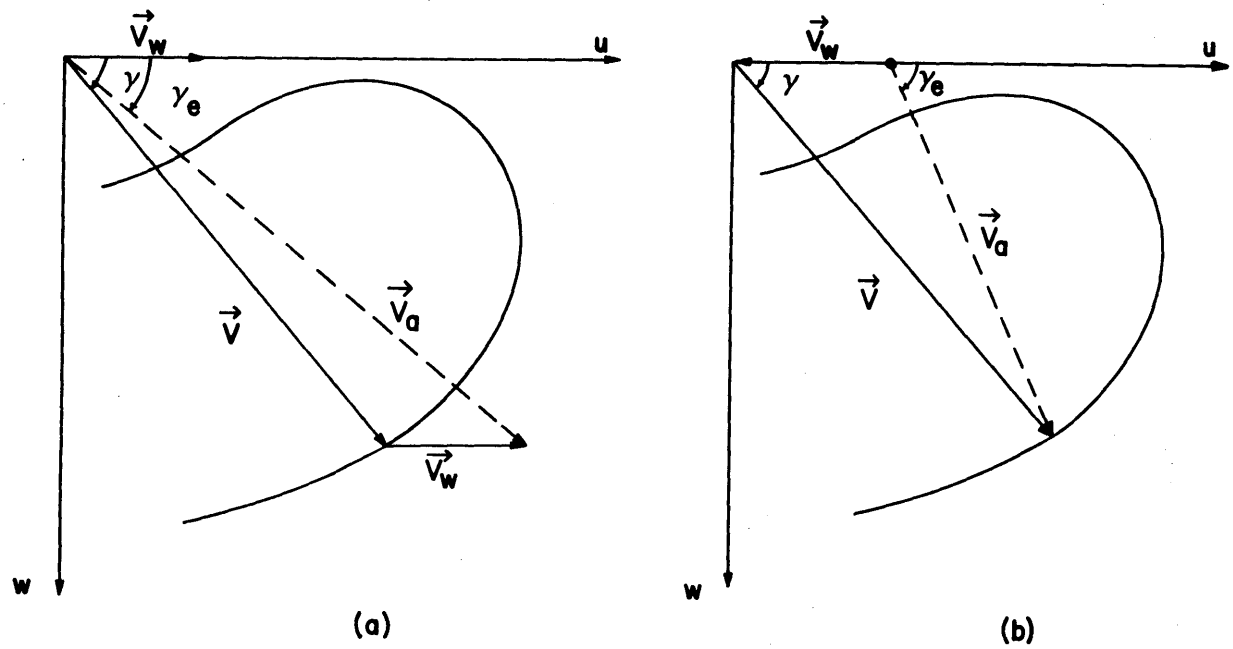


Fig. 29

flight path relative to earth. (In our present analysis, $\hat{V}_w$ is always parallel to the u-axis, but in general it may have any orientation so far as the use of the gliding diagram is concerned, since $\hat{V}_w$ is, in the general case, the velocity of the air relative to the earth.)

If we assume, for the moment, that the gliding diagram of Fig. 27 corresponds to that of a rigid wing aircraft (such as a sailplane or glider), where the wing area and shape remain permanently fixed, the wing loading $W/S$ may be increased by increasing the weight $W$ of the craft. Since the shape and size of the craft have not been altered by this weight addition, the aerodynamic characteristics $[C_L(\alpha), C_D(C_L)]$ will remain exactly the same. From eqs. (127) and (128), it is evident that the only change in the gliding diagram will be an increase in the length of the vector $\hat{V}$, since $V$ is proportional to $(W/S)^{1/2}$. Thus, for a rigid aircraft, a family of curves can be drawn, each curve corresponding to a particular value of the wing loading $W/S$, as shown in Fig. 30. Since the value of $W/S$ is constant during flight for a given aircraft (or glider), only a single curve on the gliding diagram applies, and this sets the only possible flight speeds and directions which the craft can attain in an equilibrium glide, under given wind conditions.

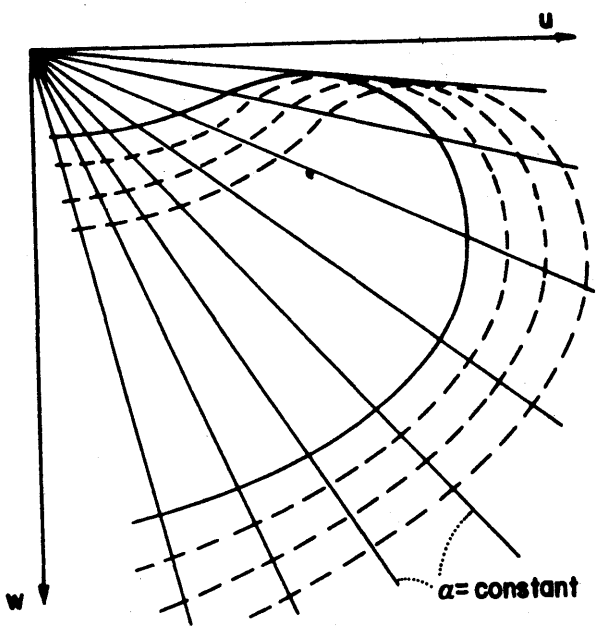


Fig. 30

In the case of the bird, the flight conditions are much more flexible. Although the bird's weight W is essentially constant during a given glide, the wing shape, area, and aerodynamic characteristics can be varied in flight due to the bird's voluntary control over the geometry of the wing. The bird can alter its wing loading W/S at will by so adjusting the wing shape that the effective lifting area S is increased or decreased. The maximum lifting area is obtained when the wings are held horizontal and fully extended; W/S is then a minimum. As the wings are flexed,* or drawn in, the effective area producing lift is decreased and W/S is therefore effectively increased. As the wing is smoothly "reefed-in" from the fully extended position to the highly flexed condition, W/S increases from a minimum to a maximum.

If it is assumed that the bird is rotated through an angle of attack range in an airstream and $C_L$ and $C_D$ are measured while holding the wing shape rigid, and this procedure repeated for small successive shape changes as the wing is progressively flexed, a series of curves will be obtained for the gliding diagram, one for each constant shape of the wing (with its corresponding value of W/S), as shown in Fig. 31.** Due to the change in wing shape, however, successive curves may no longer be obtained by a simple increase in vector length, as for the rigid wing case, since the aerodynamic parameters $C_L$, $C_D$, and L/D may be somewhat different functions of $\alpha$ for each successive curve (i.e. each stage of the flexing or wing deformation process). Due to the ability of the albatross to vary W/S in flight, the successive curves for increasing values of W/S will generate a continuous region of usable flight conditions in the u-w plane, and thus greatly expand the range of flight speeds and directions which the bird can attain under given wing conditions, as compared to a rigid wing aircraft (which can use only a single curve on the diagram). In particular, the variable wing geometry of the bird allows it to fly any of a broad range of speed and direction combinations, even under conditions where $\hat{V}_w$ is continuously changing.

---

*A description of the flexing process, together with a discussion of its aerodynamic significance, is presented later (page 61).

**The angle of attack range covered by each curve is, of course, determined by the requirement that the bird must be able to trim (i.e., to attain a zero value for the pitching moment, $C_m = 0$) at each $\alpha$ value within the range. Unless the bird can attain trim by suitable deflection of the feet, tail, and wing surfaces, equilibrium flight is not possible since the required constant angle $\alpha$ cannot be maintained.

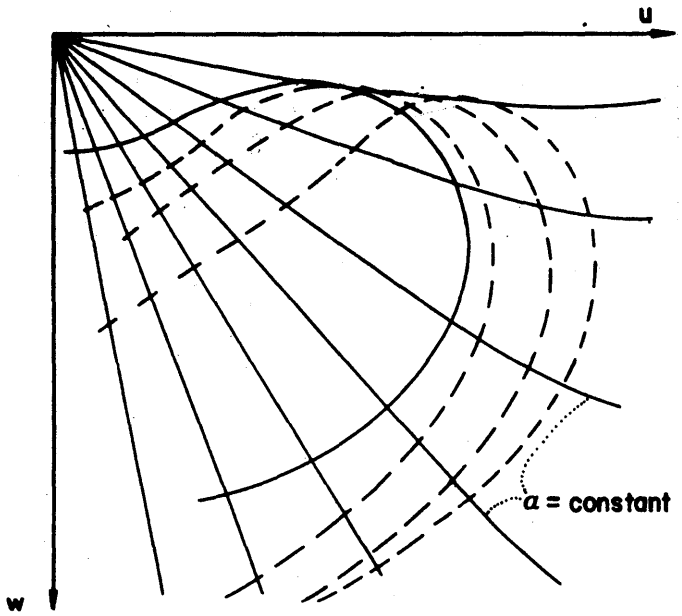


Fig. 31

It is not possible, of course, to construct the actual gliding diagrams for the successive wing shapes generated by the flexing process. Such polars would be extremely difficult, if not impossible, to obtain with live birds, and it is questionable if wind tunnel tests with mounted specimens would yield data of sufficient accuracy, although such tests might be very valuable in revealing general trends in the variation of $C_L$, $C_D$, L/D, and W/S with wing flexing. The schematic curves of the present gliding diagrams are, therefore, intended only to represent the general effects introduced by the ability of the bird to vary the effective value of W/S in flight. The exact relations for the albatross may be somewhat different from the curves shown in the figures, but the general features are expected to be similar. It is clear that any really quantitative analysis of the leeward glide must be based upon an actual experimental gliding diagram for the albatross.

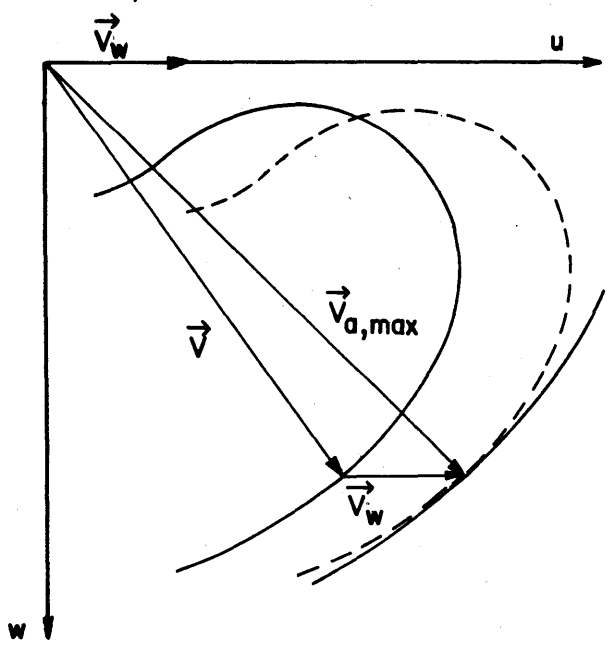


Fig. 32

In order to visualize the flight conditions necessary for the albatross to reach the surface with maximum kinetic energy, we make use of the gliding diagram shown in Fig. 32. At the end of the leeward turn the bird possesses a relatively large absolute velocity component $\hat{u}_2$ ($= \hat{V}_w + \hat{V}_c$) in the x-direction, and a small sinking velocity $\hat{w}_2$. For the present, we shall neglect the variation of the wind speed with altitude in the shear layer and, hence, assume that $\hat{V}_w$ is constant. We shall also assume, for purposes of analysis, that the bird endeavors during the glide to maintain all the initial kinetic energy associated with $u_2$ and $w_2$ and to convert its potential energy of altitude as completely as possible into additional kinetic energy. To do this, the bird must obviously glide with the aerodynamic velocity $\hat{V}$ which, when added to the wind velocity will make $\hat{V}_a$ a

maximum for the particular wing loading being used. The value of the wing loading should, of course, be that which makes $\hat{V}_{a,max}$ an absolute maximum. (This condition is somewhat altered when the wind variation $V_w(z)$ is considered, as will be shown later.) The maximum absolute velocity $V_{a,max}$ is obtained by translating the entire gliding curve (corresponding to the optimum wing loading) to the right by the amount $\hat{V}_w$, and determining the radius of the largest circle which will just enclose the translated curve. It is obvious from this figure that the velocity $\hat{V}$ for $\hat{V}_{a,max}$ is not necessarily equal to $\hat{V}_{max}$, as shown; the velocity $\hat{V}$ corresponding to $\hat{V}_{a,max}$ depends entirely upon the shape of the gliding curve for the optimum wing loading (or wing shape).

In order to reach the conditions pictured in Fig. 32, the bird must undergo a vertical acceleration to attain the sinking speed w corresponding to $\hat{V}$; most of the potential energy of altitude lost during this period is converted into increased kinetic energy of the absolute motion. Once the bird has attained the airspeed $\hat{V}$ corresponding to $\hat{V}_{a,max}$, no further conversion of potential energy to kinetic energy is possible. The remaining potential energy will merely be dissipated in overcoming the aerodynamic drag as the bird glides down.

This limit placed on the attainable kinetic energy recovery of the bird points out an interesting fact in regard to the maximum flight altitude used by the albatross in dynamic soaring. In general, the maximum altitude reached by the bird in the windward climb is observed to be less than 60 feet. This is usually assumed to be the upper limit of the shear layer. But, it is evident from the relations just considered that even if the bird could rise much higher than 60 feet so that it had a much larger amount of potential energy at the start of the leeward glide, it could not convert all of this into useful kinetic energy. For, once the bird attained the terminal aerodynamic velocity corresponding to $\hat{V}_{a,max}$, it would merely glide down with the constant velocity $\hat{V}_{a,max}$; all the remaining potential energy would be dissipated in accommodating the aerodynamic drag. Thus we see that, from an energy standpoint, the bird has nothing to gain by rising much above the top of the shear layer ($z = z^*$) so long as $z^*$ is sufficiently large that the bird has adequate time to accelerate to its terminal aerodynamic velocity before reaching the surface.

In the case where the bird endeavors to cover maximum distance to leeward during the glide, it should obviously travel with the velocity $\hat{V}$ corresponding to maximum L/D, as shown in Fig. 33.* In this effective wing loading is such as to make $\gamma_e$ a minimum. It is clear that the optimum wing loading to be used for distance travel to leeward will depend upon the shape of the envelope curve of maximum lift-drag ratios generated by the $\gamma_{min}$ points ($L/D_{max}$ points) of the individual gliding curves for the various wing shapes.

On first sight it would appear desirable for the albatross to gain as much altitude as possible in the windward climb if the bird is attempting to make maximum headway to leeward. By gliding down at $\gamma_{e,min}$, the bird could cover more distance by starting at a higher altitude. However in climbing to a high altitude, the aerodynamic speed $V_c$ during the turn will be reduced according

---

*This is true only when $\hat{V}_w$ is constant, as we are presently assuming. When $\hat{V}_w$ varies with z other factors enter (see page 61).

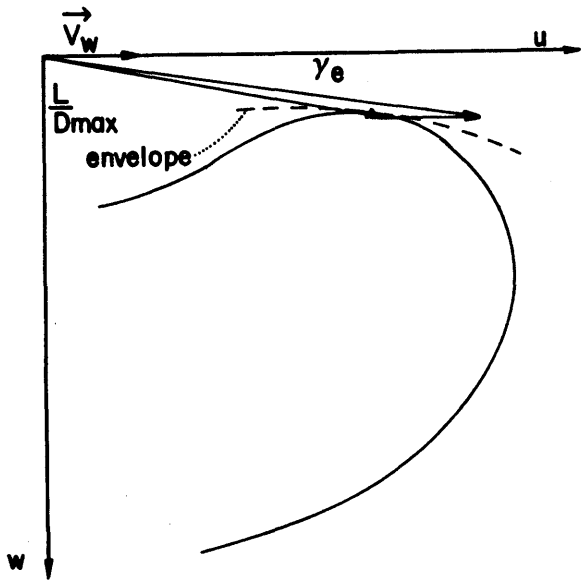


Fig. 33

to eq. (90) and the bird will end the turn with a smaller value of $u_2$ in the leeward direction. If $u_2$ is less than the u-component of $\hat{V}_a$ for $(L/D)_{max}$, the bird will then have to lose altitude in accelerating up to the proper gliding speed, and will thus lose at least some of the advantage of the high initial altitude. If $u_2$ is greater than the required u-component, then full advantage may be taken of the altitude gain since $\gamma_e$ will be even less than the equilibrium glide value, during the period of deceleration. Which of these two conditions prevails will depend, of course, upon the relative values of $V_c$ and $u$ for $(L/D)_{max}$. It is interesting to note that observations show that the bird nearly always flies at very low altitudes. In this case, however, the bird is usually attempting to follow the observer's vessel, and hence is most probably trying to get more energy from the wind than to gain leeward distance.

Effects of the Wind Profile.- The fact that in the actual leeward glide the bird is sinking through the shear layer, where the wind is continuously decreasing, introduces some additional complexities into the mechanics of the glide. Consider the bird at some altitude z near the top of the shear layer [where the wind speed is $V_w(z)$] and gliding down with the aerodynamic and absolute velocities $\hat{V}_1$ and $\hat{V}_{a1}$, as shown in Fig. 34. After the bird has lost a small amount of altitude, its absolute velocity will still be essentially $\hat{V}_{a1}$, but due to the decrease in wind speed with altitude loss, the aerodynamic velocity will have increased to $\hat{V}_2$ and will have decreased the angle of attack of the bird, as indicated in the figure. Since the bird will then be flying at an airspeed greater than its equilibrium gliding speed, it will decelerate, and hence will lose kinetic energy. In order that there be no change in the vector $\hat{V}_a$, and hence no change in the kinetic energy, it is necessary that the aerodynamic velocity $\hat{V}$ satisfy the condition

$$\hat{V} = \hat{V}_{a1} - \hat{V}_w(z) \qquad (130)$$

at each point in the shear layer. Here $\hat{V}_{a1}$ is constant and $\hat{V}_w(z)$ is the profile of the horizontal wind.

As is obvious from the gliding diagram of Fig. 34, it is impossible for the bird to satisfy eq. (130) with a fixed wing geometry (corresponding to a single gliding curve), since the bird cannot fly at the values of $\hat{V}$ required to keep $\hat{V}_{a1}$ constant. However, since the wing loading of the bird can be varied in flight, it is possible for the bird to fly the entire range of

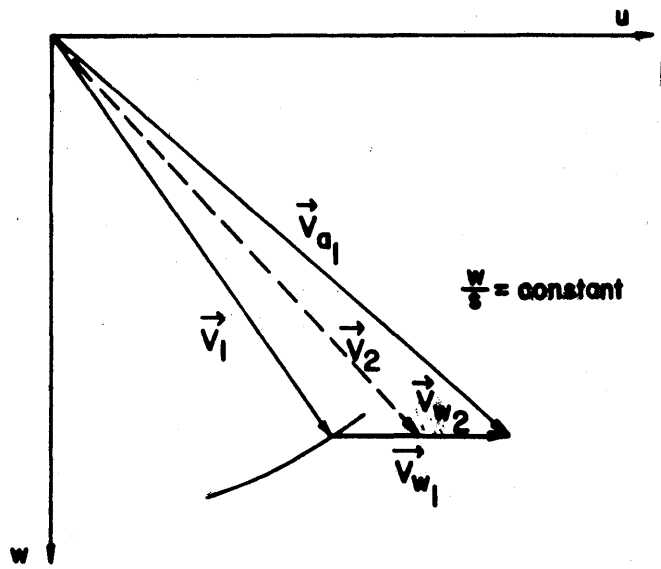


Fig. 34

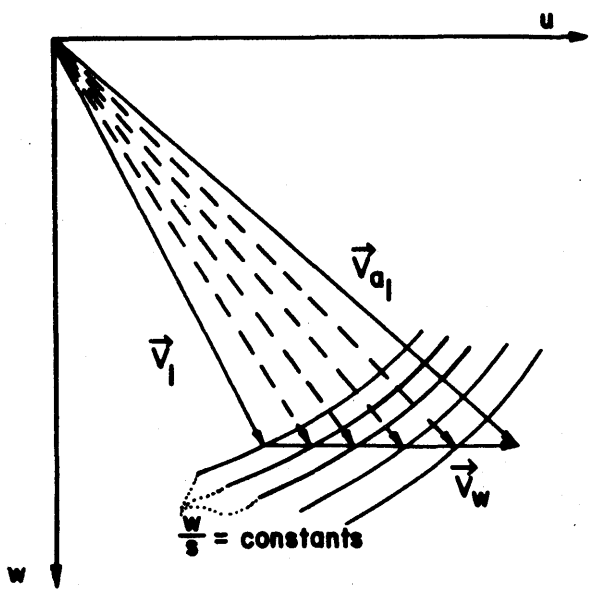


Fig. 35

values of $\hat{V}$ indicated in Fig. 35, merely by continuously varying the value of W/S and trimming at the angle of attack corresponding to the proper aerodynamic glide angle $\gamma$ (or L/D) at each level in the shear layer. (The aerodynamic forces existing during the glide are assumed to be quasi-steady, of course, so that the statically determined gliding diagram is valid.) The varying conditions imposed by the shear layer can thus be adequately accommodated by the bird by proper variation of the wing loading and angle of attack, and the maximum absolute velocity $\hat{V}_a$ can be maintained throughout the glide.

The great flight flexibility afforded the bird by its ability to vary the wing loading is thus clearly shown by the gliding diagram. As previously noted, since W/S can be controlled as well as $\alpha$, the gliding diagram becomes a whole surface of equilibrium glide points composed of a continuous series of curves of constant W/S. The bird can fly at the equilibrium glide velocity denoted by any point on the surface instead of being limited to points on a single curve.

In the foregoing discussion, it is assumed, of course, that $\hat{V}_{a1}$ is not so large that all required values of $\hat{V}$, as $\hat{V}_w$ decreases, lie outside the usable region of the gliding diagram. Thus, it is desirable that the bird start the glide with a value $\hat{V}_{a1}$ somewhat less than the maximum attainable with the optimum wing loading; this will allow the wing loading to be increased appropriately as the dive progresses. On the other hand, the possibility certainly exists that the bird could dive at the maximum value of $\hat{V}_{a1}$ and decelerate to some lesser value during the glide. Which procedure results in the smallest loss of kinetic energy, and which procedure the bird actually uses is a matter for detailed experimental investigation of the leeward glide by photographic

analysis. Also, in practice, the bird may not increase the wing loading continuously to accommodate the wind speed at each altitude, but may use some relatively constant average increase in W/S which, nevertheless, will allow a beneficial gain of kinetic energy in the glide.

It is an interesting fact of observation that the albatross does indeed flex its wings into a shallow W form during the leeward glide - a condition clearly predicted by the foregoing analysis. In addition, the glide is usually very steep, almost a dive. This is in accord with the gliding diagrams for high performance sailplanes which are aerodynamically similar to the albatross, since the aerodynamic velocity for the maximum speed glide is very strongly inclined ($\gamma$ large). This observation would tend to indicate that the albatross was generally endeavoring to extract maximum energy from the wind rather than in proceeding downwind. As noted above, however, this condition may be a result of the presence of the observer.

For the case where the bird desires to proceed to leeward, the same effects of the shear layer apply as for the maximum kinetic energy case. In particular, it may be noted (Fig. 36) that if $\gamma_e$ of the initial glide path relative to earth is too small, corresponding to $\hat{V}$ for $(L/D)_{max}$, it will be impossible for the bird to maintain $\hat{V}_{al}$ constant as $\hat{V}_w$ decreases, since all the required aerodynamic velocities lie outside the region of equilibrium flight conditions attainable by the bird.

The Effective Wing Loading. - In view of the importance of the variable wing loading in the leeward glide mechanics, it is of interest to consider the method by which the albatross varies its effective W/S in flight. When the wing is held horizontal and fully extended, the elemental lift forces on the wing surfaces act in essentially parallel directions, as shown in Fig. 37(a).

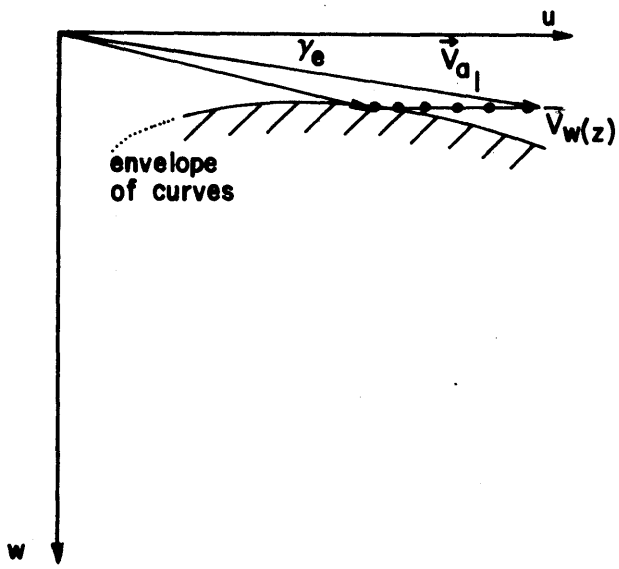


Fig. 36

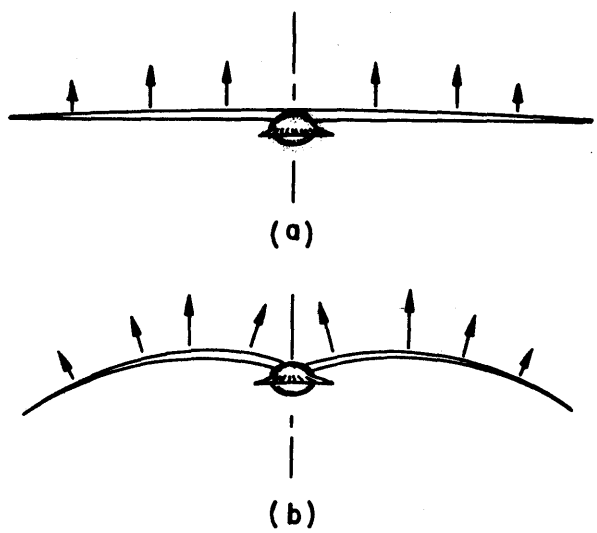


Fig. 37

When the wing is flexed, however, the surfaces assume a nonplanar form like that pictured in Fig. 37(b) ("gull wing"), and the elemental force vectors are no longer parallel. Only a component of the local force vectors acts to produce lift. The lateral force components cancel one another because of the symmetry of the wings, and the only resultant force is a reduced lift. The result of flexing the wings, therefore, is a decrease in the effective lift force, or equivalently, a decrease in the aerodynamically effective wing area. Since $W$ is constant, this effectively amounts to an increase in $W/S$. The flexing may also cause some overlapping of wing feathers, especially at the wing joints, and this further reduces the effective area. The changes in wing geometry which result from flexing may be expected to produce appreciable changes in the aerodynamic relations $C_L(\alpha)$, $C_D\ (C_L)$, $L/D\ (C_L)$, and $C_m\ (C_L)$ for the wing.

In defining the aerodynamic coefficients and wing loading $W/S$ for variable geometry wings such as the albatross possesses, some question may exist as to the proper area $S$ to use. In practice, any reference area may be chosen since the gliding diagram as given by eqs. (127) and (128), can be constructed without reference to either $C_L$ or $S$. The effective parameter is actually the product $C_L S$. Reference to Fig. 28 shows that the basic relation governing the gliding velocity is

$$L = W \cos \gamma \tag{131}$$

where $\gamma$ depends only on the ratio $L/D$ of the aerodynamic forces. If we take a given wing (or entire bird) of given shape, and measure its aerodynamic forces as functions of angle of attack $\alpha$ and airspeed $V$, we obtain

$$L = k_1 V^2 \tag{132}$$

where $k_1$ is a constant parameter (with regard to velocity $V$) which depends on a) the size of the particular wings, b) the shape or geometry of the wing and c) the orientation of the wing relative to the airstream. In the usual terminology

$$k_1 = 1/2\ \rho\ C_L\ S \tag{133}$$

Since $L$ and $D$ are measured directly, as functions of $\alpha$, $\gamma$ as a function of $\alpha$ (or $k_1$) is known. Thus eqs. (127) and (128) can be written as

$$u = \left(\frac{W}{k_1}\right)^{1/2} \cos^{3/2} \gamma \tag{134}$$

$$w = \left(\frac{W}{k_1}\right)^{1/2} \cos^{1/2} \gamma \sin \gamma \tag{135}$$

Since $k_1$ and $\gamma$ are known (measured) functions of $\alpha$, the gliding diagram can therefore be constructed without any explicit reference to any area. In this sense, $k_1$ might be called the "effective" wing area and shape parameter.

From a physical standpoint, it would be logical, of course, to use the projected planform of the flexed wing as the reference area, provided $C_L$ is also defined on this same basis.

The Low Altitude Turn to Windward

As the albatross approaches the surface near the end of the leeward glide, it is moving with very high absolute velocity and appreciable airspeed, especially for the case where it has endeavored to attain maximum kinetic energy during the glide. The glide is terminated with a pullup maneuver which reduces the sinking speed w to zero and converts all of the bird's momentum to the horizontal direction. The bird rolls into a nearly vertical bank and turns sharply from the leeward direction. In many instances the turn may be initiated simultaneously with the pullout.

The extent of the turn at this point depends upon the type of flight path the bird wishes to follow, as will be discussed in a later section. For the present case of the simple basic cycle, the bird is assumed to complete a full 180° turn to windward, whence it proceeds with the windward climb of the next cycle.

Energy Loss in the Windward Turn.- The turn to windward is made at essentially constant altitude very close to the surface, so close in fact that the primaries of the lower wing tip at times actually cut the water surface. The reason for the extremely low altitude of the turn was briefly indicated in a previous section.

Near the surface the wind speed has some small value $V_w(z_t)$ where $z_t$ is the altitude of the turn. Since the albatross banks nearly 90° in the turn, and since the spans of these birds vary from roughly 8 to 11 feet, $z_t$ will be on the order of 4 to 5 1/2 feet. From the turn diagram of Fig. 38, it is obvious that since the bird can only turn relative to the air, it will complete the upwind turn with an absolute velocity

$$\hat{u} = \hat{V}_c + \hat{V}_w (z_t) \tag{136}$$

where $\hat{V}_c$ is the aerodynamic velocity in the turn, and is essentially equal to the aerodynamic velocity which the bird possesses following the pullout maneuver.

By means of an analysis directly analagous to that for the high altitude turn to leeward, it is found that the bird loses kinetic energy in the amount

$$2 \frac{W}{g} V_c V_w (z_t) \tag{137}$$

in performing the windward turn. This is equal to the work which the centripetal force $\hat{F}_c$ has done on the air, since $\hat{F}_c \cdot \hat{V}_w$ is negative throughout the turn. From an energy standpoint, it is clearly desirable to have $V_w(z_t)$ as small as possible, so the turn must be made as near the surface as is

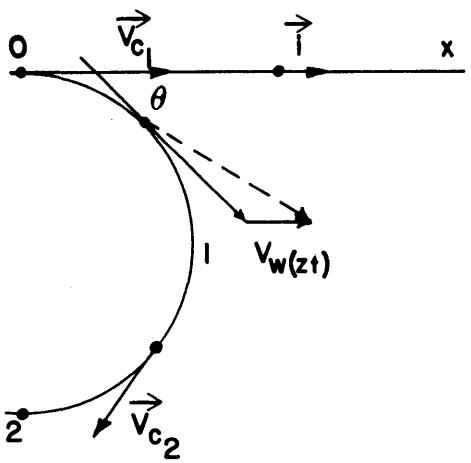


Fig. 38

practical. It is particularly advantageous in the case of the windward turn to have $V_w(z_t)$ very small, since $V_c$ may be rather large. It is often noted that when appreciable waves exist, albatrosses often perform the turn deep in the troughs of the wave trains. The wind speed in the troughs is a minimum, as will be discussed subsequently. (See page .)

In general the albatross does not make a complete 180° turn to windward with $V_c$ near its maximum. Rather, as will be discussed more fully later, it executes only a partial turn following the leeward glide and then coasts crosswind for some distance while $V_c$ decreases. When $V_c$ has become relatively small, the bird completes the turn. By this procedure, the bird loses less kinetic energy to the wind in performing the total windward turn. The crosswind coast, of course, has enabled the bird to cover distance along its desired flight path, as well as decreasing the energy loss of the turn. Using eq. (104) and the diagram of Fig. 38, the net energy loss in performing the windward turn in two 90° segments is

$$w = \int_0^{\pi/2} \frac{W}{g} V_{c_1} V_w(z_t) \sin\theta \, d\theta + \int_{\pi/2}^{\pi} \frac{W}{g} V_{c_2} V_w(z_t) \sin\theta \, d\theta = \frac{W}{g} (V_{c_1} + V_{c_2}) V_w(z_t) \tag{138}$$

where $V_{c_1}$ is the (high) airspeed of the first segment and $V_{c_2}$ is the (lower) airspeed of the second segment. If $V_{c_2}$ is expressed as a fraction m of $V_{c_1}$

$$V_{c_2} = m V_{c_1} \qquad (m < 1.0) \tag{139}$$

then the energy saved by the two-part turn is

$$(1 - m) \frac{W}{g} V_{c_1} V_w(z_t) \tag{140}$$

Although eq. (140) indicates that energy can be saved by making the windward turn in two parts having airspeeds of $V_{c_1}$ and $V_{c_2}$, respectively, the bird will complete the two-part turn with less total kinetic energy than if a single turn at a constant airspeed of $V_{c_1}$ had been used. The final kinetic energy possessed at the end of the two-part turn is $1/2\ W/g\ (V_{c_2} - V_{wt})^2$, while that for the single turn is $1/2\ W/g\ (V_{c_1} - V_{wt})^2$, and since $V_{c_1} > V_{c_2}$, the latter energy is the greater. This fact may appear contradictory to the prediction of eq. (140), but it can be shown that the two-part turn yields more total useful energy. To show that this is true, we note that the total kinetic energy lost by the bird in the two-part turn is, using eq. (139),

$$\frac{1}{2}\frac{W}{g}\left[(V_{c_1} + V_w(z_t))^2 - (m\,V_{c_1} - V_w(z_t))^2\right]$$

or

$$\frac{1}{2}\frac{W}{g}\left[(1 - m^2)\,V_{c_1}^2 + 2\,(1 + m)\,V_{c_1}\,V_w(z_t)\right] \tag{140a}$$

The portion of this total energy lost to the wind during the actual turn segments is, from eq. (139),

$$\frac{W}{g}\,(1 + m)\,V_{c_1}\,V_w\,(z_t) \tag{140b}$$

Thus the net useful energy available from the two-part turn is

$$\frac{1}{2}\frac{W}{g}\,(1 - m^2)\,V_{c_1}^2 \tag{140c}$$

At the completion of the single-segment turn, the bird has available an amount

$$\frac{1}{2}\frac{W}{g}\left[(1 - m^2)\,V_{c_1}^2 - 2\,(1 - m)\,V_{c_1}\,V_w(z_t)\right]$$

of the kinetic energy more than it would have for the two-part turn. However, this amount of useful energy is seen to be less than that of eq. (140c) by exactly $W/g \cdot (1 - m) \cdot V_{c_1} \cdot V_w(z_t)$, which is identical to the energy saved by the two-part turns [eq. (140)].

It thus becomes clear why the albatross generally makes a two-segment turn instead of a single one; the divided turn furnishes more useful kinetic energy and hence allows the bird to cover more ocean surface per cycle.

In the case of the leeward-glide conditions for maximum leeward distance travel, $V_c$ will be relatively small, and the bird would most probably execute a full 180° turn following the glide.

Steepness of the Turn. - From an aerodynamic standpoint, the windward turn could be made using any reasonable bank angle of the wings. It is of interest, therefore, to consider the significance of the fact that the bird actually uses an almost vertical bank in performing the windward turn. It appears that the reason for the extremely sharp bank and turn is to lessen the distance that the bird is carried downwind while making the turn. This factor becomes important if the bird is attempting to make headway to windward, or to follow some special flight path other than directly downwind. It is also important in the case where surface waves exist, since the turn would then be made deep in the narrow trough region where the wind speed is a minimum (see page 82).

To see how the degree of bank influences the leeward displacement of the bird, we integrate the x-component of the absolute velocity $\hat{V}_a$ over the time required to perform the turn. Since the turn is generally made in two parts, with different aerodynamic velocities,* separate integrations are carried out for each of the two turn segments. Using the diagram of Fig. 38, we have

$$x_1 = \int_o^{t_1} \hat{V}_a \cdot \hat{i}\, dt \tag{141}$$

where $x_1$ is the leeward displacement during the first part of the turn and

$$\hat{V}_a = \hat{V}_{c_1} + \hat{V}_w(z_t)$$

Thus, using eq. (141),

$$x_1 = \int_o^{\pi/2} (\hat{V}_{c_1} + \hat{V}_w(z_t)) \cdot \hat{i}\, \frac{r}{V_{c_1}}\, d\theta \tag{142}$$

$$x_1 = \int_o^{\pi/2} r \cos\theta\, d\theta + \int_o^{\pi/2} r\, \frac{V_w(z_t)}{V_{c_1}}\, d\theta \tag{143}$$

or

$$x_1 = r\left(\frac{\pi}{2}\, \frac{V_w(z_t)}{V_{c_1}} + 1\right) \tag{144}$$

Similarly, upon integrating over the second part of the turn we obtain

$$x_2 = r\left(\frac{\pi}{2}\, \frac{V_w(z_t)}{V_{c_2}} - 1\right) \tag{145}$$

The net displacement to leeward, x, for the complete turn is therefore

$$x = r\left[\left(\frac{\pi}{2} V_w(z_t)\right)\left(\frac{1}{V_{c_1}} + \frac{1}{V_{c_2}}\right)\right] \tag{146}$$

This shows that x is directly proportional to the radius of turn (relative to the air) for given values of $V_w(z_t)$, $V_{c_1}$, and $V_{c_2}$.

The relation between the radius of turn r and the angle of bank $\beta$ is given by[3,12]

---

*This is especially true when an observer's vessel is present and the bird is regulating its flight path so as to follow the ship.

$$r = \frac{W}{S} \frac{2}{\rho g} \frac{\csc \beta}{C_L} \tag{147}$$

Thus, for given values of $C_L$ and $W/S$, r varies directly as $\csc \beta$. For the range $0^\circ \leqq \beta \leqq 90^\circ$, r assumes the values $\infty \geqq r \geqq W/S \cdot 2/\rho g \cdot 1/C_L$ where the minimum radius of turn

$$r_{min} = \frac{W}{S} \frac{2}{\rho g} \frac{1}{C_{L_{max}}} \tag{148}$$

is set by the maximum value of $C_L$, $C_{L_{max}}$, and the minimum value of $W/S$, which can be attained by the bird.

From eqs. (146) and (147), it is evident that for given wind speed and airspeeds in the turn segments, the downwind distance travelled during the complete turn will be a minimum when $\beta = 90^\circ$, that is, when the bird executes a vertical bank in the turn.

While the steeply banked turn is desirable for minimizing leeward drift, it is not efficient from the drag-energy standpoint. To make a small radius of turn, $C_L$ must be large; then $C_D$ and the drag will also be large. However, as noted on page 67, the steep bank is beneficial when waves exist since it allows the bird to execute its turn in a region where the wind speed is a minimum, so that less kinetic energy is lost in the turn. Apparently, the bird finds the steeply banked turn more beneficial, especially when pursuing other than a downwind flight path and when soaring over surface waves. Since the bird performs the turn near the surface, it has practically no potential energy available and nearly all of the energy needed to accommodate the drag must be furnished from the bird's kinetic energy supply. Consequently, the bird is continuously decelerating throughout the turn. In fact, from the time the bird terminates the leeward glide until it commences the following high altitude turn to leeward, it will be in a state of deceleration. For this reason, the values of $V_c$ will not be constant as assumed in the analyses of this section, but will decrease somewhat during the turn.

## THE COMPLETE CYCLE

By combining the four basic phases analyzed in the preceding sections in such a way that the conditions at the end of one phase coincide with those at the beginning of the next, the complete basic soaring cycle of the albatross is obtained. This somewhat idealized cycle, devoid of all flapping, is intended to make clear the essential features of the energy extraction processes and associated flight mechanics involved in true dynamic soaring. In reality, the basic cycle described is not usually observed in this simple form. Rather, under actual flight conditions its four basic phases are integrated with secondary flight modes to yield the host of varied flight patterns characteristic of albatross flight. Still, despite the complexity and irregularity of a given flight pattern, it implicitly contains the four phases of the basic cycle, since these phases constitute the primary means whereby the albatross

can extract useful energy from the steady horizontal wind.* (If the wind is unsteady, that is, if it varies with time at a given point, a second type of dynamic soaring, gust soaring, is possible, but unsteady wind conditions do not appear to be very prevalent at sea. The mechanics of gust soaring are treated in Section IV.)

The essential features of the basic soaring cycle can be summarized as follows. The albatross accomplishes the windward climb by using its large initial horizontal momentum to balance the decelerating aerodynamic forces, and climbs from the region of very low wind speed near the surface to an altitude where the wind speed has essentially reached its full strength. During this climb the bird gains potential energy in the form of altitude, but loses considerable kinetic energy as it decelerates horizontally. Some energy is extracted from the wind as the bird rises, but the larger part of the potential energy comes from the initial kinetic energy of the bird itself. In the high altitude turn to leeward, the bird accelerates rapidly and extracts a large amount of energy from the wind. This energy appears as the increased kinetic energy of the bird following the leeward turn. The turn to leeward generally provides the principal energy for dynamic soaring flight in shear layers. In the leeward glide, the potential energy of altitude is partially converted to additional kinetic energy and the bird reaches the region of low wind speed near the surface with a very high absolute speed. Here the low altitude turn to windward can be accomplished without a very large loss of kinetic energy, and the bird can utilize the energy gained in the leeward turn for practical purposes.

It is important to note that, according to the results of the preceding sections, the high altitude turn to leeward is the principal means whereby energy is extracted for dynamic soaring. This fact does not appear to have been generally appreciated by most previous investigators with the exception of Idrac. The principal energy supply has usually been attributed in the past to the potential energy "gained" during the windward climb. This energy was supposed to be derived from the wind by virtue of the wind gradient, wherein the aerodynamic velocity could be maintained as the bird climbed. The potential energy thus gained was then converted to kinetic form. It is clearly true that if a wind gradient of sufficient magnitude existed from the ocean surface up to great altitudes, correspondingly large amounts of potential (and kinetic) energy could indeed be obtained from the wind. However, the ocean shear layers are generally not very deep, and the velocity gradients are suitably large only in a shallow region near the surface. Hence the practical energy which can be extracted by the bird during the windward climb appears to be rather small.

To gain some idea of the relative amounts of energy available from the windward climb as opposed to the leeward turn, let us consider the energies

---

*In some cases, the leeward glide may be replaced with a lateral glide across the wind or even slightly upwind. In such cases, the bird is travelling upwind with maximum speed and hence avoids the downwind displacement of the leeward glide by gliding transverse to the wind. The gain in kinetic energy during the high altitude turn is greatly lessened by this procedure, of course. (See Section VI, page 94.)

involved in a typical flight cycle. It is assumed that the albatross begins the climb from an initial altitude of 5 feet and rises to a maximum altitude of 50 feet, where it begins the leeward turn. If the weight of the bird is taken as 20 pounds (Diomedea exulans), the corresponding gain of potential energy will be 45 feet × 20 lb = 900 ft lb. However, a large part of this energy is derived not from the wind but from the initial kinetic energy of the bird. Hence the net energy extracted from the wind is considerably less than 900 ft lb. Actually, the rate at which potential energy is extracted from the wind at each point of the climb is proportional to the ratio of the wind speed $V_w$ to the total airspeed $(V_w - u)$. Thus a realistic value for the potential energy furnished by the wind might be only around 40% of the total, or roughly 360 ft lb. For the leeward turn, it is assumed that the bird begins the turn with an absolute speed of 5 mi/hr, moving into a wind whose speed is 35 mi/hr. The airspeed of the bird is therefore 40 mi/hr. The turn to leeward is performed at constant airspeed, and thus completed with an absolute speed of 40 + 35 = 75 mi/hr to leeward. The kinetic energy gained in the turn is, using eq. (94),

$$\Delta KE = 2 \frac{20}{32.2} (58.6)(51.3) = 3740 \text{ ft lb} \qquad (149)$$

It is thus evident that the leeward turn results in the extraction of approximately 10.4 times as much energy from the wind as does the windward climb, for this particular case.

The really essential requirement in dynamic soaring is the availability of adjacent air regions having different wind speeds, such as exist at the top and bottom of the shear layer. The existence of a continuous gradient of wind speed (as actually exists in the shear layer) is not an essential requirement. As far as the basic mechanics are concerned, dynamic soaring could be carried out just as well if the shear layer were reduced to an infinitely thin surface of discontinuity separating the regions of still and moving air. In fact, the flight maneuvers of certain phases of the basic soaring cycle might be considerably simplified if the actual shear layer could be replaced by a surface of discontinuity.

It is interesting to note the rather close similarity between the conditions required for dynamic soaring and those for the operation of a Carnot heat engine. In the case of soaring, a region of relatively low wind speed must exist which the bird can enter, before any practical use can be made of the kinetic energy gained in the region of high wind speed. In the case of the Carnot engine, there must exist a region of relatively low temperature into which the heat can flow before any practical use can be made of the energy associated with the region of high temperature.

## ADVANCED FLIGHT PATTERNS OF THE ALBATROSS

The four phases of the basic soaring cycle constitute the means by which the albatross is able to extract its flight energy from the wind. This simple cycle does not, in itself, provide a means for practical utilization of the energy gained. By suitably spacing and varying the length of the basic phases and properly interspersing certain secondary flight maneuvers, however, the

bird is able to construct an almost infinite variety of advanced flight patterns which enable it to travel in practically any desired direction over the water. Under adequate wind conditions, the albatross can proceed upwind, crosswind, and downwind with ease, and can follow a ship for hours or even days, regardless of the vessel's course and speed.

## Flight Paths

Despite the variety and complexity of the advanced flight patterns, all appear to be based on the same general principle. Under sufficient wind conditions, the bird gains more energy in the leeward turn than is required for maintaining the basic cycle; this excess energy is used to extend the duration of the basic phases or to provide power for additional periods of coasting flight. By use of such additional or secondary flight segments, the bird is able to regulate quite precisely its net travel, or displacement, relative to earth. The manner in which this is accomplished is most readily illustrated by means of simple plan view diagrams of possible flight patterns.

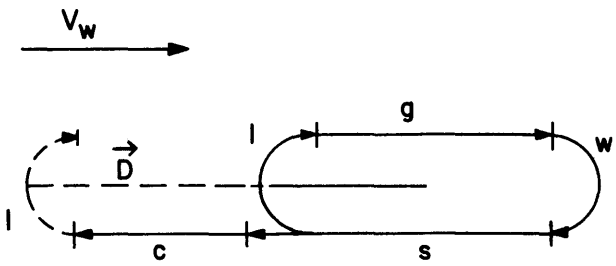


Fig. 39

In the diagrams, the flight path segments corresponding to the four phases of the basic cycle are denoted by c, l, g, and $w_k$ for the windward climb, high altitude turn to leeward, leeward glide, and low altitude turn to windward, respectively. The secondary skimming or coasting segments are denoted by s.

Fig. 39 shows one complete cycle of a possible pattern which results in a net travel directly to windward. Following the glide g and turn $w_k$, the bird merely coasts (with continuous deceleration) at essentially constant altitude while covering distance to windward. The coast or skim s is made at a low altitude just above the water, where the wind speed is very low. The duration of the skim s is under the control of the bird, but must be terminated with sufficient kinetic energy remaining to meet the requirements of the windward climb. Thus, for each given wind condition, there exists a maximum for s which cannot be exceeded. For net travel to windward, the distance s + c must be greater than the glide distance g plus the leeward displacement due to the turns l and $w_k$. In order to progress directly upwind, all turns must be made in the same direction (i.e., all turns are either clockwise or counterclockwise); otherwise a lateral displacement will occur for each cycle.

The net displacement of the bird is defined as the vector $\hat{D}$

$$\hat{D} = \int_{t_o}^{t_1} [(\hat{V}_a \cdot \hat{i})\,\hat{i} + (\hat{V}_a \cdot \hat{j})\,\hat{j}]\,dt \qquad (150)$$

where $\hat{V}_a$ is the absolute velocity of the bird and $t_o$ and $t_1$ are the times corresponding to the start and finish of a cycle, that is, $t_1 - t_o$ is the period of the cycle. The vector $\vec{D}$ is obtained by connecting corresponding points of successive cycles, as shown in Fig. 39 by the dashed vector. The magnitude of the displacement vector, $s_o$, is the straight line distance between any two successive, corresponding points.

The net displacement velocity is defined using eq. (150),

$$\hat{V}_D = (t_1 - t_o)^{-1} \hat{D} \qquad (151)$$

It thus has the same direction as $\hat{D}$, but a magnitude of $s_o/(t_1 - t_o)$. The net displacement velocity is the important factor in determining the direction and rate of travel of the albatross. The vector $\hat{V}_W$ denotes the wind direction relative to the flight path.

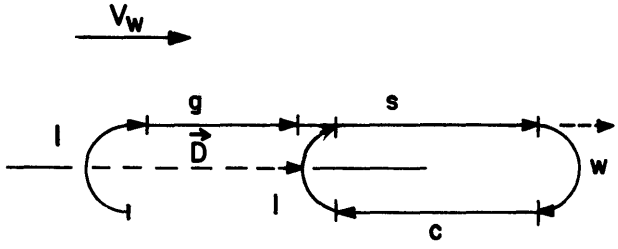


Fig. 40

For direct downwind travel, the same procedure as for the windward case can be used, only the skim is made following the leeward glide, as shown in Fig. 40. As noted previously, the glide g can be made rather steeply, as for gaining maximum kinetic energy, or it can be made at the minimum inclination angle $\gamma$, so as to cover the most leeward distance in the glide. The particular type of glide which the bird uses in a given case will, of course, affect the relative lengths of the segments g and s. Which glide procedure gives a maximum value for g + s (and hence maximum leeward travel) for a given altitude loss can be established only when the aerodynamic characteristics of the albatross have been quantitatively determined.

By banking in opposite directions on the leeward and windward turns, the direct upwind and downwind paths discussed above can be converted to the diagonal trajectories shown in Figs. 41 and 42. The direction of travel can be varied by adjusting the length of the skim path s (or other path segments). In the limiting case shown in Fig. 43, the bird's displacement velocity is perpendicular to the wind direction, since $g + s \doteq C$. Alternately, of course, the skim could be divided between the upwind and downwind legs such that $g + s_1 \doteq C + s_2$.

The lateral component of the displacement $\hat{D}$ per cycle can be appreciably increased by adding lateral skim segments as shown in Fig. 44. This figure shows the particular case where $\hat{D}$ has a downwind component. The low altitude skim can be made exceptionally efficient if the waves are large by coasting along the lee side of a wave crest, since then additional static energy can be derived from the declivity air currents generated by the wind in moving up the back of the wave. The mechanics of this process will be considered in more detail subsequently (page 78).

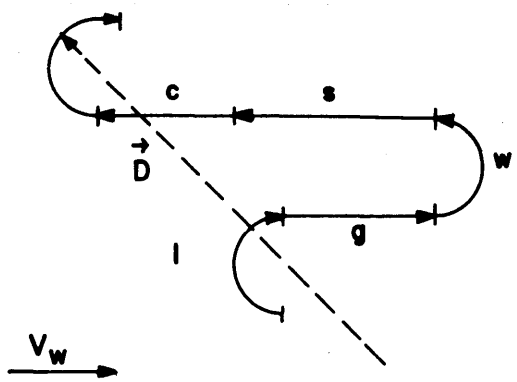


Fig. 41

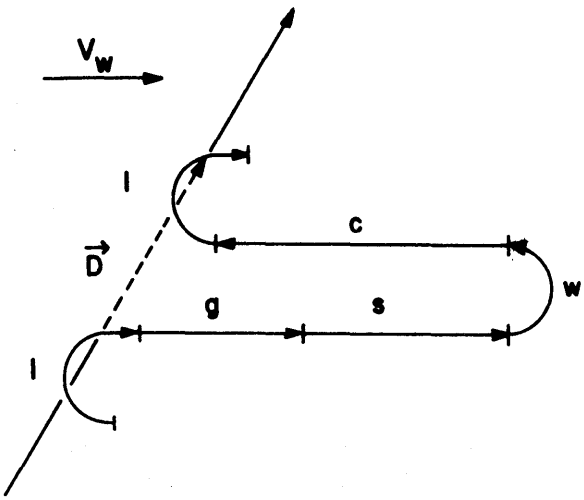


Fig. 42

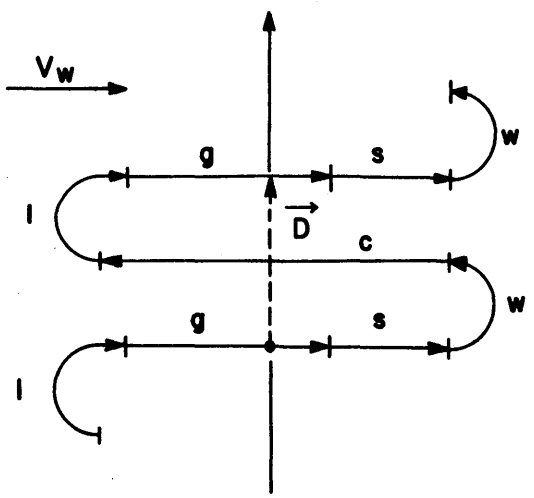


Fig. 43

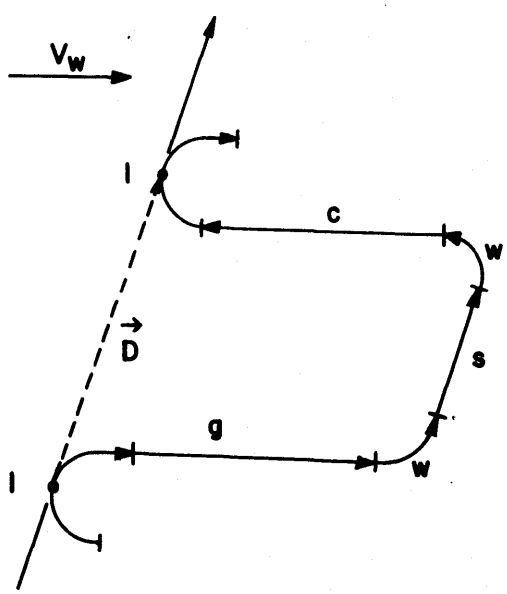


Fig. 44

The lateral skim segment can also be divided into two (or more) parts to yield additional variations to the resultant flight path. Pictured in Fig. 45 is the flight path used by the albatross in following a ship which is moving perpendicular to the wind direction. The bird adjusts the length of the various flight segments according to the wind strength so as to effect a resultant flight path which periodically brings it directly over the vessel's wake, which it carefully examines for any edible refuse.

Using suitable combinations and variations of the flight patterns discussed above, the albatross can travel in any desired direction relative to the wind, and with a range of displacement speeds, provided the wind speed lies within proper limits. The restrictions imposed on the travel capabilities of the albatross by wind conditions are discussed below.

## Limiting Flight Conditions

It is obvious that since the albatross extracts its soaring power from the energy of the wind, dynamic soaring must cease when the wind speed drops below that required to supply the minimum energy demands of the basic cycle. As the wind speed (above the shear layer) decreases, the kinetic energy available from the leeward turn also decreases, according to eq. (94). On the other hand, the energy requirements which the bird must satisfy from its kinetic energy supply increase in the windward climb. This is because the bird must move faster (into a decreased wind) to attain a given aerodynamic velocity and hence will furnish a greater part of the energy required for overcoming the dissipation drag and for doing work in raising the weight of the bird during the climb (i.e. for increasing the potential energy). When the wind speed has decreased to such an extent that the net kinetic energy of the bird after the windward turn is less than that needed to raise it to the top of the shear layer, the maximum altitude which can be reached in each succeeding cycle will continuously decrease and the bird will ultimately come to rest, unless it resorts to flapping flight to supply the energy deficiency. Long before this limiting energy condition is reached, however, the advanced flight patterns available to the bird will have been greatly reduced in range and scope. Travel in arbitrary directions will therefore become quite limited. In particular, all patterns depending upon a coasting segment will have been eliminated.

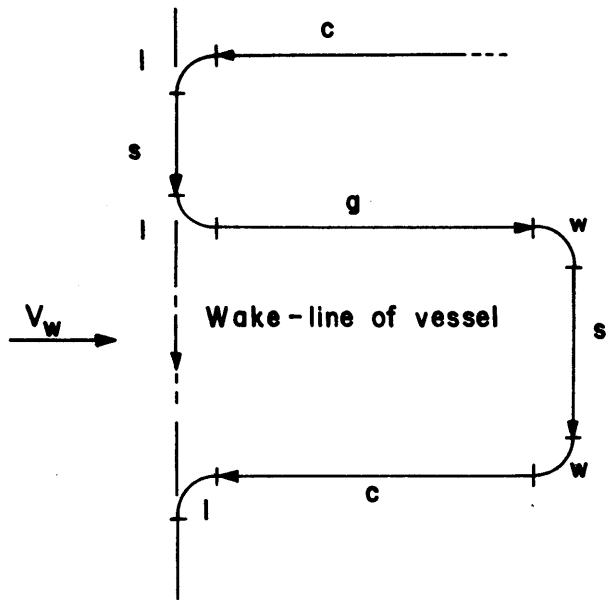


Fig. 45

The same type of limiting effects are imposed by very high wind speeds. Strong winds generate large waves and rough seas which tend to introduce severe turbulence in the lower air layers, making flight difficult. In addition, as the wind speed increases, the wave forms generated have a pronounced effect on the airflow and the velocity profile $V_w(z)$ becomes very distorted near the surface. The net kinetic energy available from the wind will then decrease as the wind increases, since the difference in wind speed at the respective levels of the leeward and windward turns becomes smaller. The same energy deficiency

effects as appear in the case of low wind speeds would then occur. In high wind speeds the bird could still perform the leeward glide; it might not, however, be able to gain any distance to windward. In fact, above a certain wind speed, the bird would necessarily be carried downwind, regardless of its desires or attempts to proceed otherwise; it might still be able to continue the basic cycle, however, and remain airborne. In winds of sufficiently high speed, albatrosses are indeed observed to be swept away to leeward. For a rational investigation and evaluation of these wind speed effects, more exact information must be obtained on how $z^*$ and $p$ vary with $V_w(z^*)$ in eq. (2) for the wind profile. That is, it must be ascertained how the shape of the velocity distribution profile $V_w(z)$ and shear layer depth $z^*$ vary (over water) as the wind speed far above the surface increases to large values.

## AUXILIARY FLIGHT MODES

### Landing and Take-Off

In addition to meeting the highly specialized aerodynamic requirements of the basic and advanced cycles of dynamic soaring flight, the albatross must also be able to perform the important maneuvers of landing and take-off. Unfortunately, the requirements for efficient dynamic soaring are quite incompatible with those for safe and easy landings and take-offs. But so critical, apparently, is the need for efficient soaring capability to the survival of the albatross that the bird's present form has evolved almost entirely to maximize the soaring performance, even to the extent of making the landing and take-off process a marginal and often dangerous undertaking.

Landing. - The albatross must be able to "land" upon both water and land surfaces. In general, the water landing is practiced much more frequently, for the bird must alight on the surface each time it feeds. During the nesting season, however, frequent landings must also be made on land. It is this latter case which, in the absence of wind, poses the primary landing difficulties.

The results of the foregoing dynamic soaring analysis showed that a relatively high value of the wing loading $W/S$ is necessary for efficient soaring; this requirement gives rise to the primary landing (and take-off) problems of the albatross. For safety in landing, the bird must approach the surface (either land or water) with a small sinking speed $w$ and small absolute velocity $\hat{V}_a$ (relative to earth). If $\hat{V}_a$ is small, the impact forces generated when the bird contacts the surface will be correspondingly small.

In order that $w$ be small, the bird must be moving essentially parallel to the landing surface at touch-down. This requires that the condition

$$L = W = C_L \frac{1}{2} \rho V^2 S \tag{152}$$

or

$$\frac{W}{S} = \frac{1}{2} \rho C_L V^2 \tag{153}$$

be satisfied. The aerodynamic velocity $\hat{V}$ depends upon the wind $\hat{V}_w$ and absolute velocity $\hat{V}_a$ of the bird,

$$\hat{V} = \hat{V}_a - \hat{V}_w \tag{154}$$

Hence, since $W/S$ is constant for the landing conditions, it is necessary that $C_L$ be large if $\hat{V}$, and thus $\hat{V}_a$, is to be small. It is also obvious from eq. (154) that the landings must be made directly into the wind in order to minimize $\hat{V}_a$. The maximum attainable value of $C_L$, $C_{L_{max}}$, is set by wing stall, so that the minimum absolute speed $(V_a)_{min}$ with which the bird can land is given by

$$(V_a)_{min} = \left(\frac{W}{S}\frac{2}{\rho\, C_{L_{max}}}\right)^{1/2} - V_w \tag{155}$$

Eq. (155) clearly shows the factors which govern the landing of the albatross, and which determine the relative difficulty of the process. For given values of $W/S$ and $C_{L_{max}}$, it is clear that $(V_a)_{min}$ is set by the wind speed $V_w$. If $V_w$ is small, $(V_a)_{min}$ will be correspondingly large. For the case $V_w = 0$, the bird must land with a minimum absolute speed of

$$(V_a)_{min} = \left(\frac{W}{S}\frac{2}{\rho\, C_{L_{max}}}\right)^{1/2} \tag{156}$$

which is equal to the aerodynamic stalling speed $V_s$,

$$V_s = \left(\frac{W}{S}\frac{2}{\rho\, C_{L_{max}}}\right)^{1/2} \tag{157}$$

If the wind speed is large, $(V_a)_{min}$ can be correspondingly reduced. In fact, when

$$V_w = \left(\frac{W}{S}\frac{2}{\rho\, C_{L_{max}}}\right)^{1/2} \tag{158}$$

the bird will have no absolute velocity, $\hat{V}_a = 0$, and can alight smoothly and gently by unloading its wing when close to the surface.

Because the basic wing loading of the albatross is relatively large for the value of $C_{L_{max}}$ which can be attained, $V_s$ [eq. (157)] is large and the landing must be accomplished at this high speed in the absence of wind. The observed value of $V_s$ is on the order of 30 to 35 miles per hour for the albatross, a dangerously high landing speed for so heavy a bird with such slender, fragile wings. When alighting on water under weak wind conditions, the albatross uses its enormous webbed feet as hydroplanes and brakes in order to lessen the shock of the landing impact. On land, this auxiliary deceleration technique is not possible and the bird endeavors to absorb some of the landing shock by pitching forward onto its well patted breast. In such cases the birds may do complete somersaults before coming to rest. Under such adverse conditions, major bones are often broken and fatalities sometimes occur. Due to the

extreme span of its wing (another consequence of specialized adaptation for efficient soaring), the albatross cannot effectively utilize the conventional wing-flapping techniques used by most other birds to kill off excess speed during the landing maneuver.

Thus, in the same manner that the albatross cannot soar without sufficient wind, it cannot safely land without it. At sea, as the wind speed decreases, the albatross is observed to alight less and less frequently, due to the difficulties involved in the landing and subsequent take off. Indeed, the uncertainty of the final landing spot under marginal wind conditions would make the capture of living prey most difficult, if not entirely futile. On land, nesting sites are always chosen where the wind is strong and constant, and nests are located on the windward side of the islands to facilitate landing and take off. Some albatross colonies are located on cliff faces and ledges in order to alleviate the landing and take off problems as much as possible. Such nest locations afford the bird considerably more room for use of its wings as a speed brake in landing; they are even more important for the take off simplification they offer, since the bird merely pitches forward into flight.

Take Off. - The high wing loading of the albatross imposes the same difficulties on the take off, in weak winds, as it does in the landing case. Actually, the take off difficulties are even more severe, since then the bird must supply energy insteady of merely dissipating it. In the take off case, eqs. (155), (156), (157), and (158) still apply, so that the existence of a wind is exceedingly helpful in reducing the ground speed (and hence the kinetic energy) which the bird must attain before becoming airborne. Since the albatross can make no real use of its wings for propulsive action prior to lift off, all energy required to accelerate the bird to take off speed must come from its own leg muscles.

On water, the albatross literally runs across the surface using its hugh webbed feet as paddles to propel it along. In many instances when the wind speed is low, some 300 feet or more of run are needed before the bird becomes fully airborne. Since the wind speed right at the water surface is relatively low, the bird must gain considerable absolute speed before it can get up into the faster moving region of the shear layer. On land, the take off is more difficult yet, since the bird's feet are not at all adapted to fast running over solid surfaces. In the usual case, the bird climbs to the top of some small hill or incline and, gaining speed as it rushes down the windward slope, launches itself into the air. If a sufficient wind is blowing, however, the take off process, as well as the landing, becomes greatly simplified and the lift off is accomplished with relatively little effort. The albatross takes great care on land, therefore, to select nesting areas which are fully accessible to strong winds. At sea, when winds are brisk, the upcurrents on the back side of waves are used to give the bird an extra boost as it takes off to windward from the crest of a wave.

## Flight Along Wave Fronts

The primary flight mode of the albatross is dynamic soaring, but the bird appears to make full use of a limited source of static soaring energy* made available by the wave fronts generated during periods of strong winds. This same phenomenon of static soaring along waves is observed in a number of other sea and shore birds, such as the shearwaters and pelicans. The energy obtained in this manner, while of only minor importance to the albatross, appears to constitute a very substantial part of the total flight energy of the latter birds. In view, therefore, of the apparently general applicability of this type of soaring, the subject is treated in this section in some detail. Other interesting, although relatively unimportant, examples of the use of static soaring by the albatross are briefly mentioned.

Static Soaring Along Waves. - When the wind at sea is strong, relatively large surface waves are generated and the air moving over these forms creates areas of appreciable upflow on their windward sides, much like the hill-generated declivity currents on land (Fig. 46). By soaring parallel to such

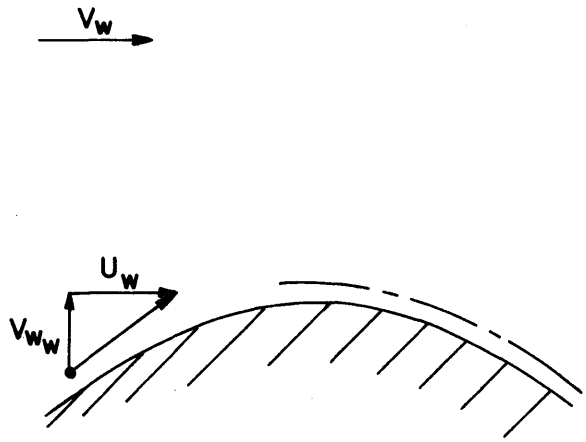


Fig. 46

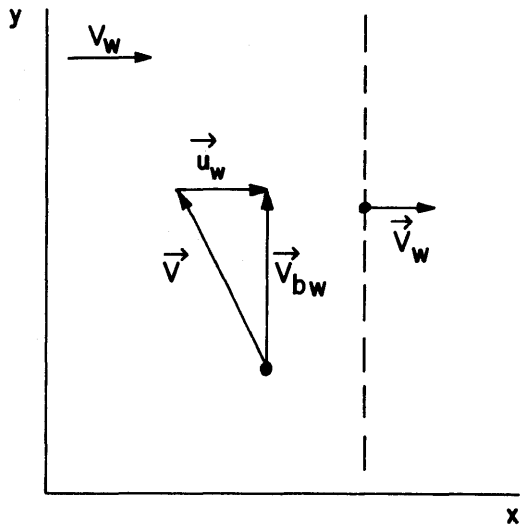


Fig. 47

a wave form and keeping within the region of strongest upflow, the albatross is able to decrease its sinking velocity during the cross-wind coasting segments of its flight cycles. This enables it to conserve its basic kinetic energy supply for use in other parts of the flight pattern, and thus allows it a greater travel range per flight cycle. The amount of energy which can be derived from the upflow depends, of course, on the magnitude of the maximum vertical velocity generated by the wave. Even when the upflow is not sufficiently strong to reduce the bird's sinking speed (relative to earth) to zero during the coast, useful energy can still be taken from the air and the length of the coasting segment correspondingly increased.

*A brief discussion of static soaring is presented in Appendix A-4.

In general, the wave form is itself moving to leeward, but more slowly than the wind. Thus, in order to fly parallel to the wave, the albatross must move downwind with the same absolute speed as the wave. The velocity regime necessary to accomplish this is pictured in Fig. 47 where

$\hat{U}_w$ = x-component of velocity of air relative to wave form

$\hat{V}$ = velocity of bird relative to air

$\hat{V}_{bw}$ = velocity of bird relative to wave form

$\hat{V}_w$ = velocity of wave form relative to earth

The bird must move relative to the air in such a manner that the x-component of $\hat{V}$ cancels the velocity $\hat{U}_w$ of the air relative to the wave. The absolute velocity $\hat{V}_a$ of the bird as seen by a stationary observer is shown in Fig. 48. The bird will be carried downwind $V_w$ feet for every $V_{bw}$ feet it travels parallel to the wave.

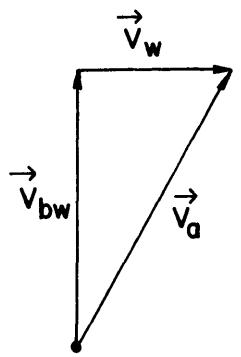


Fig. 48

All the while the bird is moving along the wave front, it will be sinking relative to the air with a speed $w_b$. If the upflow speed $w_w$ (see Fig. 46) is equal to $w_b$, the bird will move along the wave at constant altitude with all of its flight energy being provided by the air and, consequently, there will be no deceleration of the bird. If $w_b > w_w$, however, the extra energy needed to maintain constant altitude must come from the basic kinetic energy supply and the bird will decelerate. The relative magnitudes of $w_b$ and $w_w$ thus govern the length of the glide segment along the wave front.

For the albatross, with its high wing loading, $w_b$ is probably much larger than the value of $w_w$ usually available, and hence the waves provide only a minor contribution to the bird's overall flight energy. For other birds, however, it may be much more significant, especially for pelagic and coastal species having smaller wing loadings. In this latter case, it is possible that $w_w$ can exceed $w_b$ over a considerable region on the windward side of the waves and the birds can soar for relatively long distances without flapping. Pelicans, for example, although large, have low wing loadings and can be routinely observed soaring along waves of coastal waters. The upflow is apparently not sufficient to support them entirely, however, and the birds must flap periodically to maintain their momentum. Still, the length of their coasting glide is considerably extended by the existence of the upflow and the flight energy required of the bird itself must be appreciably reduced.

Mechanics of the Airflow Over Waves. - Since the strength of the vertical velocity field $w_w$ over waves determines the practical use which can be made of wave soaring by such birds as the albatross, pelican, and shearwater, it is

desirable to obtain some means for estimating the upflow field strength in relation to wave size and speed, and to wind speed. Although the shear layer introduces a gradient in the air speed above the wave surface, the effect of the wave form on the external airflow pattern decreases very rapidly with distance above the wave. Thus, the higher-velocity air above the waves would have only a slight effect on the velocity field very near the wave surfaces. For purposes of estimating the magnitude of the vertical velocity field very near the waves, it would appear acceptable, therefore, to neglect the velocity variations associated with the shear layer and to use some "average" or "effective" wind speed (relative to the wave form) for calculating the velocity field in the vicinity of the waves. With this assumption we shall now derive the vertical and horizontal velocity fields generated by the wind moving over wave forms.

The wave form is assumed to be a sine function

$$z = A \sin 2\pi \frac{x}{\lambda} \tag{159}$$

where $A$ is the amplitude and $\lambda$ the length of the waves, as shown in Fig. 49. The velocity fields $u_w(x,z)$ and $w_w(x,z)$ are determined by first finding the perturbation velocity potential $\varphi$ of the flow which satisfies Laplace's equation

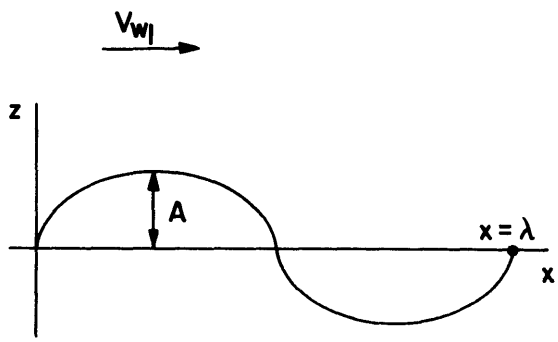


Fig. 49

$$\frac{\partial^2 \varphi}{\partial x^2} + \frac{\partial^2 \varphi}{\partial z^2} = 0 \tag{160}$$

and the boundary conditions

$$u_w\,(x, \infty) = V_{w1} \tag{161}$$

$$w_w\,(x, o) = V_{w1}\left(\frac{dz}{dx}\right)_{wave} \tag{162}$$

where $V_{w1}$ is the "effective" velocity of the air relative to the wave. The flow above the wave is assumed to be "effectively" irrotational, although the shear layer is itself rotational, of course. The field velocities are given by $w_w = \partial\varphi/\partial z$, $u_w = V_{w1} + u_w{}^1$ where, $u_w{}^1$ is the perturbation velocity satisfying eq. (160), that is, $u_w{}^1 = \partial\varphi/\partial x$.

The solution of eq. (160) is obtained by separation of variables as follows. The solution is assumed to have the form

$$\varphi\,(x,z) = F\,(x) \cdot G\,(z) \tag{163}$$

Differentiating eq. (163) and substituting in eq. (160) they yield

$$\frac{1}{F}\frac{d^2F}{dx^2} + \frac{1}{G}\frac{d^2G}{dz^2} = 0 \tag{164}$$

or

$$\frac{d^2F}{dx^2} + k^2 F = 0 \tag{165}$$

$$\frac{d^2G}{dz^2} - k^2 G = 0 \tag{166}$$

where $k$ is a constant. Solution of these two differential equations yields

$$F(x) = A_1 \sin kx + A_2 \cos kx \tag{167}$$

and

$$G(z) = B_1 e^{-kz} + B_2 e^{kz} \tag{168}$$

Applying the boundary conditions of eqs. (161) and (162), we have

$$B_2 = 0 \tag{169}$$

$$w(x, o) = \left(\frac{\partial \varphi}{\partial z}\right)_{z=o} = (A_1 \sin kx + A_2 \cos kx)\,(-B_1 k e^{-kz}) = V_{w1} A \frac{2\pi}{\lambda} \cos \frac{2\pi x}{\lambda} \tag{170}$$

whence

$$A_1 = 0$$

$$- A_2 B_1 k = V_{w1} A \frac{2\pi}{\lambda}$$

Hence

$$\varphi (x,z) = - V_{w1} A e^{-2\pi z/\lambda} \cos 2\pi \frac{x}{\lambda} \tag{171}$$

and

$$u_w = 2\pi V_{w1} \frac{A}{\lambda} e^{-2\pi z/\lambda} \sin 2\pi \frac{x}{\lambda} + V_{w1} \tag{172}$$

$$w_w = 2\pi V_{w1} \frac{A}{\lambda} e^{-2\pi z/\lambda} \cos 2\pi \frac{x}{\lambda} \tag{173}$$

It thus appears that $w_w$ is a maximum at the wave surface ($z = 0$) and midway up the windward side ($x = 0$), or at the origin in Fig. 49 where it has the value $2\pi \cdot A/\lambda \cdot V_{w1}$.

Eqs. (172) and (173) show that the local velocities are proportional to the wind speed $V_{wl}$ relative to the wave form and to the amplitude-wave length ratio $A/\lambda$. These equations may be put in a more convenient nondimensional form by use of the definitions

$$\xi = 2\pi \frac{x}{\lambda}$$

$$\eta = 2\pi \frac{z}{\lambda} \qquad (174)$$

$$R = 2\pi \frac{A}{\lambda}$$

Thus

$$\frac{u_w}{V_{wl}} = R\, e^{-\eta} \sin \xi + 1 \qquad (0 \leq \eta \leq R) \qquad (175)$$

$$\frac{w_w}{V_{wl}} = R\, e^{-\eta} \cos \xi \qquad (0 \leq \xi \leq 2\pi) \qquad (176)$$

and eq. (159) for the wave surface becomes

$$\eta = R \sin \xi \qquad (177)$$

Eqs. (175) and (176) give the horizontal and vertical velocity fields $u_w$ and $w_w$ for all wave forms and wind conditions. Figures 50(a) and 50(b) present plots of $u_w'/V_{wl}$ and $w_w/V_{wl}$ for an amplitude ratio of $R = 1.0$, for constant values of $\eta$. For other amplitude ratios, chart values of $w_w/V_{wl}$ are multiplied by the actual value of R. With $R = 1$, eqs. (175) and (176) yield simple sine and cosine waves, respectively, of amplitude $e^{-\eta}$. The local velocity disturbances caused by the wave surface thus decrease very rapidly with altitude. This rapid decrease in $w_w$ with altitude is the primary reason why wave-soaring birds must fly very close to the surface, especially in cases where $V_{wl}$ is relatively small in value. The smaller petrels, with very low wing loadings, are well adapted to this type of soaring. It should be noted that the horizontal perturbation velocity $u_w'$ is negative in the wave trough region. Thus the absolute velocity of the air is a minimum in the trough, and the bird can make its windward turn most efficiently in this region, as previously discussed.

As a practical example, let us determine the vertical velocity at the origin ($x = 0$, $z = 0$) of a wave with $\lambda = 300$ feet and $A = 15$ feet, for $V_{wl} = 20$ feet/second. This is probably a relatively strong wind compared to the average which occurs with waves of this size, except in storms. From eq. (174)

$$R = 2\pi \cdot \frac{15}{300} = \frac{\pi}{10}$$

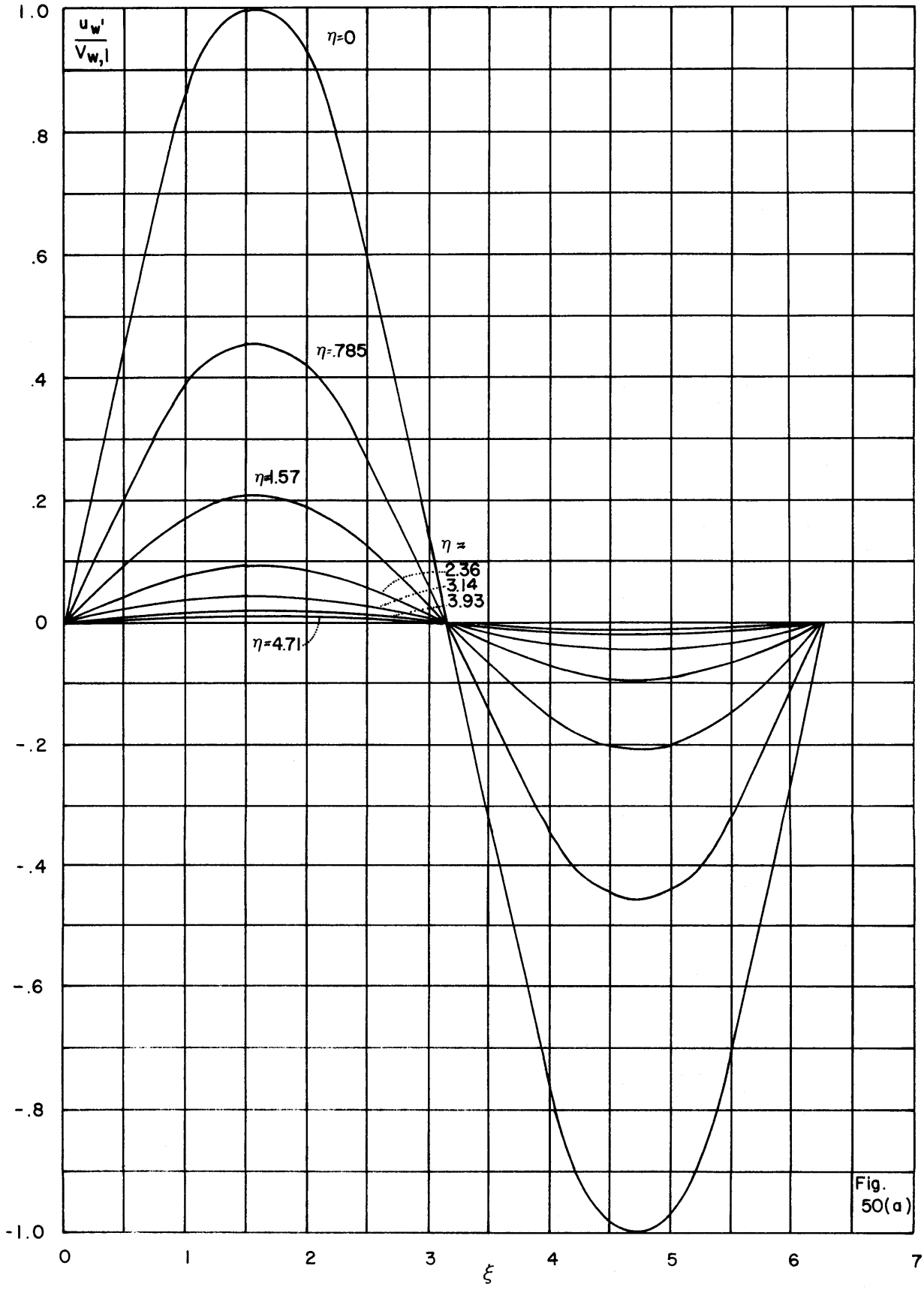
$\frac{u_w'}{V_{w,1}}$
η=0
η=.785
η=1.57
η =
2.36
3.14
3.93
η=4.71
1.0
.8
.6
.4
.2
0
-.2
-.4
-.6
-.8
-1.0
0
1
2
3
4
5
6
7
ξ
Fig. 50(a)

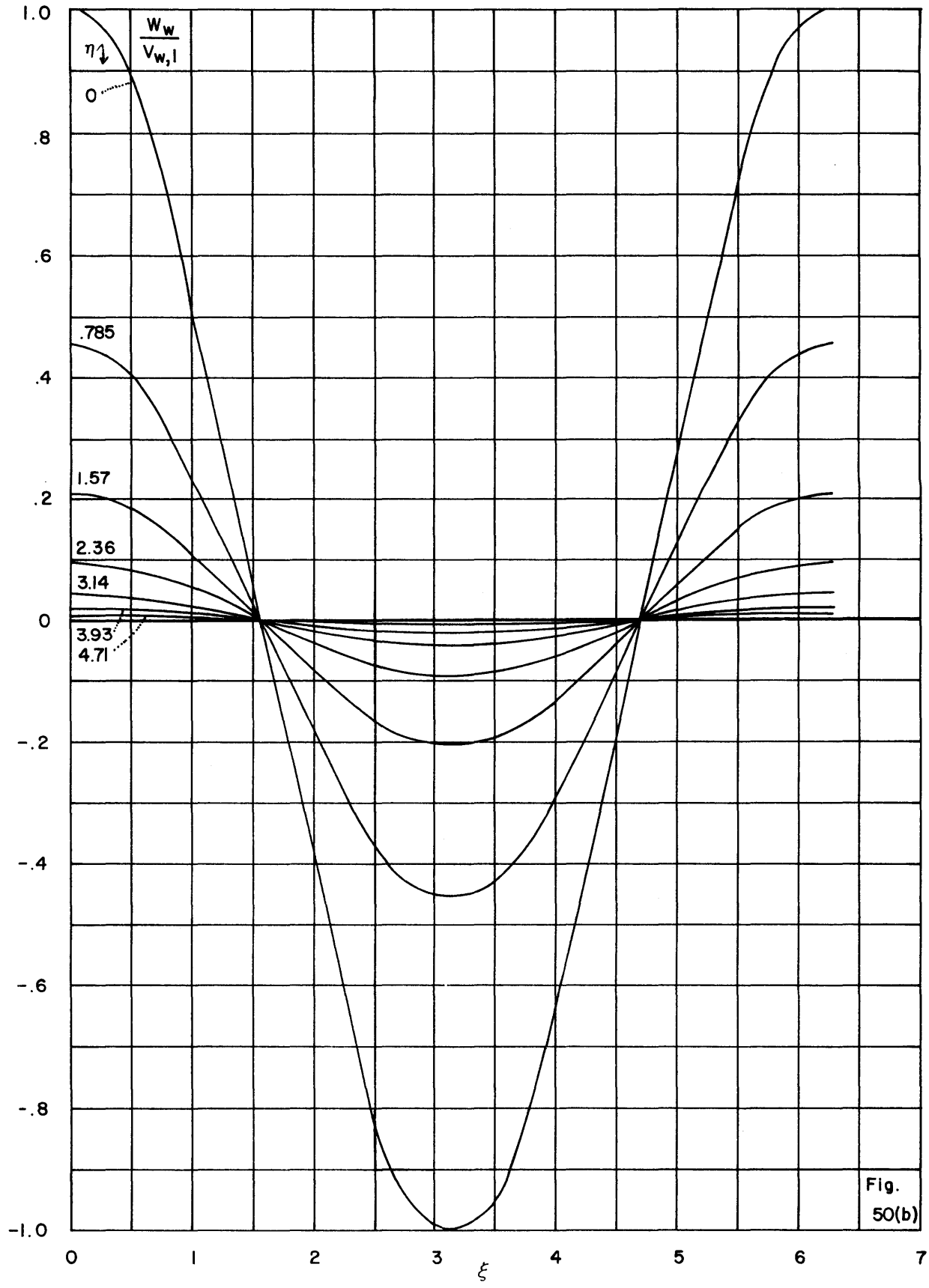
1.0
.8
.6
.4
.2
0
-.2
-.4
-.6
-.8
-1.0
$\frac{W_w}{V_{w,1}}$
$\eta$
0
.785
1.57
2.36
3.14
3.93
4.71
0
1
2
3
4
5
6
7
$\xi$
Fig. 50(b)

Thus

$$\frac{w_w}{V_{wl}} = \frac{\pi}{10} w_w = 6.28 \frac{ft}{sec} \tag{178}$$

For the point $x = 0$, $z = 1/2$, $A = 7.5$ feet, we have $\xi = 0$, $\eta = R/2 = \pi/20$. Thus, from Fig. 50, or from eq. (176)

$$w_w = (20) \frac{\pi}{10} (e^{-\pi/20}) = 5.40 \frac{ft}{sec} \tag{179}$$

At present, direct experimental measurements must be relied upon to furnish the necessary data for practical use of eqs. (175) and (176). Thus by measuring the effective absolute wind speed $V_w(z')$ and the wave speed $v_w$, the effective relative airspeed $V_{wl}$ is obtained as $V_w(z') - v_w$. Estimation of $A$ and $\lambda$ for the waves then provides the data needed for calculating the velocity fields $u_w$ and $w_w$. The "effective" values of $V_w(z')$ and $V_{wl}$ could be estimated by measuring $u_w$ and calculating the corresponding value of $V_{wl}$, using eq. (175), for actual sea conditions. In any event, eqs. (175) and (176) allow us to make some reasonable prediction of the magnitude of the vertical (and horizontal) flow velocities near waves of various sizes, so that an approximate quanitiative analysis of wave soaring by various birds can be carried out when sufficient experimental data on the wave and bird characteristics are available.

Two possible cases of wave soaring are of interest, although only one appears to have any practical significance. These cases are pictured in Fig. 51. The first [case (a)] is that just discussed, where the wind speed is greater than the wave speed $v_w$ and hence the relative airspeed $V_{wl}$ has a positive value. The second [case (b)] is that where a swell generated by distant winds, or a previous day's storm, moves through still air. In this case, $V_{wl} = -v_w$. Aerodynamically, conditions are exactly as for (a) as regards wave soaring. However, the upcurrent region will now appear on the front face of the wave, rather than on the rear side. The flight forces on a bird using such waves are directly analagous to those acting on a surf board riding the face of a large breaker. Since only the wave <u>form</u> (not the water itself) is moving relative to the air, there will be no significant boundary layer generated in this case.

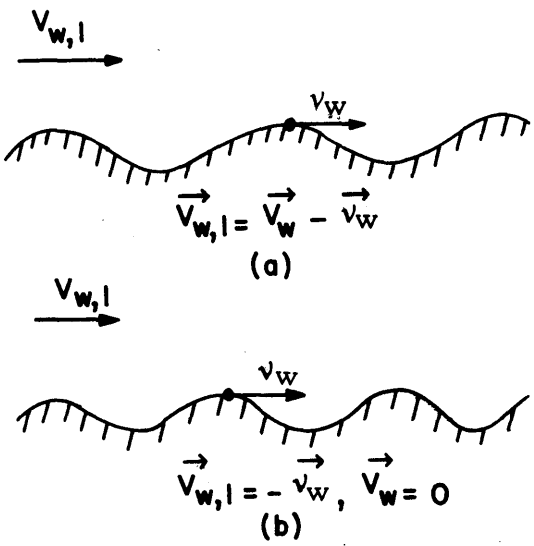


Fig. 51

In the special case where the wave and wind speeds are equal, no relative air motion $V_{wl}$ is developed and hence $u_w = w_w = 0$. Thus, static soaring is impossible, even though both wind and waves are present.

Other Examples of Static Soaring by Albatrosses. - It does not, in general, appear that thermal air currents of a size, strength, and distribution sufficient to support continuous static soaring by the albatross (or by other sea birds) occur over the ocean. This may be due to a number of causes, among them being the fact that the incident sunlight which strikes the ocean is absorbed and converted to heat over a considerable depth of water, instead of being concentrated and producing a high temperature at the surface, as is the case on land. Only in the vicinity of islands and over other bodies of land do useful thermal currents arise. It is interesting to note, however, that despite the fact that dynamic soaring is the principal flight mode of the albatross, the bird is still quite adept at static soaring, even under complex and rather artificial conditions. Balancing itself in some adequate upflow, the albatross is able to maintain almost perfect aerodynamic equilibrium, and sails along with the vessel for amazingly long periods of time. This static soaring characteristic of the albatross has enabled observers to make a number of excellent close-up photographs of these birds. It is an impressive indication of the albatross' versatile flight powers that it can, after months of continuous dynamic soaring, immediately upon encountering a ship, find and balance itself in the limited upflow regions.

Albatrosses can, and sometimes do, circle to enormous heights in thermal currents over their nesting islands.[4] The high wing loading of the bird, however, requires very strong and extensive currents to carry it to any appreciable altitude since both the radius of turn and aerodynamic sinking velocity are increasing functions of $W/S$.[3,12]

## IV. AEROECOLOGY OF THE ALBATROSS

The preceding section was concerned with development of the aerodynamic basis of albatross flight. In the present section, the ecological significance of some general observations on albatross behavior will be examined and discussed in light of the bird's aerodynamic properties. As in Section II, the present discussion applies to albatrosses in general, and to the Wandering Albatross in particular.

"Aeroecology" we define as that part of the total ecology of a bird (or other flying organism) which is governed primarily by the aerodynamic properties of the bird, and is concerned with the interaction of these properties with the environment. As noted in Section II, the albatross (and other soaring birds) is dependent upon its environment not only for food but also for its direct means of locomotion. The aeroecology of soaring species, therefore, constitutes a most significant part of the total ecology of these birds.

Unfortunately, our present knowledge of the detailed behavior and life patterns of albatrosses, especially at sea, is quite insufficient for an adequately comprehensive ecological analysis to be made. Not only are the necessary behavioral data on albatrosses lacking, but our understanding of many aspects of the birds' physical environment is limited. The critical variations of shear-layer properties with wind speed and water conditions, for example, have not yet been investigated in sufficient detail.

This present scarcity of information is a reflection, no doubt, of the great difficulties involved in making comprehensive field studies of pelagic

animals and environmental phenomena, especially when the animals are capable of such extreme mobility over such vast ranges of sea as are the albatrosses. Reasonably complete and accurate ecological analyses of the albatrosses will be possible only after a much more complete collection of data has been obtained on the birds and their environments by carefully planned and extensive field studies.

Although its basic environment appears deceptively simple, the albatross' unique form and flight patterns clearly indicate a very high degree of specialization for its pelagic existence. Wind and water are the two essential elements on which its life depends. The wind provides the energy which allows the bird to cover vast stretches of ocean in its search for food, while the ocean waters provide the squid, shrimp, and fish of its principal diet. Thus, the albatrosses are generally found where belts of strong and continuous winds exist in conjunction with fertile ocean currents. It is a significant fact, therefore, that of the thirteen species comprising the family Diomedeidae, nine are to be found in the southern hemisphere between latitudes 30° and 60° where the strong belt of prevailing westerlies overlies the food-rich currents of the cold southern oceans. In addition to the prevalence of adequate food and wind conditions, the earth's surface in this region is nearly all water thus presenting the albatross with a practically unobstructed expanse of ocean completely circling the globe. Three of the remaining species are found in the North Pacific Ocean where the necessary environmental conditions are also prevalent, but with perhaps somewhat less intense wind conditions and a more restricted (but still vast) range of open sea.

The aerodynamic suitability of the albatross for sustained flight in ocean shear layers is obvious from the results obtained in the preceding Section **III**. The adequacy of the bird's form for efficient dynamic soaring, under the existing wind conditions at sea, is clearly evidenced by its amazing speed and range capabilities. This highly specialized form, however, makes the bird critically dependent upon the continued existence of these same wind conditions and also upon the constancy of the shear layer profile generated by the wind-water interaction.* Any appreciable change in either could prove disasterous unless the change occurred over a sufficiently long period of time to allow evolutional adaptation to the new conditions. This dependency on sufficient wind is particularly acute, for the albatross has only very limited flapping-flight endurance and is incapable of sustained flight in calm air.

---

*In this respect, it should be noted that the relative temperature of the air and water may exert a pronounced effect on the stability of the surface air and hence on the velocity profile of the shear layer. Thus, the characteristic ranges of particular species of albatrosses may depend in considerable measure upon the existence of surface water temperatures compatible with the generation of shear layer profiles suited to their aerodynamic characteristics. For example, it is noted that certain species of albatrosses cease to follow southbound ships in Antarctic water as soon as pack ice is encountered. This may be evidence of an adverse change in the shear layer due to the rougher surface created by the ice, or to the lower water temperatures encountered.

In view of the critical need of the albatross for continuous winds, an extended period of calm conditions at sea could conceivably destroy a large number of birds. However, at least two major factors act to prevent this. First, and most important, the albatross is generally a solitary bird when at sea and the population is dispersed over relatively vast areas. The concentration of albatrosses in the southern oceans is estimated to be on the order of one bird per 100 square miles, on the average. This distribution characteristic of the albatross not only lessens the competition for food, but also insures that localized calms will at most affect only a relatively few birds; the probability of calm conditions existing over an extremely large part of the ocean surface for any extended period is practically nil, as the continued survival of the large albatross populations in their highly specialized forms clearly proves. The ability of the albatross to cover such vast areas of ocean is, of course, the result of its specialized aerodynamic capabilities, which in turn permit it to utilize the shear-layer energy for its flight needs. In regard to the second factor, the young of most albatrosses remain at the nest for long periods during which time they are alternately fed by the parents, so that the chances of all three birds being overtaken by disaster at any one time are also relatively remote. The breeding islands of many species of albatrosses are spread out over a large geographical range.*

Perhaps an even more important factor, from a survival standpoint, than periods of absolute calm are extended periods of low wind speed, for the possibility of this latter condition occurring is much greater. A period of low wind speed results in a reduction in soaring capability, and flapping flight must be used as an auxiliary power source to keep the albatross airborne. This frequent wing flapping leads to an increased need for food, due to the expenditure of muscular energy. However, simultaneous with this need comes a decrease in the bird's ability to locate and secure its prey. This results from the fact that the travel ability is greatly reduced since very little "excess" energy is available in low speed winds for use in the auxiliary travel-flight patterns, and hence the bird cannot reconnoiter the necessary surface areas to locate sufficient food. In addition, a low wind speed adversely affects the albatross' ability to catch its prey once it has been sighted. The bird feeds primarily on live marine animals; these animals are generally capable of rapid motion to escape predators. The success of the albatross in snaring its prey depends, therefore, upon a swift and accurate initial attack. Since the albatross does not dive for its prey,** it must

---

*This fact may possibly be of some significance in the Pacific and Indian Oceans where the relatively frequent tsunamis could destroy entire nesting colonies. In this respect it would be interesting to note the nature of the ocean floor in the vicinity of the actual nesting islands used by the various albatrosses, since the local destructiveness of the tsunamis depends in considerable measure on the slope of the local ocean floor. The suitability of certain islands for albatross nesting may depend, among other factors, upon a relative immunity to tidal wave damage.

**It appears that the tube-like nostrils of the albatross may be a significant reason why these birds do not dive from altitude for prey. High speed dives such as performed by terns and pelicans would be quite dangerous. The tube-noses of the albatross open directly (continued at bottom of next page)

alight on the surface at a precise location or else make a quick seizure of its quarry while still on the wing, and then alight to devour its meal. When the wind speed is low, the bird must possess a relatively high absolute speed upon alighting or when seizing its prey on the wing, even when moving directly into the wind, and the ease and accuracy of the landing or seizure will be reduced. More important, the extreme difficulties attending the subsequent take-off in low winds require vigorous leg and wing action and a large amount of energy must be expended by the bird.

Thus, under the conditions of decreasing wind speed, the muscular energy required of the bird to secure its food mounts rapidly, while the basic ability to catch its prey is reduced. At a sufficiently low wind speed the energy output required exceeds the possible gains and the bird conserves its energy by either resting on the surface or by continuing its basic orbit with only infrequent attempts at catching prey. It is a fact of observation that the frequency with which the albatross alights to feed decreases rapidly as the wind speed decreases, and the bird ultimately settles on the surface to await a freshening of the wind.

It appears probable that the average wind speed at sea is the primary environmental factor which has determined the presently existing form of the albatross. The present form of the bird, although very efficient, is such that additional gains in dynamic soaring effeciency might be attained in high winds by further aerodynamic refinements of structure such as increased wing loading, higher aspect ratio, larger span, and generally higher L/D. Such refinements would, however, result in a detrimental reduction in flight capabilities at the lower wind speeds. Although such a highly specialized bird might be capable of magnificent soaring performances in strong winds, it would be almost completely helpless in the lower range of wind speeds used by the existing albatrosses. Such a bird would quickly perish if the average frequency of occurrence of very strong winds ever became insufficient to meet its flight needs. Such evolutional forces are no doubt actively at work today, eliminating any grossly overspecialized birds which may be produced as mutants. The present form clearly represents an adequate balance of all existing environmental forces. When more complete data become available on albatross aerodynamic characteristics (such as L/D), it should become possible to draw some inferences as to the nature of the "average" or "effective" wind conditions at sea.

---

forward and (if they are directly connected with the lungs) the very high impact pressure generated when the bird entered the water from a high speed dive would certainly force an appreciable amount of water into the bird's lungs. Diving birds like the pelicans, on the other hand, have no external nostrils and are thus exempt from this danger.

The shape and forward orientation of the tube-noses of albatrosses is quite suggestive of the pitot-static tube used in aircraft to determine the airspeed. In view of the importance of a knowledge of the airspeed in dynamic soaring, as evidenced by the preceding analyses, it is possible that the tube-noses of albatrosses could actually function as an airspeed monitoring device. This, of course, is a subject for more detailed investigation.

It does not appear that the albatross is placed in any great jeopardy by its intimate dependency on the sea wind and its vagaries, for the bird through natural selection is well adapted to such conditions. The present properties of ocean winds have existed and will no doubt continue to exist for vast periods of time. The weakest link in the bird's survival chain appears to be the fact that albatrosses nearly always return to the same islands to breed. Apparently, they have been using these islands for vast periods of time, for the urge to return to specific locations to nest is instinctive. Attempts to resettle certain colonies of North Pacific albatrosses from their home island to one with equal or superior environment for nesting have been unsuccessful. Fortunately, most albatross species have representative colonies on several different islands, so that gross molestation of the nesting birds on any one island would not have totally disasterous effects on the population as a whole. It does appear, however, that the most immediate threat to albatross survival (on an evolutional scale), as with many other birds, is man, either directly or through the unnatural predators he introduces on the breeding islands. The species Diomedea albatrus, once enormously abundant, is now on the verge of complete extinction as a result of the merciless slaughter of the nesting birds for their feathers on their principal breeding island of Torishima.

The relatively unique ability of the albatross to travel "upwind" is a very important property, especially during the breeding season when the parent birds must return to the nesting islands after traveling appreciable distances to secure food. Since the albatross inhabits areas where prevailing winds are strong and constant, such as in the southern latitudes, it is quite necessary that the bird be able to travel upwind. For, without this capability, parent birds could return to their nests only by making a complete circle around the globe with the wind; otherwise, they would have to await a complete reversal of the wind's direction in order to reach their islands. Very few birds are capable of making sustained progress into a headwind, even with extensive use of flapping power.*

The ability of the albatross to locate with unerring accuracy its relatively tiny nesting islands after traveling over many thousands of miles of open sea indicates that its powers of navigation are acutely developed. Although still totally unexplained, the manner in which the albatross navigates is, in all probability, similar to that used by other birds which travel long distances over water in their seasonal migrations (for example, the arctic tern). The navigating faculties of the albatross are much more frequently used, however, than those of the migrating species since the albatross is constantly ranging out to sea and returning, under all weather conditions, during its breeding season.

Some additional ecological factors concerning albatrosses are discussed in the following section.

---

*Gulls are, however, often observed taking advantage of the relatively low wind speed near the surface of the ocean during periods of high wind. The birds are able, by flying within the shear layer, to make rapid progress to windward when this would be impossible at higher altitudes.

## V. ECOLOGICAL COMPARISONS OF OCEAN AND LAND SOARERS

The structural form and characteristic actions of birds in their natural surroundings are the result of a carefully balanced compromise to best satisfy the complex of existing environmental forces. Thus the particular forms and functions evolved by many birds are direct indications of the presence and active influence of very specific environmental conditions. In general, the more highly differentiated and specialized the structure, the more intimately adapted is the bird to exploit some beneficial factor in its surroundings.

In the case of soaring birds such as the albatross and the vulture, one is immediately impressed by the unique ability of each to perform sustained flight without flapping. It is obvious that these birds have acquired the remarkable power to extract their flight energy from the air through which they fly, without having to resort to the laborious flapping so characteristic of most species of birds. At the same time, however, one is also impressed by the great differences in the structure and flight habits of the albatross and vulture. Since both birds are masters of soaring flight, these differences suggest that the nature of their environmental energy sources and, indeed, of their total environments must be quite different. It is of interest, therefore, to compare briefly some of the more outstanding differences of these two birds, and to ascertain the ecological reasons for these differences.

The primary advantage of soaring flight is that it enables a bird to remain airborne for extensive periods of time in order to examine vast areas of surface in its continuous search for food. Such sustained flight is possible only because the extensive flight energy required is made available to the bird from the air itself, and does not have to be supplied from internal muscular energy by flapping. It is obvious, therefore, that the nature and structure of the particular atmospheric energy source used by each type of soaring bird will exert a dominating influence on the resultant characteristics of the bird. Thus the aerodynamic factors which govern soaring flight under the various meteorological conditions come to dictate the form of soaring birds.

The ability to perform certain and efficient soaring flight is not the only requirement the soaring bird must meet, however. Once food has been sighted, the bird must alight to claim it. Thus arises the need to perform safe and accurate landings, along with the subsequent take-offs. The physical requirements of these maneuvers are in turn governed by the nature of the terrain over which the bird operates; these requirements are generally incompatible with those for efficient soaring so that some compromise is necessary. The resultant form of the bird is therefore governed not only by the meteorological conditions of the atmosphere, but also by the particular terrain of the environment. The existing forms, attained through evolutional development, quite adequately balance all the essential demands of the environment as is evidenced by the birds' continued survival. Other secondary, but important, requirements are imposed by such factors as nesting, roosting, migration, and the like.

The aerodynamic requirements for efficient static soaring by the vulture in thermal convections over land have been discussed in previous studies by the author;[1,2,3] the requirements for dynamic soaring by the albatross in ocean shear layers have been established in the preceding sections of the present study. These requirements establish the basic properties the birds must possess in order to effectively exploit the meteorological conditions of their particular environments. The essential aerodynamic factors may be summarized as follows.

The albatross, in order to perform continuous dynamic soaring in ocean shear layers, must possess a high aerodynamic efficiency (L/D) and a high wing loading W/S. These requirements can be met by increasing the aspect ratio A to a large value by means of a large wing span b. That the albatross indeed meets these requirements is easily verified by the characteristically large span, aspect ratio, and wing loading of the bird. The albatross operates almost exclusively over the ocean where it is free of all surface obstructions, and hence can alight and take off without danger to its fragile, large-span wings, under sufficient wind conditions. The great span of the wings precludes the possibility of using strong flapping to aid in the take-off (or landing) but, on the other hand, the bird has complete freedom to "run" for long distances over the water to effect a take-off, much like a conventional airplane. In addition, over the open sea strong winds are nearly always available to lessen the burden of the take-off and to increase the ease and accuracy of the landing. Thus, the free, open surface of the sea not only provides the wind conditions needed for dynamic soaring, but is also well suited to the type of landing and take-off the albatross must use. On land during the breeding season, however, the albatross must choose its nesting locations with care, so as to adequately provide for its restricted low-speed aerodynamic capabilities, as was discussed in Section III.

The vulture, on the other hand, engages primarily in static soaring and its aerodynamic characteristics are quite different from those of the albatross. In order to perform efficient static soaring by circling within the relatively confined upflow regions of thermal shells, the vulture must possess a very low value of W/S and a low sinking speed $w \equiv dz/dt$. While a large value of L/D is desirable, it is the low value of w which is more important in static soaring. The attainment of a low value of W/S is incompatible with a large value of A unless the wing span is also large. In the case of the vulture, however, which generally has to operate from very rough, forested terrain, take-offs and landings must be made in narrow, restricted areas by direct ascent or descent, making full use of all available flapping power. Under such conditions, large span wings like those of the albatross would not only be useless but very dangerous. The vulture must therefore have a relatively short wing span (compared to body length); for a low wing loading this leads to a correspondingly small value for A. The vulture indeed possesses a very low wing loading, a relatively small span, and a low aspect ratio.

The low aspect ratio of the vulture would, in general, lead to a rather low aerodynamic efficiency in circling flight and hence to a detrimental increase in the sinking speed. However, the bird has evolved an ingenious means for attaining a relatively high aerodynamic efficiency with a very light

wing of small geometrical span and aspect ratio by use of the slotted wing tip. The emarginated pinions of the vulture's wing are an excellent example of the extent to which environmental forces can stimulate the development of highly specialized aerodynamic structures in birds. The mechanics of this device have been discussed in previous papers[1,2,12] and will not be considered here. The aerodynamic theory of the slotted wing tip and other multiplane systems has been covered in detail in reference 14. The theory and experimental verifications of this reference provide proof that the primary purpose of the slotted wing tip is to lower the induced drag of the wing.

The wing span of vultures actually varies over a rather wide range, from 5 feet for the Black Vulture to over 10 feet for the condors, so that in reality the condor possesses a much larger span than most albatrosses. With such a large span, however, the condor's range becomes limited to relatively open terrain, free of close vegetation and obstacles, much like that of the albatross. The Black Vulture, on the other hand, with its 5-foot span is able to land and take off from very thick vegetation as well as from open areas and hence is much more widely distributed than the condor. Yet, despite its absolute size, the condor's wing span is not nearly so large in relation to the bird's body height (above ground) as is that of the albatross, and the condor is still capable of strong flapping flight during take-off and landing, under normal circumstances. Under conditions of low wind speed, however, the condor must use the same technique as the albatross, and an appreciable ground run prior to lift-off is required.

An interesting example of adaptation to effect the most useful balance of ecological factors is afforded by the relationship between the types of food and the relative soaring altitudes of the albatross and vulture. As mentioned in the preceding sections, the albatross is limited to flight within the shear layer, and thus remains close to the surface throughout its soaring cycle. By contrast, the vulture nearly always soars at relatively high altitudes, on the order of 1000 to 5000 feet, where the thermal shells are well developed. The albatross feeds, in general, on live marine animals such as squid, shrimp, and fish, and in order to capture its mobile prey the bird must be able to move swiftly and surely. The high-speed, low-altitude flight thus greatly enhances its success in procuring food. The vulture feeds on immobile carrion, which it can easily detect from high altitudes. From such altitudes the bird's field of vision, and consequently its scanning efficiency, is greatly increased. Thus, the food types of the two birds are precisely those which can best be located and taken in a manner perfectly compatible with the basic flight patterns required for efficient soaring flight.

An important point of similarity exists between the vulture and the albatross in that both use the same wing-flexing technique to increase the effective wing loading. Wing-flexing is frequently used by vultures during glides into the wind, where an increase in the wing loading is necessary for an increased speed over the ground. Turkey Vultures and gulls make important use of wing-flexing in gust soaring. The use of wing-flexing by the albatross in the leeward glide is exactly analagous to that of the vulture and allows the bird to maintain a high absolute velocity in the leeward glide.

## VI. THE MECHANICS OF GUST SOARING

The preceding discussions have been concerned with dynamic soaring in which the variation of the wind speed with altitude, that is, the shear layer, made possible the extraction of useful energy by the albatross. In this case, the wind speed is a steady function of the altitude $z$; that is, the wind profile $V_w(z)$ does not change with time at a given point. A second type of dynamic soaring is also possible, however, which does not depend upon the variation of $V_w$ with altitude, but rather upon the direct variation with time. This second type will be referred to as gust soaring.

It does not appear, in general, that gust soaring is a significant mode of flight for true oceanic birds, since the wind conditions at sea are relatively steady. Over land, horizontal gusts generated by turbulence and local air instabilities (due to nonuniform heating of the surface) are more prevalent, and are used to a limited extent by such soaring birds as the Turkey Vulture and gull. The very erratic and uncertain nature of such gusts, however, precludes their general use for practical soaring.

### WIND VARIATIONS

In the general case, the variations in wind speed which a bird encounters at any given instant can come from two sources: that due to the change in $V_w$ with time at the local position of the bird and that due to the bird's motion in taking it to a new position where the wind speed is different. Mathematically, the variation in $V_w$ experienced by the bird is given by the total derivative

$$\frac{DV_w}{Dt} = \frac{\partial V_w}{\partial t} + u \frac{\partial V_w}{\partial x} + v \frac{\partial V_w}{\partial y} + w \frac{\partial V_w}{\partial z} \tag{180}$$

where $\partial V_w/\partial t$ is the "local" derivative and the remaining three terms comprise the "convective" derivative. Here $u$, $v$, and $w$ are the magnitudes of the orthogonal velocity components of the bird relative to earth.

In the steady shear layer previously considered,

$$\begin{aligned} \frac{\partial V_w}{\partial t} &= 0 \\ \frac{\partial V_w}{\partial x} &= 0 \\ \frac{\partial V_w}{\partial y} &= 0 \end{aligned} \tag{181}$$

since the x-axis is taken parallel to the wind vector, $\hat{V}_w = V_w(z)\,\hat{i}$. Hence we have

$$\frac{DV_w}{Dt} = w \frac{dV_w}{dz} \tag{182}$$

which yields the time-altitude relation

$$w = \frac{dz}{dt} \tag{183}$$

In the case of pure gust soaring, we have

$$\frac{DV_W}{Dt} = \frac{\partial V_W}{\partial t} \equiv \frac{dV_W}{dt} \tag{184}$$

assuming, of course, that the wind increases simultaneously at every point according to the same function $\hat{V}_W(t)$ throughout a sufficiently large region surrounding the bird. For the most general case, where the wind velocity field is varying with time and position, eq. (180) must be used. An example of such a situation is a shear layer in which the wind above the layer is rapidly changing with time, and thus causing changes in the wind profile. This section considers primarily the case wherein eq. (184) applies, that is, the case of pure gust soaring.

## EQUATIONS OF MOTION IN GUST SOARING

Consider a bird at altitude $z_o$ at time $t = 0$, moving with the horizontal absolute velocity $\hat{u}$ directly into a wind of uniform speed $\hat{V}_{WO}$, that is, the wind speed is everywhere equal to $V_{WO}$ in a large region surrounding the bird. If now the wind increases uniformly according to some function $V_W(t)$ throughout the region, the bird will accelerate vertically and begin to climb if the strength of the gust is sufficient (that is, if $F_Z > W$). The motion during the climb is governed by exactly the same differential equations as for the shear layer [eqs. (23) and (24)]. Since $V_W$ is now an explicit function of time, however, it is desirable to state the linearized forms of these equations in terms of $t$ rather than $z$. Thus we obtain

$$\frac{du}{dt} = g\left(C_D + C_L \frac{w}{V_W - u}\right) \frac{1}{2} \rho \frac{(V_W - u)^2}{W/S} \tag{185}$$

$$\frac{dw}{dt} = g\left(C_L \frac{1}{2} \rho \frac{(V_W - u)^2}{W/S} - 1\right) \tag{186}$$

where $C_L$, $C_D$, and $V_W$ are functions of time. These equations may be solved in exactly the same manner as for the shear layer case to yield $u(t)$ and $w(t)$. Alternately, if the functions $x(t)$ and $z(t)$ are obtained from a photographic record of the gust flight path, the functions $C_L(t)$, $L/D(t)$, and $V_W(t)$ can be calculated.

The exact relationship of the equations of motion for gust and shear layer soaring is clearly brought out by the fact that any flight path produced by a windward climb in a shear layer can be duplicated exactly by a correpsonding gust function $V_W(t)$. Let us suppose that a photographic analysis of a climb in a shear layer has been obtained and has yielded the flight path functions $u(z)$, $w(z)$, $C_L(z)$, $L/D$ $(C_L)$, and $V_W(z)$. The analysis also gives the basic time-altitude relation $z(t)$. Then by relating $z$ in $V_W(z)$ to its equivalent

time by $z(t)$, the appropriate gust function $V_w(t)$ is obtained. In the same manner, the corresponding functions $u(t)$, $w(t)$, and $C_L(t)$ are obtained. It is clear that the increase in wind speed with time will then produce exactly the same wind speed at each altitude as does the shear layer, and flight conditions in the two cases will be identical. If the gust were of long enough duration, the bird could also gain useful kinetic energy by executing a leeward turn when the gust had reached its maximum strength.

The analogy can obviously be extended so that a complete basic cycle in the shear layer can be reproduced by the corresponding gust function. To duplicate the basic cycle, the gust function $V_w(t)$ would have the general form shown in Fig 52. The segments 1, 2, 3, and 4 of the gust correspond respectively

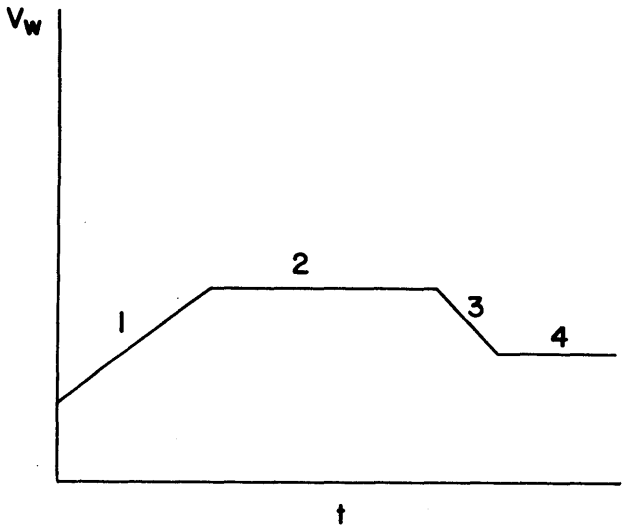


Fig. 52

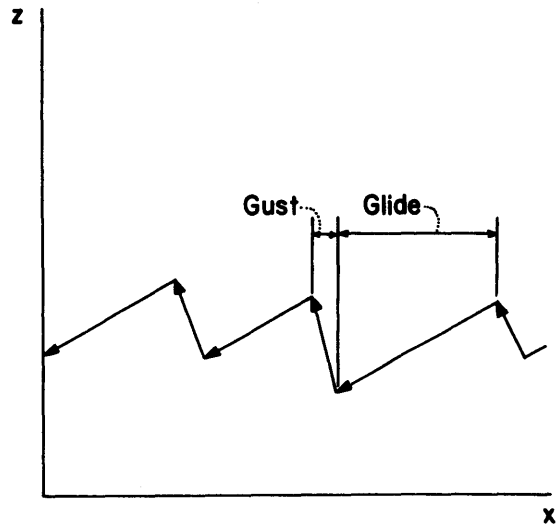


Fig. 53

to the windward climb, leeward turn, leeward glide, and windward turn in the shear layer. If a gust function of this type actually existed in the atmosphere and were periodic, useful gust soaring directly analagous to shear layer soaring would be possible. The flight path would have the additional beneficial feature (at least for vultures) that it need be no longer restricted to a narrow region near the surface, but could be generated at relatively high altitudes. Unfortunately, gusts of such highly specialized structure are not observed in nature to any extent, and soaring birds are therefore unable to realize the large kinetic energy gains which would otherwise be available from use of such wind variations.

In the general case of gust soaring, the only energy obtained is the potential energy gained during the climb. For example, Fig. 53 shows a flight path which might result from gust soaring. The bird climbs during the period of the gust, and extracts some energy from the wind. This energy is stored in

the potential form. Then, upon subsidence of the gust, the bird commences a glide until another gust is encountered. As in the case of the analagous windward climb in shear layers, the functions $C_L(t)$ and $L/D\ (C_L)$ as well as the wing loading, play an important part in determining the efficiency of the climb.

The analysis of the equations of motion for the windward climb in shear layer soaring indicated that a large value of the wing loading was desirable for an efficient gain of altitude. Thus it appears that a high wing loading is also desirable for gust soaring. It is interesting to note, therefore, that land birds such as the Turkey Vulture and the gull, which have very low basic wing loadings, but which frequently soar in gusty weather, fly under such conditions with their wings very strongly flexed so as to gain a favorable increase in wing loading.

## VII. CONCLUDING REMARKS

The intent of this study has been to develop on as rational and as quantitative a basis as possible the fundamental aerodynamic principles underlying the dynamic soaring flight of albatrosses in ocean shear layers. With the aerodynamic basis of albatross flight firmly established, the ecological significance of many aspects of the bird's characteristic form and behavior becomes clear. Not only can many qualitative deductions be made, but the quantitative nature of the aerodynamic analyses allow the actual numerical investigation and correlation of many ecological factors when adequate field data are available.

This paper, being primarily concerned with the analysis of the flight dynamics, has not endeavored to carry out any detailed numerical correlation of albatross ecological factors. However, with the availability of adequate quanititative data on specific albatross flight paths and travel patterns, combined with adequate oceanographic and meteorological information on the specific environments, it should become possible to describe the primary ecosystems of the various species of albatrosses to a highly quantitative degree.

With the availability of accurate recordings of flight paths, it will become possible to determine the exact aerodynamic properties of the albatrosses, that is the flight speeds, $L/D\ (C_L)$, $C_D\ (C_L)$, and $C_L(z)$, by use of the general equations of motion. The direct determination of such information by experimental measurement would be practically impossible. The flight path recordings can, when used with the equations of motion and energy, be used to determine the actual wind shear profiles $V_w(z)$ over the oceans. Once the aerodynamic capabilities of the various albatrosses have been quanitiatively determined, it should be possible to relate many factors of basic ecological importance, such as the speeds and directions of travel with regard to wind strength and direction, the density patterns of distribution at sea, the total range distribution, seasonal speeds and directions of movements, and distances covered in forages at sea during the nesting season.

When quanitiative data on the aerodynamic characteristics of several different but associated species become available, it should be possible to

establish the reasons for the most significant aeroecological differences between the various species on the basis of their differences in structural form and flight capabilities.

In order to bring out the essential aerodynamic features of the flight processes, attention has been devoted primarily to the idealized basic soaring cycle. Although observations indicate that the basic cycle as treated herein is the primary mode of dynamic soaring used by the albatross, the equations of motion and energy developed in the study bring to light possibilities of other soaring modes which should be looked for in field studies. For example, the energy balance given by eq. (86) suggests that an albatross may be able to proceed directly to windward by a simple series of windward climbs and dives, without performing any leeward or windward turns. The condition necessary for this to be possible is

$$\int_T D\, w \sin\varphi \, dt - \int_T D\, u \cos\varphi \, dt \leqq \int_T L\, V_w \sin\varphi \, dt$$

where $T$ is the period of the climb-dive cycle. Indeed, the aerodynamic results of the present paper present a whole new set of questions calling for a great amount of careful and accurate field observations on the albatrosses.

Finally, the general relations developed in the analyses of albatross soaring in shear layers and land bird soaring in gusts can be utilized to investigate the feasibility of dynamic soaring by man in areas where meteorological conditions appear favorable. The unsteady character of such flight, together with the need for great maneuverability, however, will make dynamic soaring in aircraft a very difficult task, even under adequate wind conditions.

Gloucester Point, Virginia
17 April 1964

# VIII. APPENDICES

## A-1. REFERENCES


1. C. D. Cone, Jr.: Thermal Soaring of Birds. American Scientist, Vol. 50, No. 1, March 1962.

2. C. D. Cone, Jr.: The Soaring Flight of Birds. Scientific American, Vol. 206, No. 4, April 1962.

3. C. D. Cone, Jr.: The Theory of Soaring Flight in Vortex Shells. Soaring, Vol. 25, Nos. 4, 5, 6, April, May, June 1961.

4. R. C. Murphy: Oceanic Birds of South America. Vol. 1, The Macmillan Co., 1936.

5. G. M. Mathews: Remarks on the Albatrosses and Mollymauks. Ibis, Vol. 4, 1934.

6. L. E. Richdale: Post-Egg Period in Albatrosses. Otago Daily Times, Dunedin, 1952.

7. C. C. Dixon: Some Observations on the Albatrosses and Other Birds of the Southern Ocean. Transactions of the Royal Canadian Institute, Vol. 19, 1933.

8. F. W. Hutton: Remarks on the Flight of Albatrosses. Ibis., Vol. 3, 1903.

9. P. Idrac: Experimental Studies of the "Soaring" of Albatrosses. Comptes Rendus, 1924.

10. W. Jameson: The Wandering Albatross. William Morrow and Co., 1959.

11. A. G. Davenport: Wind Loads on Structures. Technical Paper No. 88 of the Division of Building Research, National Research Council, Ottawa, Canada. March 1960.

12. C. D. Cone, Jr.: The Design of Sailplanes for Optimum Thermal Soaring Performance. NASA TN D-2052. September 1963.

13. C. D. Cone, Jr.: The Induced Drag of a Decelerating Airfoil. Flight Publications, Box 195, Yorktown, Va. February 1962.

14. C. D. Cone, Jr.: The Theory of Induced Lift and Minimum Induced Drag of Nonplanar Lifting Systems. NASA TR-139. February 1962.

15. C. D. Cone, Jr.: A Method for Measuring the Properties of Atmospheric Vortex Shells. Flight Publications, Box 195, Yorktown, Va. December 1961.

## A-2. SYMBOLS

The following list includes definitions of the principal symbols used in the paper; symbols which are infrequently used and which are adequately defined within the text are not repeated here.

| | |
|---|---|
| $a$ | acceleration |
| $A$ | aspect ratio |
| $b$ | span |
| $C_D$ | drag coefficient |
| $C_L$ | lift coefficient |
| $D$ | drag |
| $\hat{D}$ | displacement vector |
| $E_d$ | dissipation energy |
| $\hat{F}_c$ | centripetal force |
| $F_x$ | horizontal component of aerodynamic force |
| $F_z$ | vertical component of aerodynamic force |
| $g$ | gravitational acceleration constant |
| $\hat{i},\hat{j},\hat{k}$ | orthogonal unit vectors |
| K.E. | kinetic energy |
| $L$ | lift |
| $p$ | wind profile exponent |
| P.E. | potential energy |
| $r$ | radius of turn |
| $R$ | resultant aerodynamic force magnitude |
| $S$ | wing area |
| $t$ | time |
| $u,v,w$ | orthogonal components of absolute speed |
| $V$ | aerodynamic speed (linearized) |

| | |
|---|---|
| $V_a$ | absolute speed |
| $V_c$ | aerodynamic speed in turns |
| $V_R$ | aerodynamic speed (exact) |
| $V_w$ | wind speed |
| $w_k$ | work |
| W | weight |
| x,y,z | orthogonal space coordinates |
| $\alpha$ | angle of attack |
| $\beta$ | angle of bank |
| $\gamma$ | glide inclination angle |
| $\delta$ | boundary layer thickness |
| $\Delta$ | increment (prefix) |
| $\theta$ | $\tan^{-1} D/L$ |
| $\rho$ | density of air |
| $\sum$ | summation (prefix) |
| $\varphi$ | inclination of $\hat{V}_R$ to x-axis |
| $\omega$ | angular velocity |

Superscripts

| | |
|---|---|
| * | condition at top of shear layer |
| ^ | vector quantity |

Subscripts

| | |
|---|---|
| max | maximum |
| min | minimum |

## A-3. CLASSIFICATION OF NATURAL SOARING FLIGHT

Birdflight in which the wings remain stationary or rigid may be divided into two types. In gliding flight the bird glides through the air with a continuous loss of altitude, and ultimately comes to earth. In soaring flight the bird is able to fly a level course or even gain altitude by using the energy of the moving air.

The principles of fluid dynamics allow us to state the two atmospheric conditions necessary for a bird to remain in the air without flapping its wings. One of the following must be true for sustained soaring:

(1) the air must have a vertical component of velocity, or otherwise

(2) the motion of the air must not be of uniform speed with regard to space and/or time.

These two requirements form the basis for the classification of soaring flight. Soaring which is based on the utilization of the vertical motions of the air is called static soaring. It is almost exclusively the form used by land soaring birds. Soaring using the non-uniformities of the wind is called dynamic soaring. This form is occasionally practiced by land birds in gusty or stormy weather, but the available evidence indicates that this form is of much less importance than static soaring to land birds. For sea soarers such as the albatross, dynamic soaring is used almost exclusively.

Static soaring may be subclassed according to the manner in which the vertical air velocity is produced. These are (1) declivity winds and (2) thermals.

Declivity currents arise when the wind moving parallel to the earth encounters an obstacle, such as a hill. The air is forced upward as it approaches and passes over the obstacle thus producing a vertical velocity component that can be utilized by the birds. It is obvious that in order to have declivities of sufficient strength to support soaring, we must have strong surface winds and/or very large obstacles. Declivity winds are thus so restricted that they are in general of small value to soaring birds, whose primary reason for flight is to cover large areas of land in search of food.

Thermals occur when surface layers of air become so warmed and/or moisture-laden by contact with the sun-heated earth that they are less dense than the layers above them and tend to overturn, forming rising bodies or bubbles of air. The formation of thermals depends only on the presence of sufficient sunshine and thus their distribution is universal over all land areas. Due to their wide and continuous distribution, thermals appear to offer the sustaining means necessary for practically useful soaring flight. The year round availability of thermals is the reason why the highest degree of soaring is observed in temperate and tropic regions. It is because of the availability of thermals that soaring is possible over broad flat plains in a form equal or superior to that observed in mountainous country where declivities are always

available. (It is interesting to note that even in mountainous country, thermal soaring is quite as widely used as is declivity soaring – hills are excellent thermal producers.)

This availability of thermals is the condition upon which the very existence of the large soaring birds such as the vultures depends. This is the only atmospheric condition which will permit them to travel so effortlessly over such wide areas in search of food, and they have adapted themselves to exploit it to the fullest extent.

Dynamic soaring may be subclassified as shear-layer soaring and gust soaring. In shear-layer soaring the bird uses the difference in wind speeds which exists between the top and bottom of the shear layer to provide the energy for its flight. In gust soaring the bird uses the differences in wind speed which occur with time. Both types of dynamic soaring are treated in detail within the present paper.

## A-4. AERODYNAMICS OF NATURAL SOARING FLIGHT

As a bird flies through the air, it experiences a resultant force due to the air pressure and frictional stress distributions over its wings and body. The component of this force normal to the flight direction is called lift, while the component opposite to the flight direction is called drag. (Note that lift need not always act normal to the horizon.) If the bird is flying a straight course at a constant speed, the sum of all forces acting on it must be zero. Hence, it is necessary that the resultant aerodynamic force be equal to the bird's weight. When the forces are resolved along the flight path, it is necessary that a thrust force exist equal to the bird's drag. For a gliding bird moving through still air, there is no aerodynamic thrust force. Hence, the bird must glide down toward the earth at such an angle that the resultant aerodynamic force exactly balances the weight.

In the glide at constant velocity $V$, the force component balancing the drag is $W \sin\gamma$. Since the bird has a velocity in the direction of the force the weight is doing work against the drag at the rate $WV \sin\gamma$. Since the vertical component of the bird's velocity (the sinking velocity) is $V \sin\gamma$, the bird is losing potential energy at the rate $WV \sin\gamma$, and we see that the loss of altitude is furnishing the energy to power the glide. Suppose now that the bird were gliding down through an enormous box of air, but that this box was rising vertically (relative to the earth) with the speed $V \sin\gamma$. Then, although it would still be sinking relative to the air at the rate $V \sin\gamma$, the bird would be flying parallel to the surface of the earth with a velocity $V \cos\gamma$. If the box of air were moving upward with a speed greater than $V \sin\gamma$, the bird would actually be gaining altitude with respect to the earth. In this case the power for flight comes from the energy of the rising air. This simple picture gives the basic principle of static soaring flight.

If a bird wished to make a turn, it is necessary that a component of the aerodynamic force act toward the center of the turn to provide the necessary centripetal acceleration. This is accomplished by banking the wing through

some angle $\beta$. In this way a component of the lift acts to pull the bird around the turn. Since the lift is no longer acting in a vertical plane, the lift force must be greater in a turn if it is to balance the weight force.

The mechanics of dynamic soaring in shear layers and in gusts is discussed in detail within the present paper, so that the aerodynamic details are not considered here. Due to the unsteady nature of dynamic soaring, it is a much more complex phenomenon than static soaring flight.

## A-5. CLASSIFICATION AND RANGES OF ALBATROSSES

Order: Procellariiformes

Family: Diomedeidae

Genus: Phoebetria

Species: Phoebetria fusca (Sooty Albatross)

Range:* South Atlantic and Indian Oceans, eastward to Australia; confined chiefly to temperate latitudes. Breeds at Gough Island and the Tristan da Cunha group in South Atlantic.

Species: Phoebetria palpebrata (Light-mantled Albatross)

Range: Circumpolar in the pan-antarctic belt, ranging from about the 35th parallel southward into the zone of pack ice and beyond the antarctic circle. Breeds at Antipodes, Campbell, Auckland, Macquarie, Kerguelen, Crozet, Prince Edward, and South Georgia Islands.

Genus: Diomedea

Species: Diomedea melanophris (Black-browed Albatross)

Range: Southern oceans generally, from the tropic of Capricorn to latitude 60° S., and occasionally beyond. Breeds at Campbell and Auckland Islands; at Kerguelen and the Prince Edward Islands, South Georgia, the Falklands, Staten Islands, and at the Ildefonso and Diego Ramirez Islets, near Cape Horn.

Species: Diomedea chrysostoma (Gray-headed Albatross)

Range: From south temperate latitudes to the edge of pack ice. Breeds at Campbell Island south of New Zealand, at Kerguelen, the Prince Edwards, Crozets, South Georgia, the Falklands, and the Diego Ramirez Islands.

---

*Data on ranges of sourthern albatrosses are taken from Murphy.[4]

Species: Diomedea chlororhynchos (Yellow-nosed Albatross)

Range: Ranges widely over the southern oceans, and breeds upon Gough Island and the islands of the Tristan da Cunha group in the Atlantic, and at St. Paul Island in the Indian Ocean.

Species: Diomedea bulleri (Buller's Albatross)

Range: Confined to the South Pacific Ocean between the New Zealand region and the West Coast of South America. Breeds at the Snares Islands, and at several islands of the Chatham group.

Species: Diomedea cauta (White-capped Albatross)

Range: Southern oceans, chiefly in temperate latitudes, and apparently less common in the South Atlantic than in the Pacific and Indian Oceans. The subspecies salvini is known to breed only at the Bounty Islands, east and south of New Zealand.

Species: Diomedea irrorata (Galapagos Albatross)

Range: Breeds at Hood Island of the Galapagos and ranges to southward of the archipelago; regularly reaches the coast of Ecuador and northern Peru.

Species: Diomedea exulans (Wandering Albatross)

Range: Circumpolar in the west wind belt of the southern hemisphere, and ranging normally from the tropic of Capricorn southward to latitude 60° S., occasionally entering the zone of pack ice. Breeds at northerly antarctic islands, such as South Georgia, the Prince Edward and Crozet groups, Kerguelen, Auckland, and Antipodes.

Species: Diomedea epomophora (Royal Albatross)

Range: Coastal waters of southern America and New Zealand. Breeds on Campbell Island, New Zealand, and coasts and islands of southern South America.

Species: Diomedea nigripes (Black-footed Albatross)

Diomedea immutabilis (Laysan Albatross)

Diomedea albatrus (Short-tailed Albatross)

Ranges: These are the albatrosses of the North Pacific Ocean, and range over the entire ocean area between Hawaii and the Bering Sea. Breeding of the first two species occurs on the islands of the central North Pacific Ocean, particularly on the leeward islands of the Hawaiian archipelago.

## A-6. DYNAMIC SOARING IN AERONAUTICS

The possibility of achieving dynamic soaring flight in sailplanes has long intrigued soaring enthusiasts as a means for opening up a new realm of soaring energy. It is of interest, therefore, to briefly consider such possibilities in light of the foregoing analysis of natural dynamic soaring.

### Use of Shear Layers and Regions

It does not appear that practical use of ocean shear layers for dynamic soaring by sailplanes is possible to any significant extent. The reason for this lies in the excessively large size of the sailplane needed to support a man, compared to the depth of the shear layer. An efficient sailplane large enough to support a man, and having the same wing loading and aspect ratio as the albatross, would possess a span of some 45 to 50 feet. Hence, in performing a turn with any appreciable bank, the wings of the plane would span practically the entire extent of the shear layer; and very little, if any, useful energy could be taken from the wind. It thus appears that the absolute depth of the shear layers at sea, although making dynamic soaring a certain and useful flight mode for the albatross, precludes its use for practical soaring by man. This same effect of relative size of bird and sailplane on soaring ability is also noted in the case of static soaring in thermal shells over land.[3]

The mathematical analysis of albatross soaring flight presented in the body of this paper has shown that the essential physical requirement for dynamic soaring is the existence of two regions of air in close proximity having different absolute velocities. At sea, the shear layer satisfies this condition. Over land, conditions suitable for dynamic soaring in sailplanes no doubt exist at various times and places in the form of relatively strong velocity gradients. Great difficulty is encountered in the practical use of such shear regions, however, due to the uncertainty of finding sufficiently large areas of strong wind gradients in the free atmosphere, and in the case of shears generated by surface obstructions, the very restricted and stationary nature of the shear regions. For example, relatively strong wind shears are detected at the higher altitudes from time to time, but such conditions are highly unpredictable as to time, place, and extent of occurrence. Other shear conditions generated by surface obstructions no doubt exist, such as in valleys between parallel mountain ridges (Fig. 54) and in the lee of sharp ridges (Fig. 55) where the upflow has separated but flight is restricted to the immediate vicinity of these obstructions. In addition, such flight is somewhat dangerous since the separated airflow is usually very turbulent and unsteady. It is easy to understand the enormous advantages the ocean shear layers, with their immense areas of apparently constant shear conditions, offer the albatross in its ceaseless wanderings.

One possibility for accomplishing dynamic soaring over land consists in use of the land shear layers. As previously noted in Fig. 4, appreciable velocity gradients exist over land, especially over smooth, flat land (such as deserts), where the shear layers are quite similar to those over the ocean, only thicker. It may be possible that sustained dynamic soaring is feasible over vast stretches of flat prairie land or coastal plains, using the same

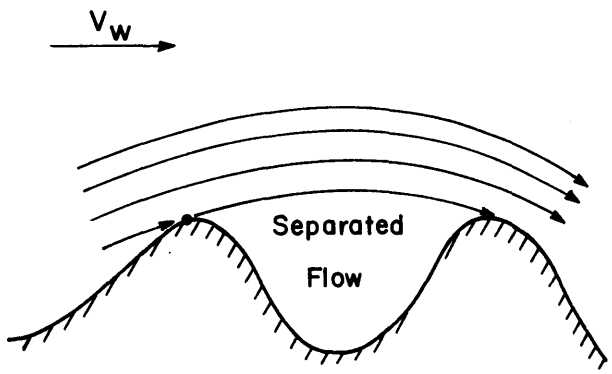


Fig. 54

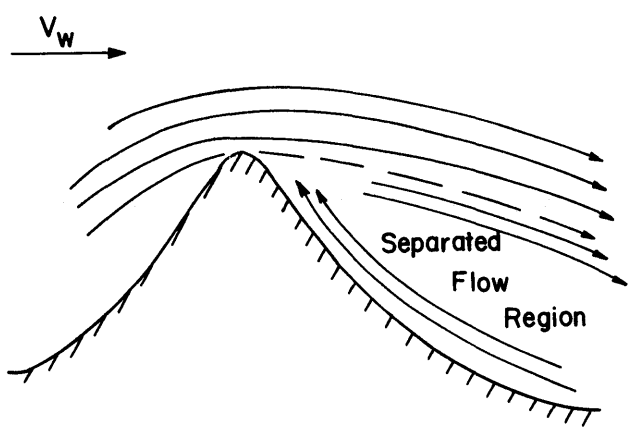


Fig. 55

flight techniques and patterns as used by the albatross over the sea. The great complexity of providing an efficient and flexible means for varying the wing loading in the leeward glide and the rapid, accurate maneuvers required, however, would make the use of such layers quite difficult and rather dangerous because of the high speeds and low altitudes involved. In any event, dynamic soaring will always be a much more difficult and exacting endeavor than the relatively simple equilibrium static soaring in thermal shells as presently used by sailplanes.

The basic principles involved in dynamic soaring by the albatross and the governing differential equations, as derived in this paper, can, of course, be directly applied to the analysis of dynamic soaring by sailplanes in various shear layers and regions over land. Meteorological measurements of the intensity of shear layers over various terrain types, when used with the basic equations of Section III will clearly indicate the aerodynamic properties a sailplane must have in order to perform dynamic soaring in a given layer and, more importantly, whether or not dynamic soaring over land is feasible (from an aerodynamic standpoint) with any type of sailplane. In this respect, it should be noted that, unlike the situation in thermal soaring, the high value of wing loading which comes with high A values in sailplanes is no longer detrimental in dynamic soaring.

## Use of Gusts

The possibility of accomplishing extended dynamic soaring with sailplanes in gusts does not presently appear very promising, except under certain specialized and infrequent wind conditions and at specific locations. The primary difficulty involved in gust soaring is, once again, the uncertainty of finding a usable gust at the time it is needed to replenish the energy supply of the craft.

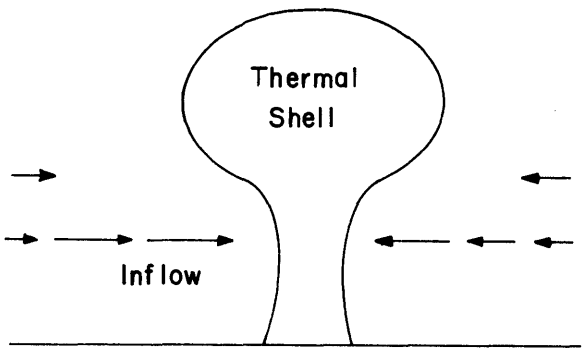


Fig. 56

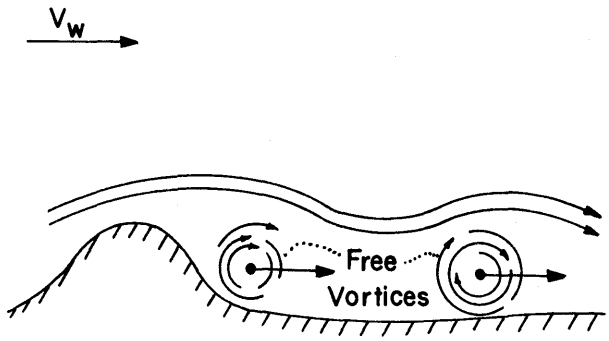


Fig. 57

Two basic sources of gusts are (1) inflows to thermal shells and (2) periodic vortex wakes in the lee of large obstacles, as pictured in Figs. 56 and 57, respectively. In the first case, the inflow toward the thermal shell creates a temporary increase (or decrease) in the absolute velocity of the air at a given point,[15] and these resultant changes in wind speed are felt as gusts. In the second case, the large free-vortices created by flow separation behind the obstacles are carried along by the wind, and produce local gusts as they move past a fixed point. Thermal-induced gusts are uncertain in nature and difficult to find, generally, while obstacle-created gusts are limited in extent and require special ranges of wind speed and direction for their orderly production.

For the case of gusts created by forming thermal shells, and for idealized vortex wakes, $V_W(t)$ functions can be theoretically predicted, but experimental research on actual gust functions is needed for the various specific terrain locations under various weather conditions before the possibility of any useful gust soaring can be established. To date, no obviously useful gust forms have been encountered by sailplanes. However, with a more detailed knowledge of characteristic gust functions, the windward climb equations of Section III can be used to establish the necessary aerodynamic characteristics of sailplanes for efficient gust soaring, and to determine the optimum $C_L(t)$ function to be used for maximum altitude gain during the gusts.

In conclusion, although special possibilities for dynamic soaring in sailplanes exist, it does not appear that dynamic soaring by man is presently possible to any useful degree. The great complexity of dynamic soaring flight, even under sufficient meteorological conditions, will always require constant and extreme maneuverability of the aircraft and continuous action on the part of the pilot. The ultimately useful exploitation of specialized sources of dynamic soaring energy will depend in great measure upon carefully planned research into the best methods for extracting such energy.